# Synthesis Of Cyclic Polymers With Active Esters For The Preparation Of Functional Materials

By

Peter Edward Trokajlo

A thesis submitted to the Faculty of Graduate Studies of

the University of Manitoba

in partial fulfillment of the requirements of the degree of

MASTER OF SCIENCE

Department of Chemistry

University of Manitoba

Winnipeg

## Abstract

Universal cyclic scaffolds of acrylate polymers with pentafluorophenyl active ester groups were synthesized using the α, ω- ring closing method and confirmed with a variety of characterization techniques. The incorporation of the active ester into the universal scaffold allows for alteration of the side groups by post polymerization modification. The preparation of this universal cyclic scaffold lays the synthetic foundation for materials that take advantage of cyclic polymer properties. Prerequisite linear poly(pentafluorophenyl methacrylate) was prepared possessing well-defined photoactive end groups and the conditions for the hetero Diels-Alder ring closing reaction were optimized.

The synthesis of a series of phenanthridine and quinolone based fluorophores was explored for post polymerization modification. A series of linear and cyclic polymers with active esters were substituted to comparable degrees with a phenanthridine-based fluorophore and of the two topologies the cyclic polymers exhibited the expected enhanced emissivity.

## Acknowledgements

I would like to thank and acknowledge the many interesting and wonderful people who have either taught me something new or have had an impact on my experience during graduate studies.

I would first like to thank my admirable supervisor Dr. David E Herbert of the Department of Chemistry at the University of Manitoba. He was always available for discussion and continually provided me guidance in the correct direction.

I would like to thank the members of the department for engaging conversations, help in using new instrumentation, and in experiment design; Dr. Mazdak Khajehpour, Ian Reinhorn, Dr. Hélène Perreault, Dr. Jörg Stetefeld, Dr. Markus Meier, Dr. Tom Ward, Dr. Horace Luong, and Dr. Elena Smirnova. I would like to thank the support staff for all their help in equipment and glassware repair and borrowing and ordering chemicals; Ms Sharon Mullen, Ms Lesa Cafferty, Mr. Terry Wolowiec, Dr. Oleg Roussak, Dr. Lilia Shamova, and Ms. Manjula Wijegunasinghe. I would like to thank Keith Travis and Dr. Jennifer. van Wijngaarden in aiding me traverse all my administrative work.

I would like to particularly thank Dr. Kirk Marat, Dr. David Davidson, and Dr. Carl Bartels for all their help, expert knowledge, and allowing me to continually pick their brains. I learnt a tremendous amount from them in the hours of discussions that we shared.

I would like to thank my committee members, Dr. Philip Hultin, Dr. Song Liu, and Dr. Emmanuel Ho, and Dr. David Herbert for their insights and attention into making this work possible.

I have had a lot of support and mentorship as a graduate student from my fellow group members, past and present; Pavan Mandapati, Rajarshi Mondal – both of whom have taught me so many practical skills in the laboratory, Kevin Szkop, Issiah Lozada, Gabriel Martins da Silva

Almeida Duarte, Bin Huang-Ivy, Talon Murray, Patrick Giesbrecht – for much discussion about how good chemistry is done, and Jason Braun.

I must express my profound gratitude to my family, Stanislaw, Ewa, and Paul for their unwavering support throughout my years of education. This work would not have been possible without them.

Thank you all

# Table of Contents

# List of Tables

# List of Figures

## List of Schemes

# 1. Introduction

## 1.1 Universal scaffolds: cyclic polymers and post polymerization modification

A universal scaffold of a cyclic polymer is a readily derivatizable cyclic framework that takes advantage of post polymerization modification to make a wide array of different functional materials. To develop a universal scaffold would lay the synthetic foundation for further chemistry of interesting materials that take advantage of the properties of cyclic polymers. Cyclic polymers have been synthesized before but the goal of this project was to configure them for a wide array of applications by using a modular synthetic strategy.

**Figure 1**. Animation of a Generic Universal Cyclic Polymer Scaffold

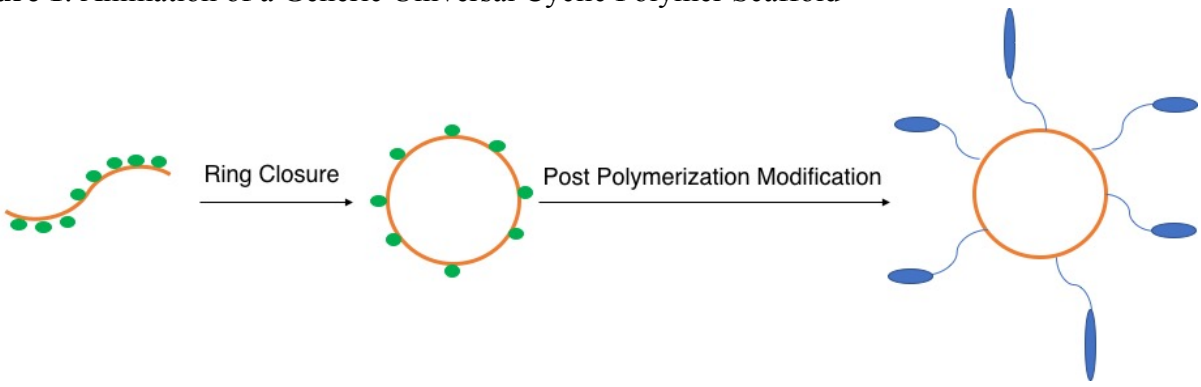


The monomer selected contained an ester moiety that could be readily substituted with a desired chemical group containing a primary amine or other suitable nucleophile.[1] The mode of post-polymerization modification (PPM) utilized involves making a polymer using a single easily polymerizable monomer containing an active ester and then substituting under mild conditions to obtain the desired material.[1] The advantage of this method over direct polymerization of various monomers with functionalized groups is that not all the targeted monomers may be compatible with the polymerization mechanism and cyclization chemistry.

New polymerization conditions would need to be developed for different functionalized targets but starting from a universal cyclic scaffold could allow for a larger variety of functionalization[2] that would be otherwise limited by a direct approach. See **Figure 1**.

The labile active esters can allow for quantitative PPM of tether-bound drugs and other useful functional molecules such as fluorophores, indicators, and biological markers. The wide array of functional molecules can permit the study of biological systems, the physical chemistry of cyclic polymers themselves, and the preparation of interesting new materials.

## 1.2 Properties and uses of cyclic polymers

The compact conformation of cyclic polymers results in a smaller volume occupied and leading to different solution behaviors for the polymer such as: larger elution volumes for gel permeation chromatography, lower intrinsic viscosity, lower solution viscosity, higher critical solution temperature, a smaller hydrodynamic volume (higher coil density), and a smaller radius of gyration.[3–5] For bulk phase properties: a higher density, higher refractive index, higher glass transition temperature, lower melt viscosity, and simulations suggest that the lack of chain ends leads to 'amoeba-like' dynamics as opposed to the conventional end-on reptation motion of linear chains.[3–5]

Cyclic polymers can be exploited for new applications because they have different properties than their linear counterparts. They are not yet widely used because of the difficulty of large-scale production.[6] As well, the door is still open to finding more applications for these systems.[6]

Examples of potential applications include:

(1) Gel properties are determined by structure and removing defective dangling chains ends and loop structures gives higher swelling ratios and lower gel fraction, statistic cross-

linking density, and shear modulus.[6,7] These gels can be achieved by using cyclic polymers as precursors in crosslinking reactions.

(2) Yamamota et al. reported a micelle composed of cyclic poly(butyl acrylate)$_n$-block-poly(ethylene oxide)$_m$, which was stable at higher temperatures compared to the micelle made of linear block copolymer.[6,8] The thermal stability of cyclic and linear mixtures varied according to the mixing ratio between the two species and could be adjusted within a window of temperatures.[8] This could lead to applications in drug delivery by designing heat-responsive devices to capture pathogens and release medicines.[8]

(3) Cyclic polymers possess enhanced fluorescence intensity and longer lifetimes which is thought to allow them to be used for organic optoelectronic devices. [6,9–13]

(4) The inability of cyclic polymers to deform to the same extent as linear polymers lowers their glomerular filtration rate in the human body which increases their half-life in the blood compared to linear systems and allows them to accumulate to greater extents in the body.[14]

Cyclic polymers can effectively utilize the 'enhanced permeation and retention' effect (EPR). EPR is a physiological consequence resulting from the rapid growth of cancerous solid tumor cells and their associated vasculature.[15] Macromolecules passively target tumor cells because of their highly porous incoming vasculature (enhanced permeability) and poor outgoing lymphatic drainage (enhanced retention).[15] The vascular tissue is more permeable in cancerous tissue than in healthy tissue thus allowing macromolecules to enter inside of the cells more easily.[14] Additionally, once inside the lack of chain ends in cyclic polymers alters the solution dynamics in such a way that passage through the outgoing biological pores is impeded.[14]

The two most successful approaches to targeting cancerous cells with drug-loaded carrier systems are passive and active targeting. Passive targeting is mediated by the EPR effect and

active targeting is based on the attachment of a specific ligand onto the drug or drug carrier that recognizes and binds distinctive receptors on the cancer cells.[16] The universal cyclic scaffolds can be readily derivatized to contain both the active pharmaceutical ingredients and the ligand bearing the targeting receptor, to utilize both forms of targeting. The improved targeting capabilities of cyclic polymers can be used to rationally design anticancer drugs.

## 1.3 Syntheses of Cyclic Polymers

Cyclic polymers frequently involve multistep syntheses and a challenge is to create the material in large amounts. In the recent decade progress in this field is allowing cyclic polymers to be synthesized with higher levels of purity with significantly less adulterating linear starting material.[6] Synthetic strategy considerations are at the heart of achieving pure cyclic material.

Two prominent synthetic strategies for making cyclic polymers are (1) ring expansion polymerization and (2) end-to-end ring closing method.[3,17] These two categories can be further subdivided into more diverse and sophisticated sets of reaction conditions but the two general classifications remain.[3,17] A ring expansion strategy involves a cyclic catalyst or initiator such as a stannane for β-butyrolactone insertion[18] or a cyclic ruthenium catalyst for cyclic poly(octenes) via olefin metathesis[19,20].

A ring expansion polymerization equilibrium strategy usually produces material of a higher purity without the need for large amounts of solvent.[17] The drawback of this technique is less control over PDI and a limit on the variety of monomers that are compatible with currently known REP catalysts and reactions.[17] The end-to-end ring closing method is less reliable at generating purities comparable to the ring-chain equilibrium method since it deals with large dilutions requiring large amounts of solvent which can lead to inefficiency in reactivity.[3] This method is advantageous because of the compatibility of combining a wide array of ring closing

reactions with a variety of linear polymer types.

**Figure 2**. Synthetic approaches for cyclic polymers

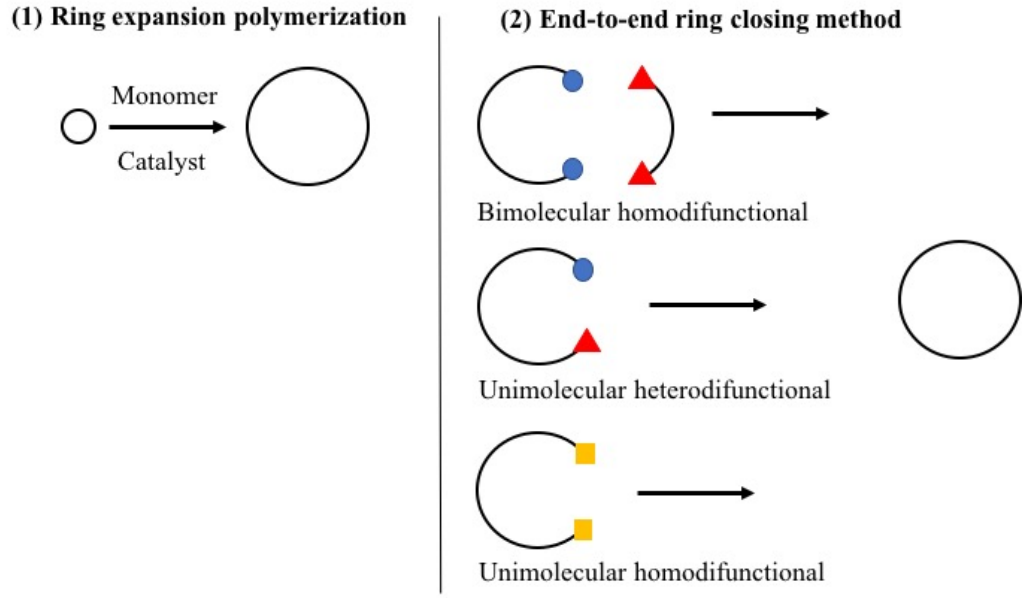


An end-to-end ring closing method was selected as the synthetic strategy for this project for the reasons above and to utilize such a strategy an α,ω- or hetero- telechelic linear polymer needs to be prepared. A telechelic polymer is a polymer possessing deliberately introduced reactive functional chain ends.[21] On a linear polymer reactive chain ends can either be the same or different (telechelic or α,ω-/hetero-telechelic) and for more complex polymer topologies a prefix is added to denote the number of reactive chain ends (di-, tri-, and poly-telechelic).[21] Since in this work only α,ω-/ hetero-telechelic linear polymers were prepared the term telechelic will be used to mean this.

Initially the intramolecular α, ω-ring closing method was initially pursued using copper(I) catalyzed azide-alkyne cycloaddition (CuAAC) 'click' reaction[22] of polymers prepared by atom transfer radical polymerization (ATRP). However, the end group chemistry of this initial approach was found to be incompatible with the active ester side groups and the hetero Diels-Alder (HDA) 'click' reaction was used alternatively for ring closure.

The specific challenge was to select a 'living' polymerization technique that would generate a polymer with distinct end groups that can join together without compromising the integrity of the active ester groups. To accomplish this the photochemical HDA was selected to close the ring because it does not generate any strong nucleophiles. Pentafluorophenyl methacrylate (PFMA) **1** was the chosen monomer bearing the active ester. Reversible addition-fragmentation chain-transfer (RAFT) polymerization was selected because of its diverse functional group tolerance and the chain transfer agent's capacity to install the diene and dienophile prior to polymerization.

## 1.4 Preparation of telechelic linear polymers using ATRP and attempted ring closure with copper(I) catalyzed azide-alkyne cycloaddition

Initial attempts at creating the cyclic scaffold with derivatizable active ester side chains were made by using the Atom Transfer Radical Polymerization (ATRP) '*living*' polymerization technique with the combination of 'click' chemistry. The α, ω-ring closure methodology was intended to follow a precedent established for cyclic-polystyrene which was successfully applied to cyclic poly(methyl methacrylate).[22,23]

ATRP is a reversible-deactivation radical polymerization (RDRP) synthetic technique used to generate polymers with control over molecular weight, polydispersity, chain topology, and composition.[24] It offers more control than conventional radical polymerization and the success of this technique is based on the dynamic equilibrium between "living" and dormant chains.[24,25]

The mechanism of ATRP involves an equilibrium between propagating radicals (the "living" polymer) and dormant species (a halide terminated polymer, $P_nX$, or alkyl halide).[24,25] The dormant species is present in solution in greater proportions than the propagating species

and it equilibrates by reacting with an activator complex, usually a transition metal (TM) in its lower oxidation state bound to an appropriate ligand (L).[24] The activator complex reversibly abstracts the terminal halide of the polymer or radical initiator and generates a deactivator complex – a higher oxidation state transition metal complex.[24] The propagating species is short lived and in the time it is present in solution it reacts with monomer. Activation and deactivation should be fast and efficient so as to permit the propagating radicals to react with only monomer in solution.[25] ATRP is considered a catalytic process and can be mediated with many different redox-active transition metals and ligand combinations.[24] It is described by the ATRP equilibrium constant, $K_{ATRP}$, which is the ratio of the rates of activation ($k_{act}$) to deactivation ($k_{deact}$). This ratio is affected by the structure of the ligand, monomer, catalyst activity, solvent polarity, temperature, and pressure.[24,26–28] The rate of the process depends on the concentration of monomer and the total radical concentration.[25]

**Figure 3**. ATRP dynamic equilibrium[24,25]

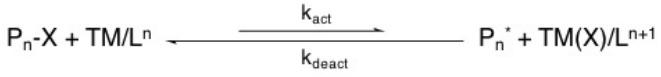


The synthetic strategy was to make linear telechelic poly(pentafluorophenyl methacrylate) with alkyne and azide end groups. Solutions of these polymers were then prepared in high dilution and copper(I) added to catalyze an azide-alkyne cycloaddition (CuAAC). The CuAAC is a 'click' reaction known for its efficiency, high yield, and orthogonality to other chemistries.[29–31]

**Figure 4**. Attempted synthetic strategy for cyclic polymers prepared by ATRP and copper(I) catalyzed azide-alkyne cycloaddition (CuAAC) 'click' chemistry

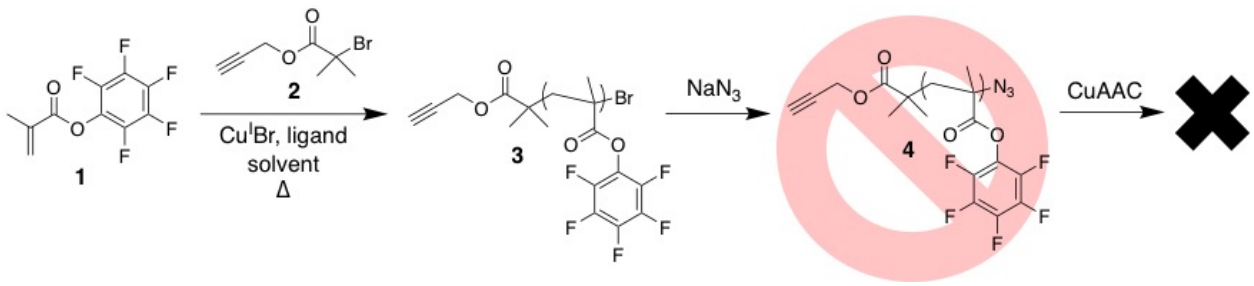


Unfortunately, side reactions resulted in the substitution of the side groups with azides when the terminal bromine end group was reacted to generate the ω azide demonstrating that this strategy was not feasible for the universal cyclic scaffolds with pentafluorophenyl groups. An alternative synthetic strategy was sought to overcome the limitations of the ATRP polymers.

## 1.5 Preparation of telechelic linear polymers using RAFT and ring closure with hetero Diels-Alder cycloaddition (HDA)

Different chemistries and polymerization techniques were explored to seek an alternative for the CuAAC α, ω-ring closure methodology. It was imperative not to generate any strong nucleophiles during the ring closing process so as not to compromise any of the active esters. The best alternative was to use a pericyclic reaction which progresses in a concerted fashion and the intermediates or transition states generated from the end groups for ring closure did not react with the active esters.

Reversible Addition-Fragmentation Chain Transfer (RAFT) is a '*living*' polymerization technique that is robust and versatile towards many monomers used in radical polymerization.[32–34] It is a complex process with many equilibria but the overall process entails sequential insertion of a monomer into C-S bond of a RAFT agent to make a macro-RAFT agent.[25] The majority of

living chains are present in the dormant form and a rapid equilibrium maintains that all of the chains have equal opportunity to grow.[25]

**Figure 5.** The RAFT mechanism (scheme adapted from reference[34])

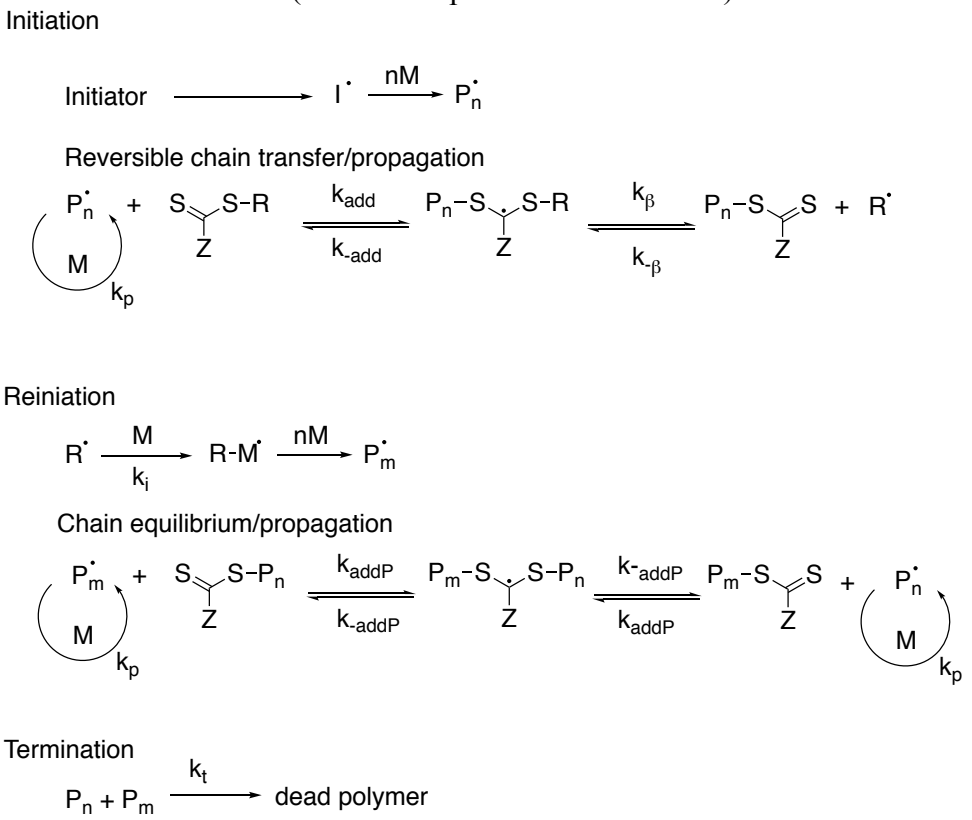


The activation and deactivation process involves a degenerate chain transfer between '*living*' polymers possessing a propagating radical and dormant polymers capped with a dithioester.[25] The process is degenerative because it involves two chemically identical polymer chains that differ only by their degree of polymerization ($P_n$ & $P_m$, **Figure 5**) but exchange their dithioester end group from the dormant to the 'living' species. If the activation and deactivation process is effective the difference in length is small which leads to a narrow molecular weight distribution.[25] The presence of the dithioester group on the end of the polymer maintains the living character.

More specifically RAFT is a reversible deactivation radical polymerization (RDRP) and with appropriate reagents and reaction conditions possesses the attributes of a '*living*' polymerization.[35] In '*living*' polymerizations all chains are initiated quickly, all of the chains grow at the same rate and survive polymerization, and, most importantly, no termination or other size reactions occur.[35,36] In RDRP '*living*' characteristics are provided through reagents that react with the propagating radicals by reversible chain transfer to maintain the majority of living chains in a dormant form.[35] Rapid equilibration between the active and dormant polymer ensures that all chains possess an equal chance for growth providing for well-defined molar masses that increase linearly with conversion and a low polydispersity index (PDI).[35]

Barner-Kowollik and coworkers have performed extensive work on different HDA reactions to alter the end groups of various RAFT polymers.[37–44] Our approach was adapted from his work on the synthesis of block copolymers whereby different polymers were made by RAFT polymerization and coupled by the HDA cycloaddition using *ortho*-methylbenzaldehydes.[45] In this synthesis a RAFT agent was selected and used to grow linear poly(methyl methacrylate)s that were terminated with a dithiolbenzoate group (the dienophile). A poly(caprolactone) was prepared with a terminal *ortho*-methylbenzaldehyde, irradiated with ultraviolet radiation to generate the diene, and link the two polymers.

Other work by Barner-Kowollik[41] and Tang et al.[46–48] applied similar 'click' chemistry to generate cyclic polymers of aliphatic polyesters and various methacrylates and acrylates. The goal of using their synthesis is to extend the system to encompass active esters on the cyclic framework. A dithioester RAFT agent shown to be compatible with methacrylates was prepared and contained a framework for the installation of further functionality which allowed the esterification of the *ortho*-methylbenzaldehyde group. The synthesis of the RAFT agent was

adapted from the work by Tang et al.[46–48] Polymerization of pentafluorophenylmethacrylate then results in the *ortho*-methylbenzaldehyde being installed at the α end and the dithiolbenzoate at the ω end. (See **Fig. 6**) The benefit of this method was that it did not require any end groups to be modified preventing purification steps from lowering the yields and additional reagents were not required to perform the cycloaddition.

**Figure 6**. Synthetic strategy for cyclic polymers prepared by RAFT and hetero Diels-Alder (HDA) 'click' chemistry

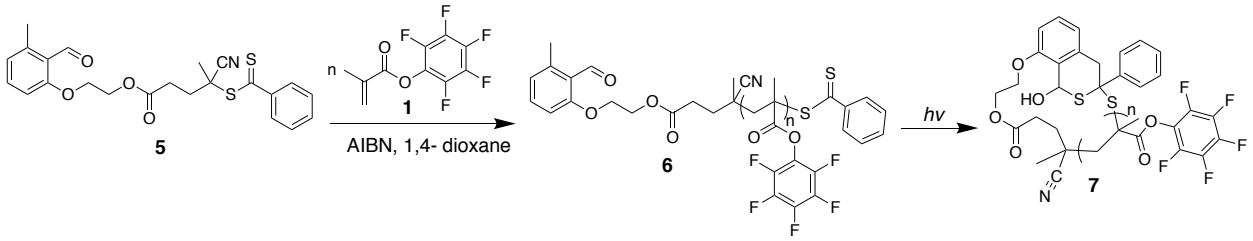


Upon irradiation in dilute solution, the *ortho*-methylbenzaldehyde undergoes a Norrish Type 2 reaction rearranging into a diene with an S-*cis* conformation, referred to as a photoenol or ortho-methylbenzaldehyde, which can react quickly with a dienophile. The mechanism of photoenolization has been an extensively studied process and is well understood (**Figure 7**).[49]

**Figure 7**. Photoenolization of the *ortho*-methylbenzaldehyde[50]

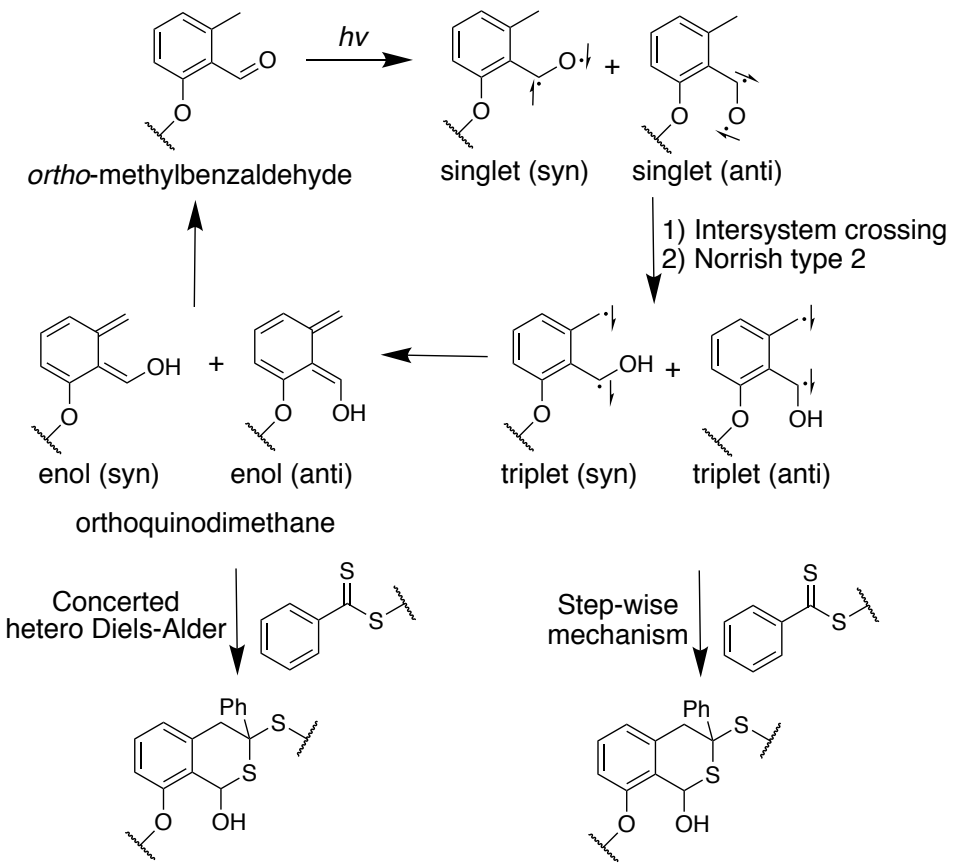


Excitation of either the syn or anti carbonyl ground state to the first excited state is followed by intersystem crossing to the triplet excited state.[50] Intersystem crossing is a radiationless electronic transition leading to an overall change in spin multiplicity of a molecule. In the triplet state, intramolecular hydrogen abstraction generates either a *syn* or *anti* triplet 1,4-biradical, referred to as a Norrish Type-II reaction, that collapses to the singlet enol.[50] Both the *syn* and *anti* enol tautomerize back to the aldehyde but it is the *anti* triplet 1,4-biradical that has the capacity to be trapped by a dienophile.[49] A photochemically driven cycloaddition usually involves a step-wise mechanism with biradical intermediates with other investigations reporting such a mechanism.[49]

Being a photochemical reaction involving triplet states, consideration of oxygen in the system is of concern. Reports claim that orthoquinodimethanes are capable of trapping triplet oxygen[49] but similar compounds[51] were too short lived or electronically incapable of sensitizing oxygen. Tang et al[46–48] has reported successful HDA of cyclic polymers in non-degassed solvents.

The quantum yields have been measured for analogous compounds elsewhere and have been shown to be solvent dependent. There is a significant enhancement in the reactivity with the addition of hydroxylic solvents such as water[50] or alcohol[52], most likely because of stabilization of the biradical through hydrogen bonding.

## 1.6 Jacobson Stockmayer Theory

For a successful ring closing reaction of a linear polymer, dilute concentrations are required for intramolecular reactivity because below a certain dilution, in a random coil conformation, the end groups would encounter each other rather than the end groups of other polymers. In the work of Tang, the concentrations required for successful ring closing were on the order of ~$10^{-5}$ to $10^{-6}$ M. As well, extensive work by Monteiro et al. has been performed on kinetic simulations of ring closure and determining the necessary concentrations and feed rates for cyclization.[5,53–55]

Monteiro et al revisited the work of Jacobson and Stockmayer by reformulating their molar cyclization equilibrium constant $K_x$ in terms of kinetic rate constants to determine the probabilities of cyclization and intermolecular chain extension.[56] Jacobson and Stockmayer provided an expression for the molar cyclization equilibrium constants, summarized by $K_x$

$$K_x = \frac{W_x(0)}{N_A \sigma_{Rx}} \quad (1)$$

Where $W_x(0)$ is the density of end-to-end vectors in space corresponding to the approach of chain ends, $N_a$ is Avogadro's number, $\sigma_{Rx}$ is the symmetry number of an n-repeat long polymer. The chains used for cyclization have to be of sufficient length and flexibility to be described by Gaussian statistics thus,

$$W_x(0) = \left(\frac{3}{2\pi\langle r^2\rangle}\right)^{3/2} \quad (2)$$

Where $\langle r^2 \rangle$ is the mean square end-to-end distance of a chain and $W_x(0)$ is in moles per litre. Thus,

$$K_x = \left(\frac{3}{2\pi\langle r^2\rangle}\right)^{\frac{3}{2}} \left(\frac{1}{N_a \sigma_{Rx}}\right) \quad (3)$$

$K_x$ is in moles per litre.

If cyclization described by an encounter pair model (See **Figure 8**) and controlled by equilibrium kinetics then the probability for closure can be determined by the Jacobson Stockmayer equation (3).

**Figure 8**. Encounter pair model of ring closure and intermolecular chain extension

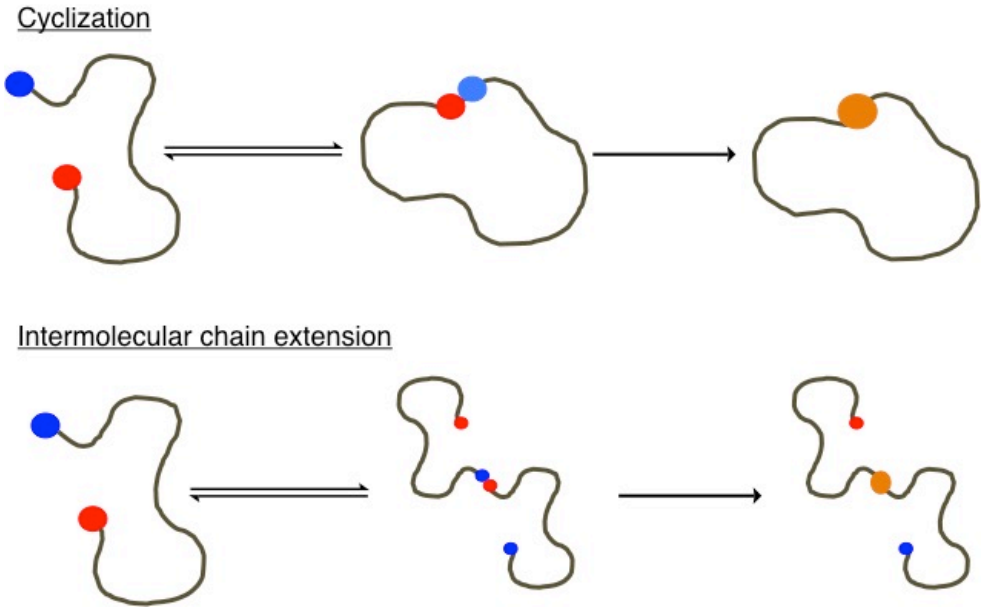

The probabilities are reformulated in terms of the Jacobson Stockmayer Case II type condensation meaning that the polymer has two different reactive functional groups used for ring closure, which will be applicable for this work.

The probabilities for cyclization ($P_C$) and intermolecular chain extension ($P_L$) are given by,

$$P_C = \left(\frac{3}{2\pi}\right)^{3/2} \frac{v_s}{\langle r^2 \rangle^{3/2}} \quad (4)$$

$$P_L = 2N\frac{v_s}{V} = \frac{2N_a c}{M} v_s \quad (5)$$

Where $v_s$ is the capture volume of the end groups, $<r^2>$ is the mean square end-to-end distance of a chain, N is the total number of polymer molecules, V is the total volume of the polymer molecules, $N_a$ is Avogadro's number, M is the molecular weight of the polymers, and c is the concentration of polymers in g/mL.

For successful ring closure the ratio for $P_C$ to $P_L$ ought to be as large as possible. For a given linear polymer in a solvent equations (4) and (5) are dependent on inherent properties of the system except for concentration. Cyclization is not dependent on the concentration of the polymer in solution but the probability of chain extension is dependent and ought to be minimized as much as is practically possible in a reaction.

The work of Jacobson and Stockmayer was used as a guide in this work. The concentration depends on the kinetics of the 'click' reaction and this could not be trivially determined so the concentrations suggested from Monteiro et al.[54] and Tang et al.[57] were used as the starting points for cyclization. Secondly, shorter linear polymer lengths were sought since chain extension dominates the kinetics when the molecular weight is increased.[53] Thirdly, cyclization is dependent on the end-to-end distance of the chain and the ends need to diffuse

within the capture volume for closure to occur. Though there is precedent for α, ω-ring closure occurring for methacrylate polymers, it was considered that the methacrylate polymers in this work might have more rigidity limiting their encounter.

## 1.7 Fluorescent enhancement of cyclic polymers

After the cyclic polymers were synthesized they were modified with a fluorescent trifluoromethyl-phenanthridine **8** and the properties of the cyclic system were investigated (**Fig. 9**). Cyclic polymers have enhanced fluorescence emission in comparison to their linear counterparts of the same molecular weight and PDI. This has been demonstrated for cyclic polymers bearing phenylazo naphthalene[10], triphenylene[11], tetraphenylethylene[12], carbazole[9], and 2-vinylnapthalene[13]. It has been suggested that the mechanism for this enhancement is due to the stronger cyclic backbone rigidity which leads to less quenching caused by aggregation.[10] Most fluorophores, including **8**, are hydrophobic aromatic organic molecules that are subject to "aggregation-caused quenching" (ACQ) both in solution and the solid state.[58] This enhancement phenomenon is referred to as the Restriction of Intramolecular Rotation (RIR). The fluorophores employed in this work, and in others[9], used planar fluorophores and the more distinctive features of RIR have been used to rationalize this enhancement in cyclic polymers. The RIR has two channels: restriction of distortion by main chain topological structures and the block effect between adjacent segments.[9] Additionally, cyclic polymers have greater bond angle and torsional strains that might hinder the formation of excimers between neighboring side groups.[59] The expected fluorescent enhancement was observed for the modified cyclic polymers **9** in this work.

**Figure 9**. Post polymerization modification of cyclic poly(pentafluorophenyl methacrylate) **7** with trifluoromethyl phenanthridine **8**

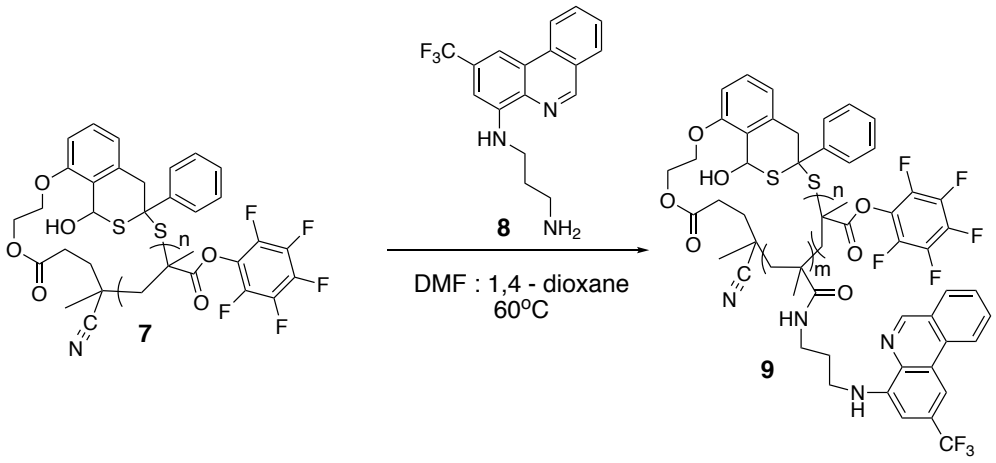

# 2. Synthesis of telechelic linear polymers with active esters

## 2.1 Introduction: synthesis of linear polymers by ATRP and ring closure by copper catalyzed azide-alkyne cycloaddition (CuAAC)

The prerequisite to making cyclic polymers with the α-ω ring-closing method are linear telechelic polymers with well-defined end-groups possessing the necessary reactivity between each other or the capacity to be changed to useful end groups. Herein, is described the synthesis and characterization of linear polymers of poly(pentafluorophenyl methacrylate).

Initial attempts at creating linear telechelic polymers were made by using the Atom Transfer Radical Polymerization (ATRP) '*living*' polymerization technique followed by end group modification for cyclization by copper catalyzed azide-alkyne cycloaddition (CuAAC).[29,31,60,61] See **Scheme 1**. The synthetic plan was intended to follow a precedent established for cyclic-polystyrene[22] which was successfully applied to cyclic-poly(methyl methacrylate)[23].

**Scheme 1.** Overview of ATRP Synthetic Strategy.

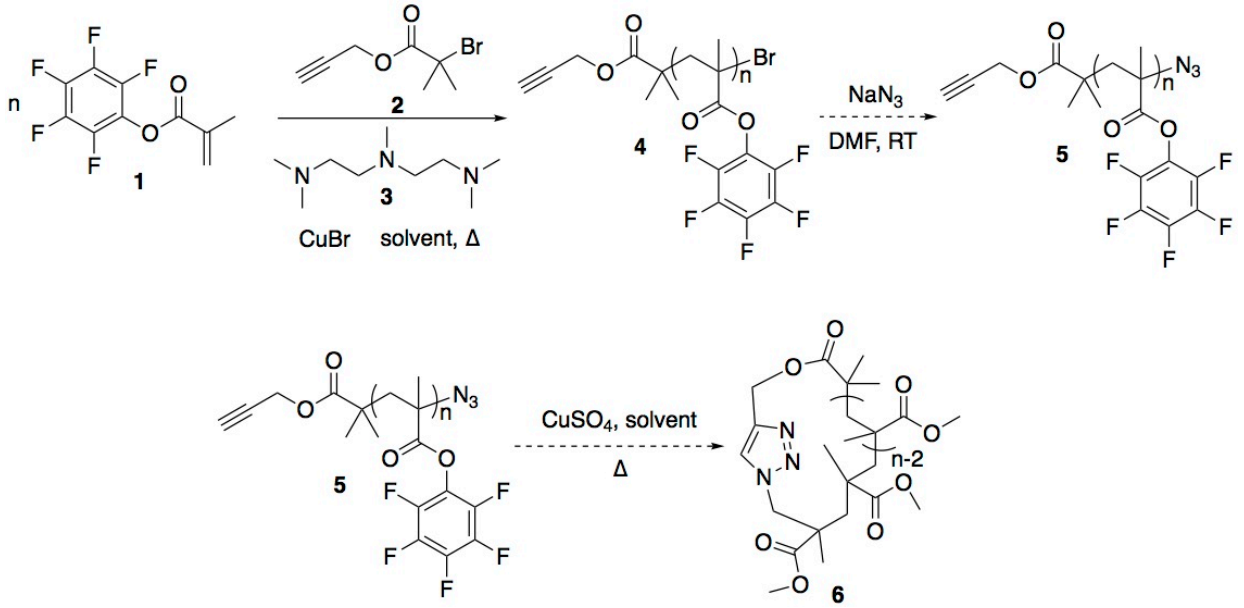


Monomer **1** and radical initiator **2**[62] were subject to ATRP conditions using CuBr as the catalyst and *N*,*N*,*N*′,*N*″,*N*″-Pentamethyldiethylenetriamine (PMDETA) **3** as the ligand in anisole solvent to generate poly(pentafluorophenyl methacrylate) **4**. In attempts to make **5**, **4** was substituted with $NaN_3$ (see below).[63] The CuAAC was the intended reaction to generate **6**.[2] Dotted arrows indicate hypothetical reactions.

ATRP is a reversible-deactivation radical polymerization (RDRP) synthetic technique used to generate polymers with control over molecular weight, polydispersity, and architecture in terms of chain topology, composition, and functionality.[24,64] It offers more control than conventional radical polymerization and the success of this technique is based on its dynamic equilibrium described earlier. [24,64]

The weakness of the strategy came down to the substitution of the pentafluorophenyl ring with azide in attempts for **5** from **4** where **7** is the suspected product. See **Scheme 2**.

**Scheme 2.** Side group substitution with azide.

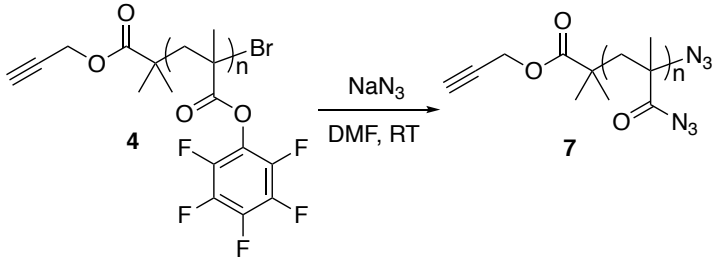


In **Figure 1** there are two characteristic azide stretches indicative of the different end and side group environments. When an excess of $NaN_3$ was used, it resulted in the complete removal of the pentafluorophenol. See **Figure 2**. The other drawbacks of applying ATRP to the ring closing reaction amount to the difficulty in altering the terminal bromine[65] and the inconvenience of characterizing its fidelity conclusively using destructive techniques such as mass spectrometry.

**Figure 1.** Stack of FTIR spectra of polymeric films of **4** and **7**. Lines: (black) $C_{sp2}$-F overtone stretch at 2660 & 2450 $cm^{-1}$ of the pentafluorophenyl side group of **4**. (green) ω - azide stretch at 2252 $cm^{-1}$ and acyl azide stretch at 2137 $cm^{-1}$ of **7**. (blue) backbone carbonyl stretch of **4** at 1778 $cm^{-1}$ and of **7** at 1700 $cm^{-1}$. (orange) C=C stretch of pentafluorophenyl ring at 1520 $cm^{-1}$ of **4**.

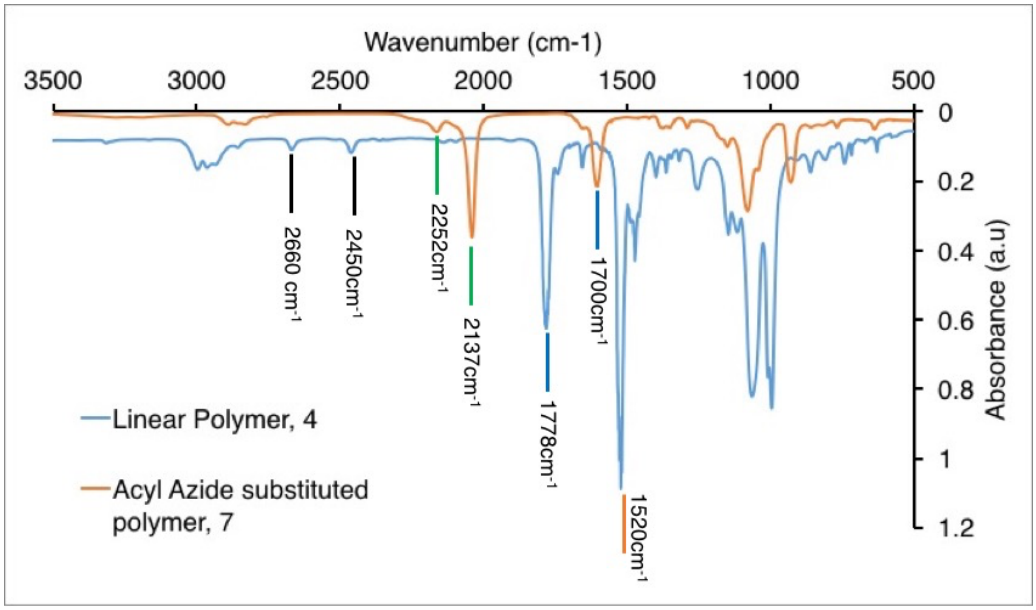

**Figure 2.** $^{19}F$ NMR of starting material **4** and **7** indicating that fluorine is no longer present in the polymeric material, and the supernatant of **7** showing the two environments of pentafluorophenol.

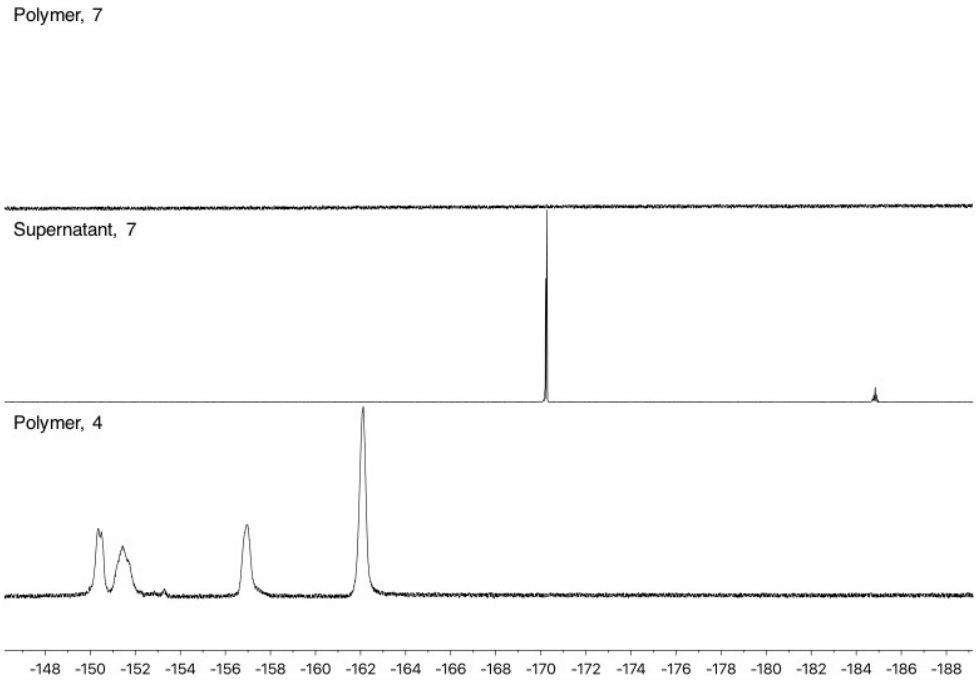


## 2.2 Synthesis of RAFT chain transfer agent bearing *ortho*-methylbenzaldehydes

As a result the synthetic strategy was switched to reversible addition chain-transfer fragmentation (RAFT) polymerization, a 'living' radical polymerization technique which could allow access to more well-defined end groups.[32,66,67] Like ATRP, RAFT gives narrow polydistribution indices, well-defined backbones, and high fidelity of end groups. [32,66,67] As well, a wide array of commercially available chain transfer agents can be readily altered and utilized to append different functional groups without compromising the living character of the radical polymerization. [32,66,67]

The synthesis of the starting materials used for the end groups of the linear polymers are summarized in **Scheme 3** (**steps a-d**). This section outlines the preparation of the RAFT chain transfer agent **15** and monomer **1**.

**Scheme 3.** Small molecules used in RAFT polymerization.

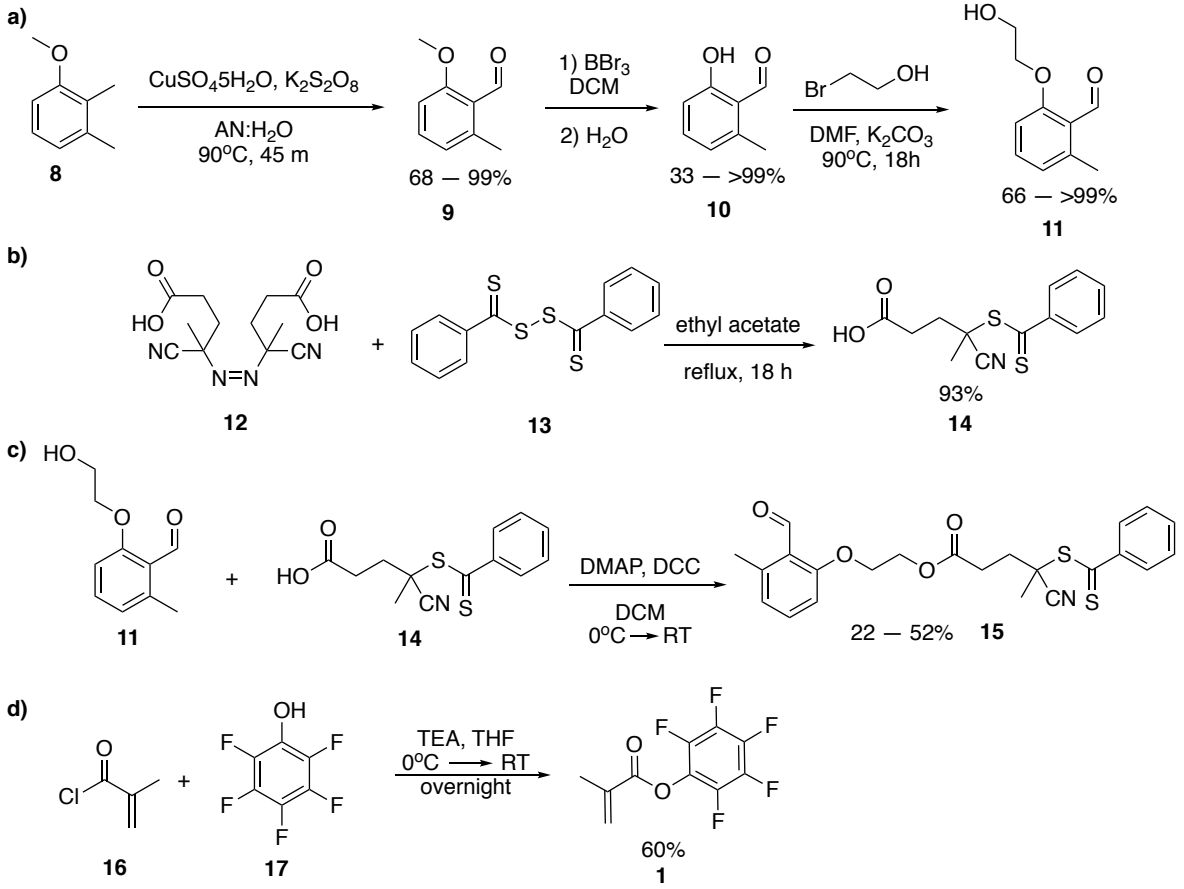


The synthesis of RAFT agent **15** can be dissected into four major steps: regioselective oxidation of 2,3-dimethyl anisole, demethylation, substitution, and Steglich Esterification onto thioester/carboxylic acid **14**. Compound **15** was purified by column chromatography and characterized by $^{1}$H NMR and UV-vis spectroscopy.

The synthesis of the *ortho*-methylbenzaldehyde, **9**, involves interesting radical chemistry itself and draws heavily upon the work of Walling et al.[68,69] Though the synthesis was adapted

from the literature much of the work of Walling et al. and others aided in the refinement and understanding of the synthesis and reactivity of **9**.[45,68,69]

Compound **9** was prepared from **8** as previously reported by Barner-Kowollik.[45] The $^{1}H$ NMR after isolation of **9** shows minor unidentified impurities but was carried forward without any further purification as suggested by the literature.[70] The product was confirmed by the appearance of the downfield aldehyde peak at 10.6 ppm and the disappearance of one of the methyl group b of **8** (**Figure 3**).

**Figure 3.** Stacked $^{1}H$ NMR spectra ($CDCl_3$, 300 MHz) of **8** and **9**. * indicates unknown impurities.

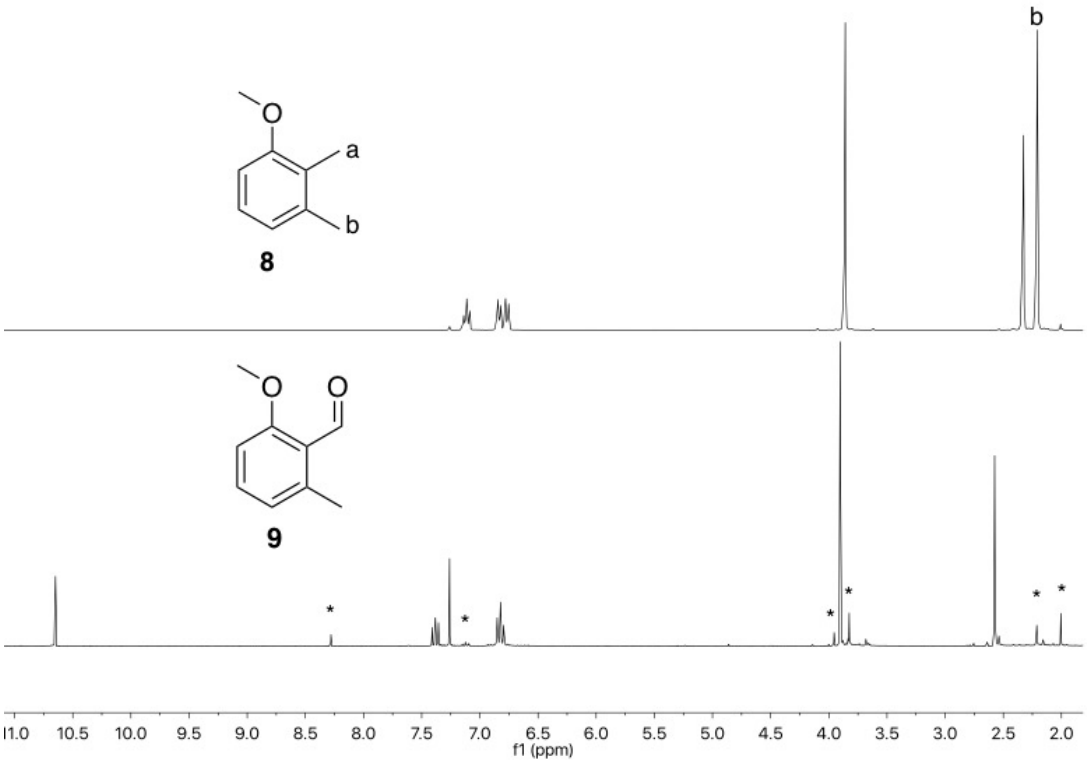


The synthesis of **10** was attempted using $AlCl_3$ and $BBr_3$. $AlCl_3$ gave incomplete conversions compared to $BBr_3$. Starting material could be seen in the crude NMR using $AlCl_3$ (**Fig. 4**) and the procedure did not afford product as readily and cleanly as previously reported.[45]

To overcome this difficulty a different Lewis acidic demethylating agent, $BBr_3$, was used. This is a good reagent since it requires mild conditions and does not affect a large variety of functional groups.[71,72] It is a highly Lewis acidic compound that coordinates to ethereal oxygens and promotes C-O cleavage to alkyl bromides and alkoxyboranes which leads to the alcohol after hydrolysis.[68,69] $BBr_3$ has been most generally used for the demethylation of methyl aryl ethers and carbonyls on aryl rings with *ortho*-methoxy groups facilitate demethylation.[73,74]

**Figure 4.** Stack $^1$H NMR spectra ($CDCl_3$, 300 MHz) of incomplete reaction using $AlCl_3$. Both **9** and **10** can be seen after work up. * - unidentified impurities.

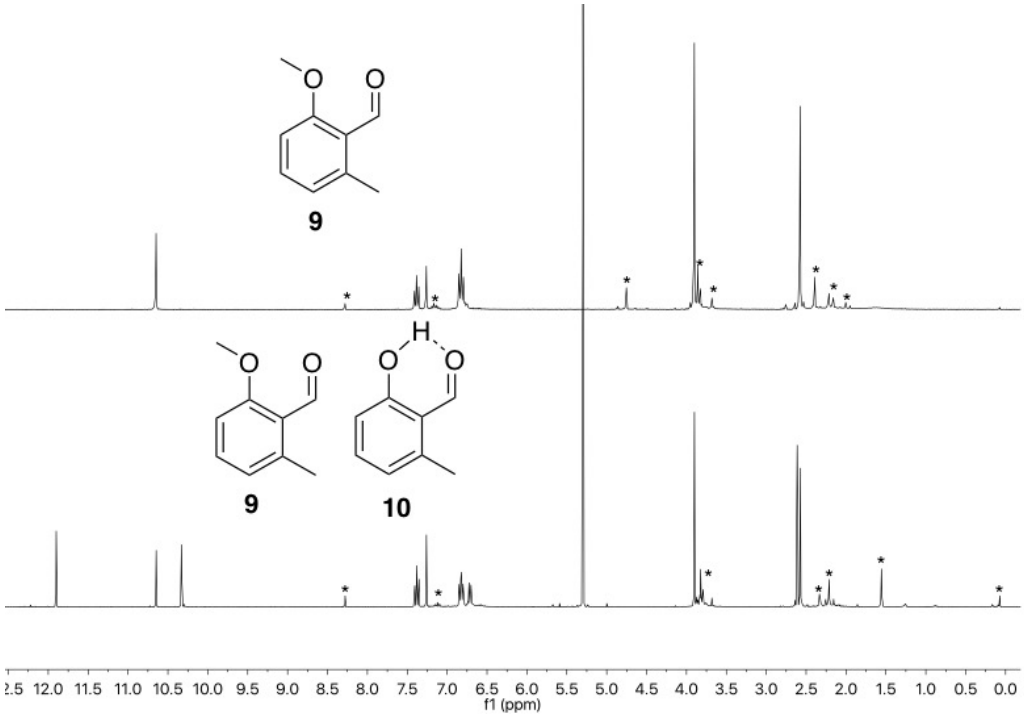


Stirring **9** with $BBr_3$ overnight in anhydrous dichloromethane followed by a water quench afforded **10** in 33 to >99% yield after isolation. The quenching step generates the product and an insoluble dark solid, presumably boronic acid, which requires filtration. The contents were stirred over anhydrous sodium thiosulfate to remove any remaining water and to reduce any $Br_2$

generated from the decomposition of $BBr_3$. The solution changed colour from a brown-red to a dark orange-yellow upon reduction of $Br_2$.

**Figure 5:** Stacked $^1H$ NMR spectra ($CDCl_3$, 300 MHz) of **9** and **10** after successful demethylation using $BBr_3$. * - unidentified impurities.

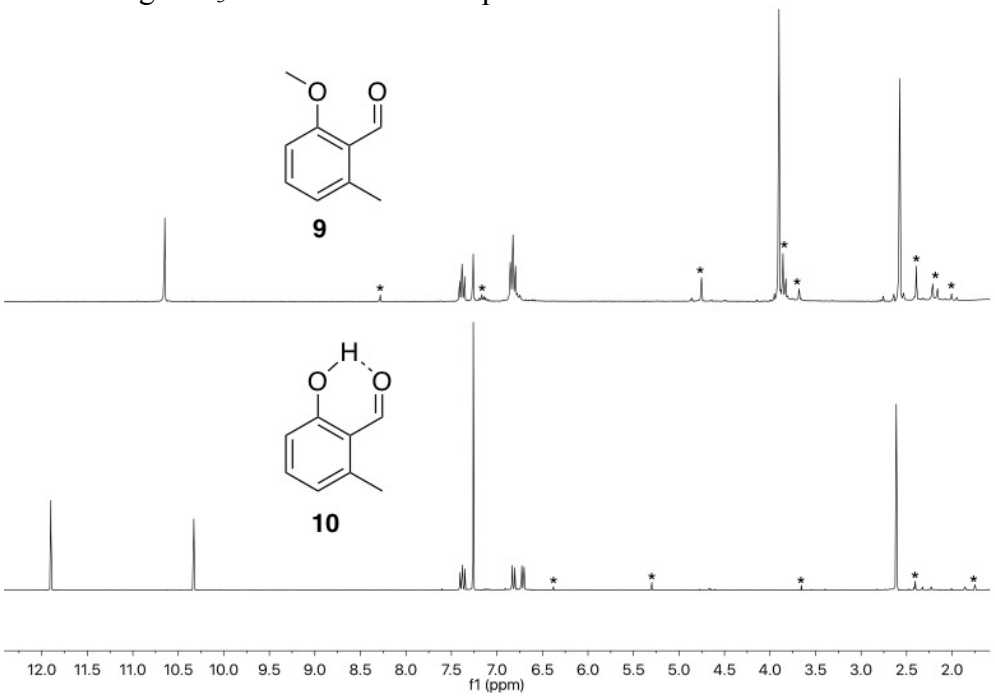


Compound **10** was confirmed by the disappearance of the methoxy peak at 3.92 ppm and the appearance of the hydroxyl proton at 11.90 ppm (**Fig. 5**). Apart from being attached to an electron withdrawing benzaldehyde, the reason for the large –OH chemical shift is due to intramolecular hydrogen bond formation. The hydrogen bond increases the partial positive charge on the proton deshielding it (See **10** in **Fig. 5**).

Compound **11** was prepared by substituting Br of 2-bromoethanol with **10**. Optimized conditions were afforded with DMF and $K_2CO_3$ at 90°C for 18 hours. After purification **11** was isolated in 66-100% yields as a brown sticky oil. The substitution was confirmed by the disappearance of the hydroxyl peak and the downfield shift of the methylene product peaks compared to the reactant (**Fig. 6**).

**Figure 6**. $^1$H NMR: Confirmation of substitution of 2-bromoethanol by the hydroxyl of **10** as evidenced by the disappearance of the hydroxyl peak and the downfield shift of the methylene peaks compared to the reactant. * - unidentified impurities. ($CDCl_3$, 300MHz)

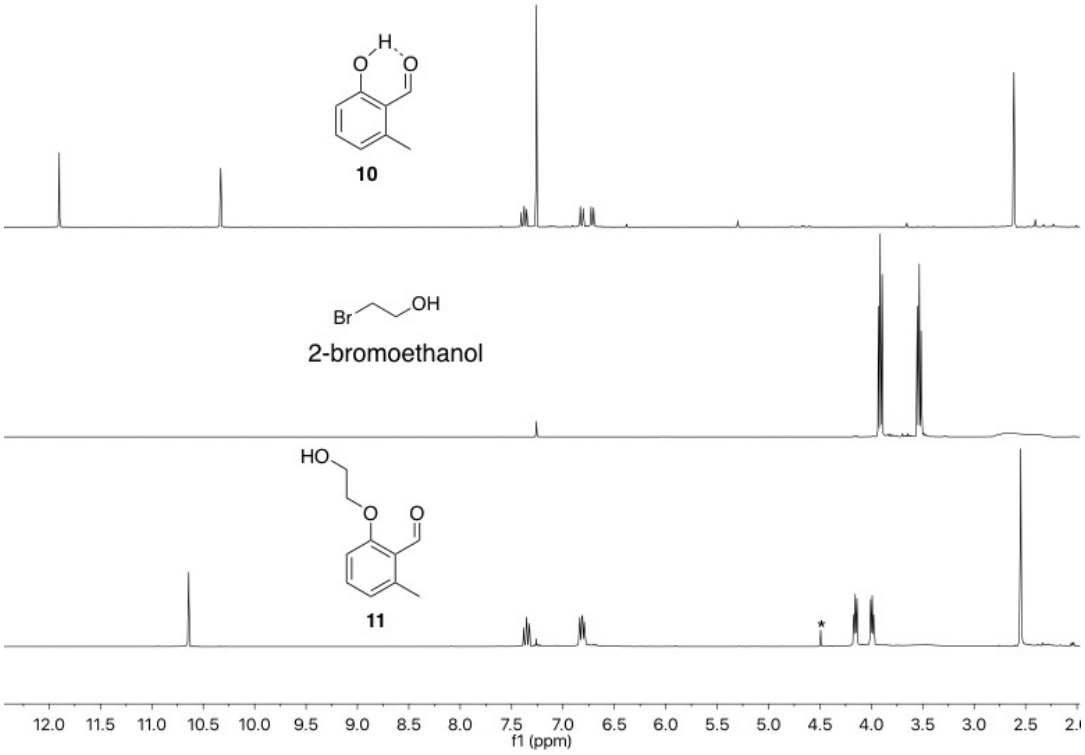


Aldehyde **11** is the product of a Williamson Ether synthesis whereby $K_2CO_3$ was used to deprotonate **10**, increasing its nucleophilicity, and partaking in an $S_N2$ reaction with 2-bromoethanol.[14] DMF was used as the polar aprotic solvent to encourage substitution rather than elimination.[14] Water soluble poly(ethylene glycol) oligomers were the suspected side-reaction products, and along with $K_2CO_3$, were washed away during purification the purification. However, the formation of the oligomers is not considered substantial since the pKa of phenols is lower than aliphatic alcohols.

Compound **14** was prepared in ethyl acetate and purified as previously reported.[75] The reason that the methylene protons of the methylene group in **14** and **15** are a multiplet is because of strong coupling between magnetically inequivalent (diasteriotopic) protons (**Fig**. **7**). Magnetically inequivalent protons of chemically similar envrionments may lead to second order

effects but not necessarily. The dithiobenzoate and the nitrile are strongly electron withdrawing groups leading to an increase in the *J* coupling constant of the neighboring methylene protons. When the difference in chemical shift is comparable to the coupling constant in *Hz* second order effects appear in the $^{1}$H NMR spectrum.

**Figure 7**. Confirmation of the Steglich Esterification of **15** can be seen by the downfield shift of the methylene linker at 4.16 and 3.99 ppm to 4.52 and 4.28 ppm. In **15** * indicates residual ethyl acetate solvent and in **14** * indicates unidentified impurities.

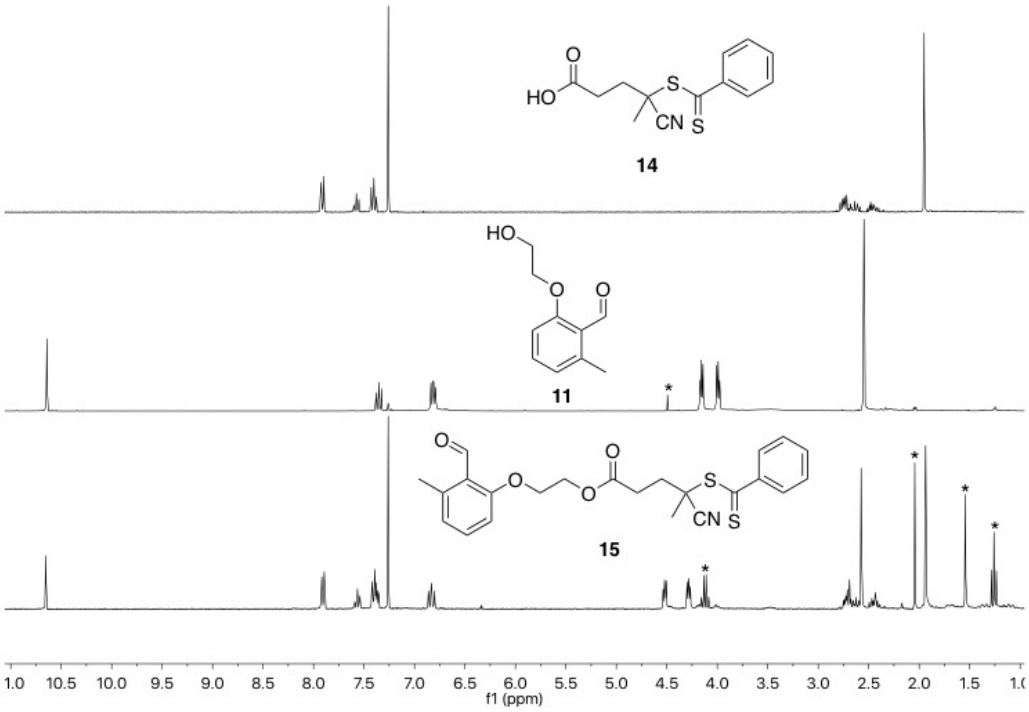


Compound **15** was synthesized by Steglich Esterification between **14** and **11**. *N,N'*-Dicyclohexylcarbodiimide (DCC) rather than 1-ethyl-3-(3-dimethylaminopropyl)carbodiimide (EDC) was found to be more effective in promoting reactivity as starting materials could be seen in the $^{1}$H NMR after work-up. Though EDC was previously reported in transesterification of **15a**[46,48,76] and **15b**[45] the reaction was slow because of solubility issues (**Fig. 8**). The EDC reagent in the form of the hydrochloride salt is used for the transesterification of carboxylic acids in aqueous media and DCC is commonly used in organic media.[77] The ester was confirmed by the

downfield shift of the product methylene peaks (**Fig. 7**). After flash chromatography the product was isolated as a bright red viscous oil in 25-52% yield.

**Figure 8**. Previously reported *ortho*-methylbenzaldehyde tethered chain transfer agents **15a** and **15b**.

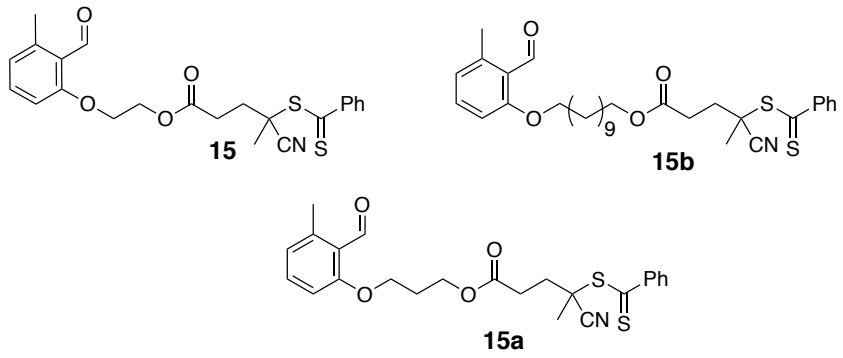


The UV-Vis trace (**Fig. 9**) shows the overlay of **11**, **14,** and **15** in dichloromethane. Compound **14** and **15** both have an (n → π*) transition at 513 nm attributed to the C=S which is the source of the red colour of the compound. This transition is most likely attributed to the red colour because the compounds absorb is the green (~ 500 nm). The broad peak from 300 to 315 nm in **15** is comprised of the (π → π*) transition from both **11** and **14**.[45] The peak at 513 nm is present in both **14** and **15** but **15** is only shown in **Figure 9**. The π → π* absorbance of **11** overlaps significantly with the emission of the Cosmedico UVB lamp.

**Figure 9**. UV-Vis spectra in dichloromethane of **14** (purple), **11** (yellow), and **15** (red) showing (n → π*) transitions. Inset: in red of **15** expanded and denoted with n → π*.

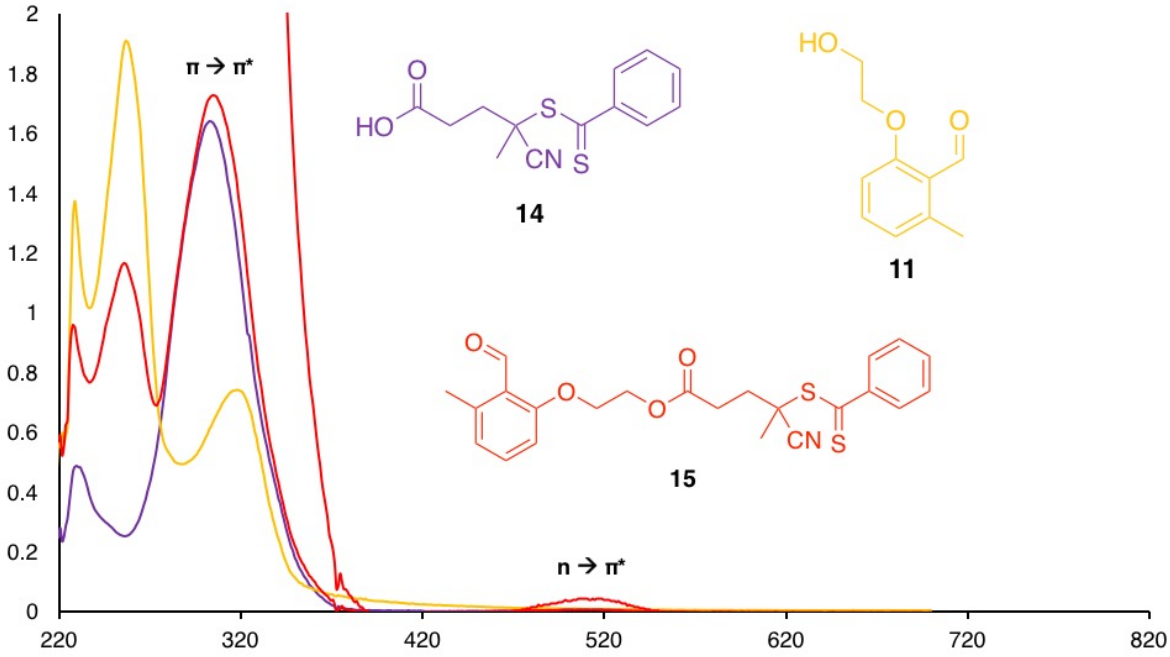


Compound **15** was then used to carry out RAFT polymerization for the synthesis of linear polymers of poly(pentafluorophenyl) methacrylate **18**. The monomer that was selected as the active ester was pentafluorophenyl methacrylate **1** because (1) of the robustness of the methacrylate backbone, (2) the resistance to hydrolysis and stability of the ester, (3) a larger variety of FDA approved polymers have methacrylate backbones and to incorporate the structure of the medicinal portion into cyclic polymers would allow for quick streamlining to test in biological systems, (4) the fluorine imparts the leaving group capability, and (5) $^{19}$F NMR can be used as a convenient NMR handle for Post polymerization modification (PPM).[78,79] Polymers of **1** have better solubility compared to other active esters such as *N*-hydroxysuccinimide (NHS) esters which have poor solubility in most organic solvents and need to be copolymerized.[79] Since **18** is a fluorinated polymethacrylate, this class of polymers usually posses high thermal resistance, large weather resistance, low dielectric constant, and low refractive index, and these

physical properties[80] could be investigated into how they can be augment or altered in a cyclic scaffold. Another class of pentafluorophenol based active esters, the pentafluorophenyl vinyl benzoates and pentafluorophenyl vinyl sulfonates, surpass the methacrylates and acrylates in terms of post polymerization reactivity rate.[79] These monomers can be involved in future projects as they are compatible with the methacrylate based chain transfer agent **14**.[81–85]

**Scheme 4**. Synthesis of pentafluorophenyl methacrylate monomer **1**.

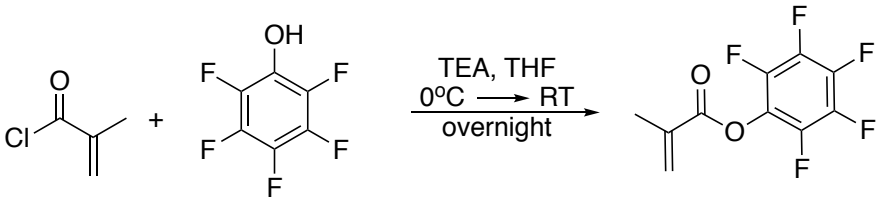


**16** **17** **1**

Compound **1** was synthesized by adding **16** in THF into a stirring solution of **17** and triethyl amine at 0°C. **Scheme 4**. This product was previously reported in my honours work. The combination of base and solvent were selected because generation of the chloride from **16** formed the insoluble $N(Et)_3$•HCl salt driving the reaction forward and simplifying purification. An unidentified impurity consistently appeared as a singlet at ~ 1.75 ppm and was removed by column chromatography to afford the pure material as a clear liquid in 60% yield. Monomer **1** was stable towards decomposition in storage at 10°C away from light for up to two years.

Monomer **1** was confirmed by an upfield shift of the two fluorine environments at 184.84 and 170.24 ppm on **17** to three different environments at 152.78, 158.20, and 162.50 ppm. As well, the proton NMR displays two distinct vinyl signals at 6.45 and 5.91 ppm integrating to 1 proton each and a single methyl group at 2.09 ppm integrating to 3 protons. See **Figure 10**.

**Figure 10.** $^{1}$H NMR spectrum of **1** after column chromatography. * water peak at 1.56 ppm. Inset: $^{19}$F NMR of the **17** and **1** comparing free alcohol and ester.

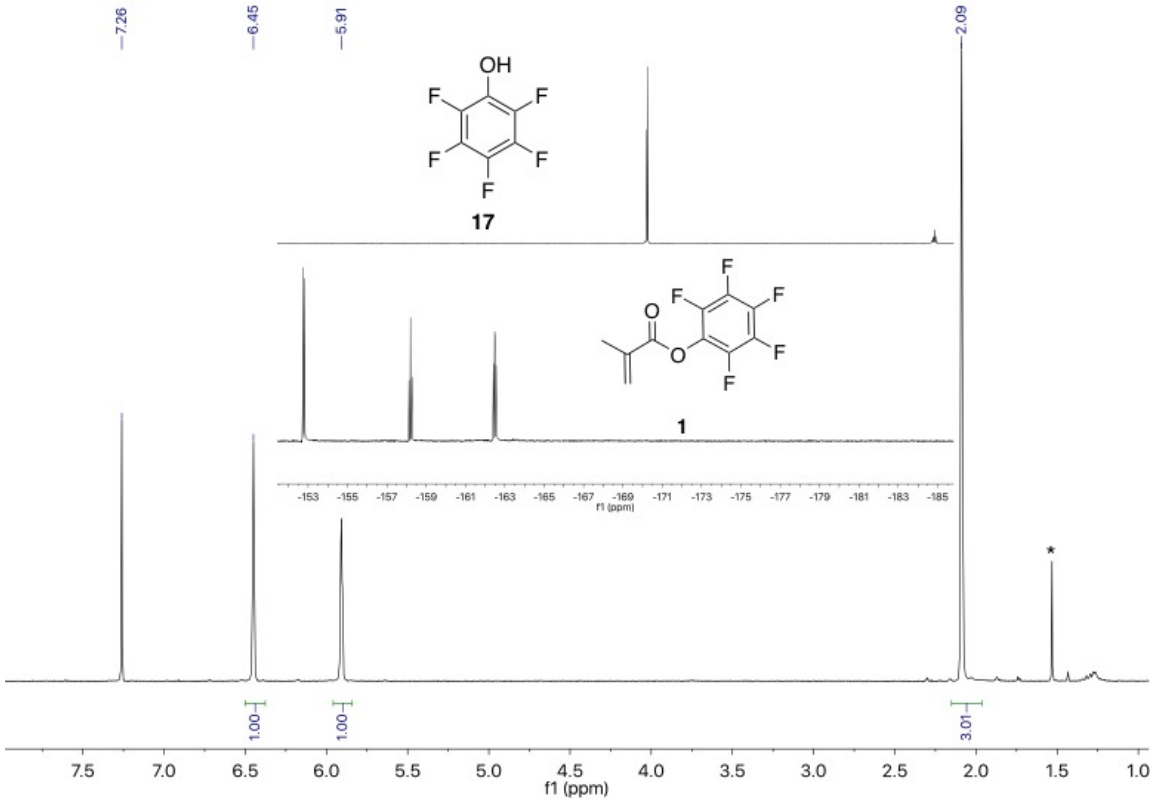


## 2.3 Synthesis of telechelic linear polymers with active esters

Under RAFT conditions, using AIBN as a radical initiator, **15** and **1** were used to generate a library of **18** with different molecular weights (**Table 1**).

**Table 1**. Preparation of linear pentafluorophenylmethacrylate polymers prepared by RAFT with varied molecular weight.

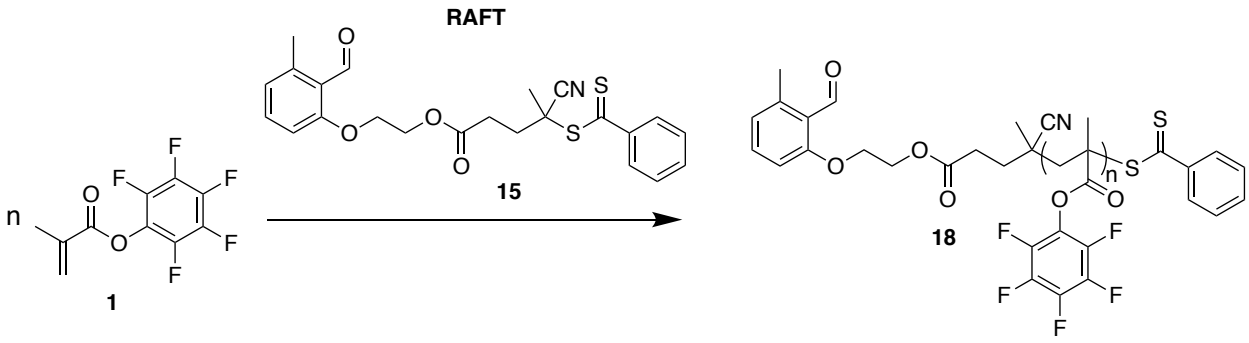


| Name | Expected n | $n_{NMR}$ ($(CD_3)_2CO$) | $n_{NMR}$ ($CDCl_3$) | $n_{GPC}$ |
|---|---|---|---|---|
| **18a** | 5 | - | 9 | 12 |
| **18b** | 10 | 27 | 18 | 23 |
| **18c** | 12 | - | 18 | - |
| **18d** | 12 | 23 | 19 | 16 |
| **18e** | 17 | - | 26 | |
| **18f** | 19 | 23 | - | - |
| **18g** | 20 | 46 | 33 | 34 |
| **18h** | 20 | 27 | 26 | 34 |
| **18i** | 22 | 51 | 42 | 51 |
| **18j** | 24 | - | 35 | 38 |
| **18k** | 26 | 52 | 70 | 73 |
| **18l** | 27 | 27 | 27 | 29 |
| **18m** | 29 | - | 133 | - |
| **18n** | 31 | 45 | - | 52 |
| **18o** | 33 | 89 | 65 | 63 |
| **18p** | 37 | 39 | - | 41 |
| **18q** | 98 | - | 161 | 155 |
| **18r** | 133 | 240 | 195 | 209 |
| **18sm** | 133 | 240 | 167 | 209 |

Expected n – molar ratio of monomer to chain transfer agent.

Reaction conditions were chosen based on related reactions with **1** (**Table 2)**. The R (-$(CN)(CH_3)C(CH_2)_2CO_2H$) and Z (Ph-) substituents on the RAFT agent dictate its compatibility towards different monomers, which forms the basis of an effective polymerization.[32] The

dithioester RAFT agents are used for more activated monomers (MAMs) such as methyl methacrylate, and methyl acrylate and, by this criteria alone, suggest promise towards **1**.[66,67] The chain transfer agent **15** has been used to generate **18** and polymers synthesized herein are consistent with the methacrylate backbone in the $^{1}$H NMR.[86]

**Table 2**. Summary of Experimental Conditions for RAFT polymers.

| Name | Ratio of CTA:Initiator | [Monomer] | Temp. (°C) | % Yield (m/m) |
|---|---|---|---|---|
| **18a** | 5.0 | 0.50 | 105 | 16 |
| **18b** | 4.8 | 5.55 | 110 | 87 |
| **18c** | 4.9 | 1.00 | 110 | - |
| **18d** | 9.3 | 0.57 | 110 | 23 |
| **18e** | 7.9 | 1.28 | 110 | 44 |
| **18f** | 16.4 | 3.17 | 105 | 26 |
| **18g** | 5.0 | 2.68 | 105 | 64 |
| **18h** | 7.0 | 0.93 | 110 | 59 |
| **18i** | 30.8 | 4.16 | 110 | 54 |
| **18j** | 6.2 | 5.55 | 105 | 53 |
| **18k** | 3.5 | 2.52 | 105 | 82 |
| **18l** | 25.5 | 3.16 | 105 | 29 |
| **18m** | 5.1 | 2.66 | 110 | 51 |
| **18n** | 6.3 | 2.38 | 105 | - |
| **18o** | 16.1 | 1.59 | 110 | 70 |
| **18p** | 10.4 | 3.17 | 105 | 43 |
| **18q** | 4.9 | 5.55 | 110 | 63 |
| **18r** | 5.0 | 5.55 | 90 | 83 |
| **18s** | 5.0 | 5.55 | 90 | 112* |

* - most likely due to experimental error

AIBN was selected because it is the most commonly used thermal initiator but any source of radicals in principle can be used.[32,66,67,87] The concentration and choice of initiator is an important consideration since side reactions can occur involving the initiator, and due to the

mechanism, there will inherently be a fraction of dead chains relating directly to the number of chains initiated so the concentration is kept as low as possible.[87] AIBN was chosen because the 2-cyanopropyl radical is a good leaving group to most propagating species in the main equilibrium.[25] As well, to achieve a narrow PDI and to increase the number of living chains requires a high chain transfer agent to radical initiator ratio which was recommended be at least 5 and higher.[32,88]

RAFT is a versatile technique because a starting point for the conditions can be adapted from a given radical polymerization condition simply by adding an appropriate chain transfer agent. A temperature around 90 - 110°C was investigated since polymerization at 90°C was previously reported[86] and 80 - 90°C for the radical polymerization[89] of **1**. In considering the balance of rate of polymerization and chain end fidelity, a higher temperature with a shorter reaction time was selected. A reaction temperature of 110°C offered higher rates of polymerization allowing adequate yields to be achieved in a shorter reaction time. A reaction time of two hours, in contrast to the eighteen-hour reaction times[89], was selected to preserve end groups since the concentration of dead polymers and end-to-end termination products increases with time.

The degree of polymerization was determined from the ratio of monomer to chain transfer agent but the results showed deviations. Since n was larger than expected this indicates that less chain transfer agent was consumed and after work-up CTA was observed in the supernatant.[66,67] The rate of polymerization depends on the monomer concentration[87,90] so either solvent was added or the reaction was performed neat to affect the conversion. 1,4-Dioxane was selected because it has a high boiling point and is commonly used in radical polymerizations to

minimize chain transfer reactions. The RAFT process is robust towards water but it was kept to a minimum to protect the dithioester.[66]

**Figure 11**. $^{1}$H NMR spectrum showing assignment of **18**.[46] Inset: zoomed in end group region. * - residual water, ** - residual solvent.

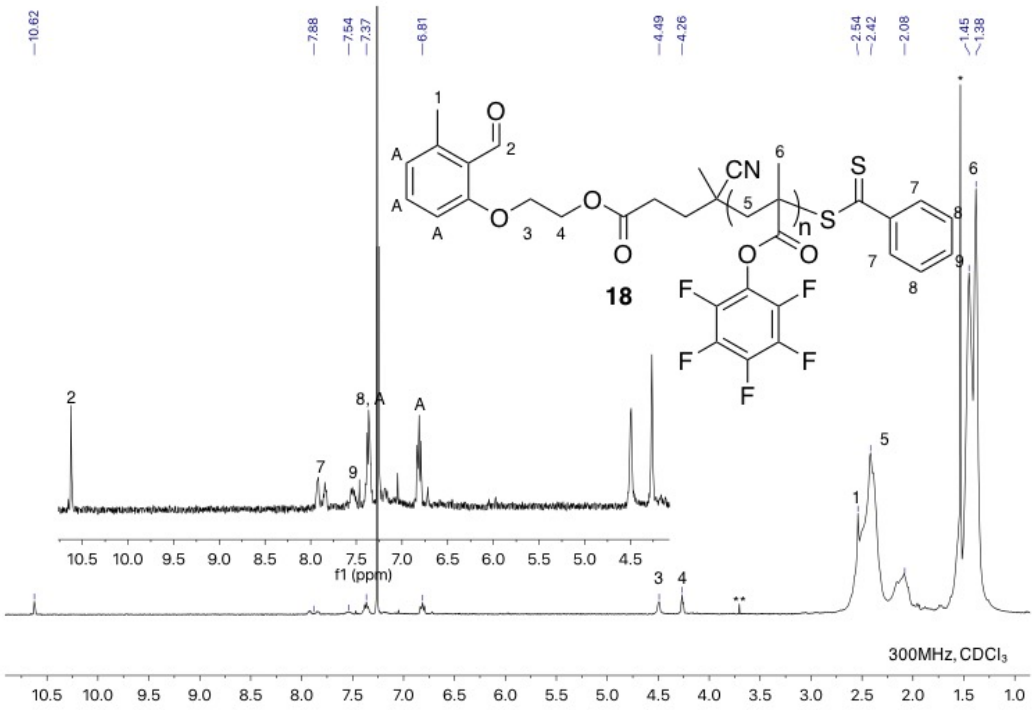


Polymer **18** was isolated as a light-pink powdery solid and the $^{1}$H NMR conveniently displayed both α and ω ends (**Figure 11**), along with features in the UV-Vis spectrum of **18** display consistent with the presence of chemical groups from **15** (**Figure 12)**.

**Figure 12**. Stack UV-Vis spectra of chain transfer agent **15** and linear telechelic polymer **18** in dichloromethane.

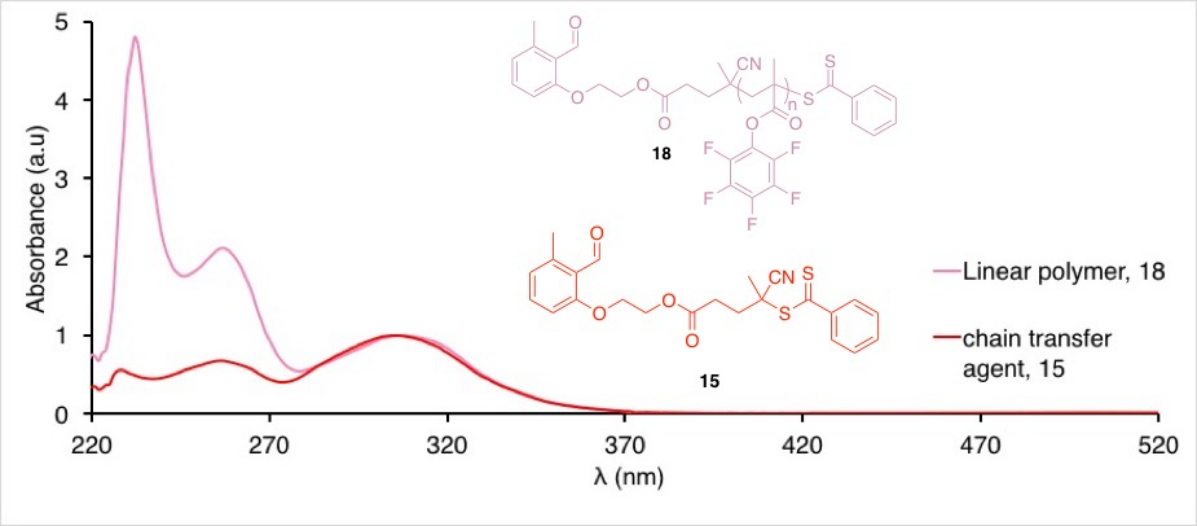


**Figure 11** shows the assignment of **18**. The chemical shifts of the end groups remain largely unchanged from the small molecule to the macromolecule and allowing for unambiguous assignment of **18**. Of note is the assignment of the ω *ortho*-protons; in the small molecule, it was a doublet which broadened out into a single peak in the polymer but for larger polymer lengths it appeared as two peaks centered around 7.88 ppm both in $(CD_3)_2CO$ and $CDCl_3$ NMR solvents. The chemical shift of the *ortho*-peak, as well as for all the end group peaks, did not change when acquiring a $^1H$ NMR in $(CD_3)_2CO$ on both 300 and 500 MHz field strength magnets.

**Table 3**. Coupling constants ($^4J_{HH}$) for ω *ortho*- protons measured by $^1H$ NMR spectroscopy.

| Polymer | Distance between peaks (Hz) for 300MHz field strength | Distance between peaks (Hz) for 500MHz field strength |
|---|---|---|
| **18h** | 26.43 | 29.64 |
| **18k** | 25.92 | 41.84 |
| **18k** | 34.54* | 54.63* |
| **18m** | 26.81 | 26.80 |

The splitting parameters (Hz) were determined in $CDCl_3$, * - $((CD_3)_2CO)$

The spacing in Hz between the *ortho* proton peaks on a 300 MHz and 500 MHz magnets shows little change for polymers **18h** and **18m**, but a larger change for **18k** in both NMR solvents. If the Hz value is the same, independent of field strength, then this indicates that the

two peaks are one peak split with a coupling constant of ~ 26 Hz – an uncommonly large value. A change with the field would indicate that these are two separate peaks. The results are ambiguous since polymers of different length indicate different changes. Further work is needed to elucidate the splitting of the *ortho*- peaks.

Gel permeation chromatography (GPC) traces were collected of linear polymers of **18** in THF and were used to corroborate the number of repeat units by comparing them against a ten-point polystyrene calibration standard. Using a UV-Vis detector (254 nm), the resultant traces show narrow monomodal distributions comparable to polystyrene standards (**Figure 13**) backing up the '*living*' character of the polymerization.

**Figure 13.** Polymer **18k** GPC trace showing a monomodal distribution and compared against polystyrene standards. $MW_n$ = 16300 g/mol, n = 63.

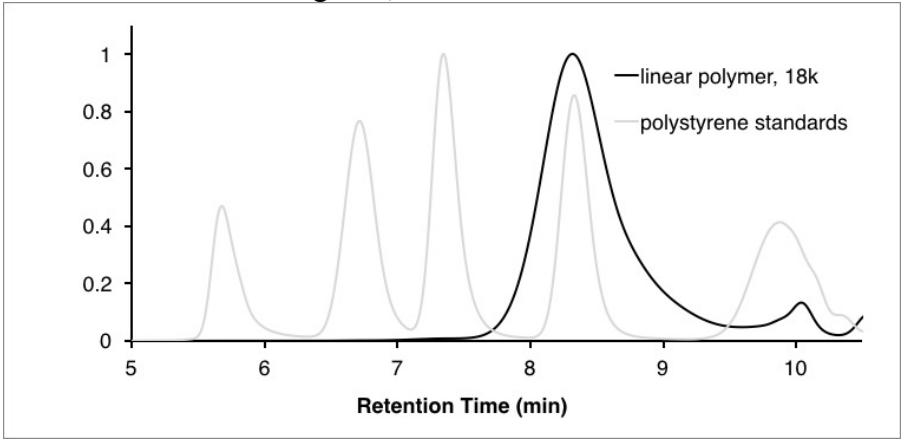


Investigation of the two methylene peaks at 4.50 and 4.27 ppm shows broadening upon polymerization from **15** as expected but in smaller polymers shows additional upfield broad peaks around 4.05 and 4.16 ppm (**Figure 14)**. Shorter polymers are expected to reveal independent chemical environments as more distinct because the shorter length contains less similar environments that would lead to broader spectra especially for polymers only 5 - 20 units in length.

**Figure 14**. Stacked $^{1}$H NMR spectra of **18g** ($n_{gpc}$ = 34) with upfield broad peaks and slide low molecular weight impurities. Polymer **18k** ($n_{gpc}$ = 73) with clean methylene region and monomodal GPC.

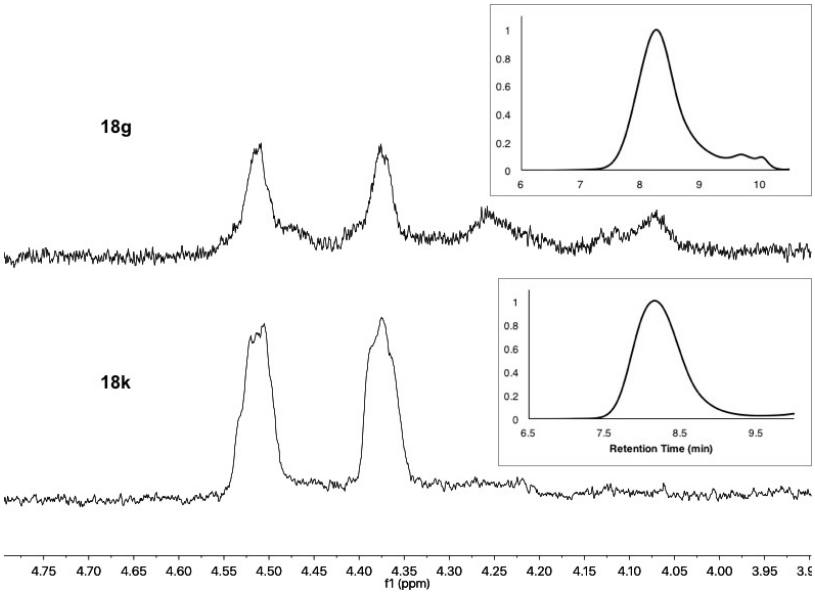


Polymer **18** was determined qualitatively to be soluble in 1, 4-dioxane, dichloromethane, tetrahydrofuran, chloroform, acetone, and diethyl ether and insoluble in dimethyl sulfoxide, dimethyl formamide, methanol, ethanol, pentane, hexane, acetonitrile, and water. **18** should be stored away from light and decomposition can be visually determined by a colour change from pink to yellowish-white (**Figure 15**).

**Figure 15.** $^{19}$F NMR spectra of **a**) decomposition after storage in THF, **b**) decomposition after storage on bench top with exposure to light, and **c**) polymer with end group integrity.

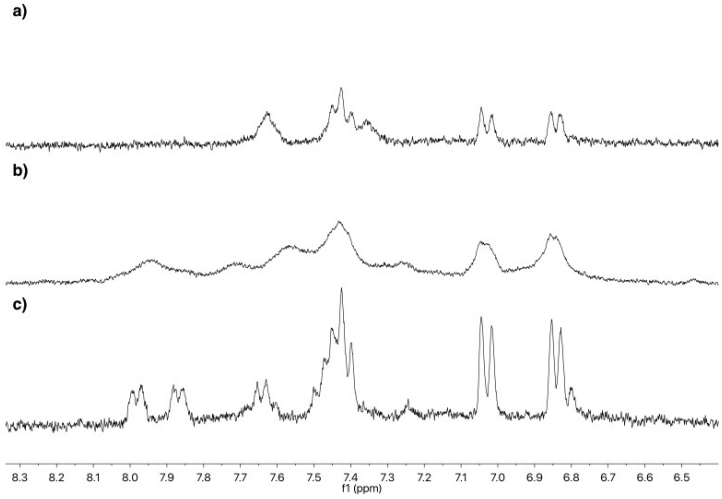

Polymer **18o** was stored in THF solvent at room temperature overnight away from light. The polymer retained its red colour but a change in the phenyl region of the dithiobenzoate occurred and it was unclear what change took place but it is advisable to store the polymer as a solid. This confirms literature precedent that storage of RAFT polymers with dithiobenzoates in THF leads to their decomposition.[91]

**Figure 16**. Proposed side-product isolated from supernatant followed by precipitation of **18** into methanol.

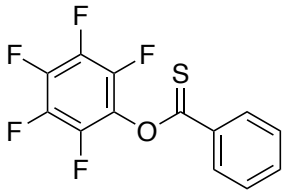


**19**

A $^{1}H$ and $^{19}F$ NMR spectra were collected of the supernatant once the polymer was isolated by precipitation. In all cases **1** was fully unconsumed as expected and $^{19}F$ NMR indicated pentafluorophenol suggesting that hydrolysis or decomposition of the monomer occurred either during the polymerization or work-up. In the $^{19}F$ NMR spectra of the supernatant mixture an additional set of peaks were also observed at -152.76, - 158.18, and -162.46 ppm attributed to an unknown impurity which was suspected to be **19**. The aromatic region of the $^{1}H$ NMR supernatant spectra was too messy to allow for assignment. Supernatants of polymers of $n_{expected} \leq 100$ contained **15**, either in-tact or as a decomposition product as determined by more than one aldehyde peak around 10.6 ppm. The solution was a red color that would turn orange or yellow either during or after rotoevaporation.

Polymer **18** was purified from the reaction mixture by dissolving in THF and adding drop-wise to a vigorously stirring solution of either hexanes, pentane, or methanol. Methanol

does not substitute the active ester and this was confirmed by the lack of peak at 3.6 ppm expected for the backbone methyl ester of poly(methyl methacrylate).

To investigate the end group fidelity the integrals of key signals in the $^{1}$H NMR spectra of the linear polymers were compared in **Table 4**. The integrals were determined by selecting identical regions for each designation and relative ratios for a given spectrum at the expected values confirm fidelity.

**Table 4**. Comparison of the end group integrals of select linear telechelic polymers ranging in molecular weight.

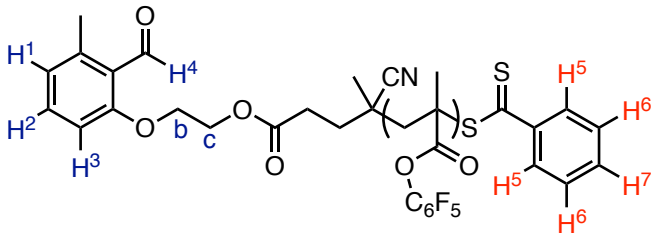


| Designation | | Integral | | | | | | | |
|---|---|---|---|---|---|---|---|---|---|
| | | **18b** | **18d** | **18g** | **18h** | **18i** | **18k** | **18o** | **Expected** |
| α | $H^4$ | 0.36 | 0.58 | 0.58 | 0.78 | 0.64 | 0.58 | 0.76 | 1.00 |
| | $H^3$ | 0.68 | 1.00 | 1.12 | 1.14 | 1.38 | 1.50 | 1.06 | 1.00 |
| | $H^1$ | 1.58 | 1.30 | 1.82 | 1.26 | 1.90 | 1.54 | 1.08 | 1.00 |
| | b | 2.00 | 2.00 | 2.00 | 2.00 | 2.00 | 2.00 | 2.00 | 2.00 |
| | c | 1.70 | 2.04 | 2.24 | 2.00 | 1.96 | 2.34 | 1.98 | 2.00 |
| ω | $H^5$ | 1.80 | 2.00 | 1.84 | 1.36 | 1.92 | 2.54 | 1.00 | 2.00 |
| | $H^7$ | 1.10 | 1.42 | 1.66 | 1.36 | 2.36 | 1.64 | 0.72 | 1.00 |
| | $H^6$ and $H^2$ | 3.14 | 3.42 | 3.32 | 2.26 | 3.52 | 3.72 | 2.40 | 3.00 |

The integrals indicated that the end groups were not present on the polymer in equal proportions. However, the small molecule chain transfer agent did not readily afford expected integrals as well and this might have arisen due to the impact of the quadrupolar $^{33}$S nucleus on the protons' T1 relaxation time (**Table 5**). The protons of a single end group have incongruent integrals for both the α and ω ends.

**Table 5**. Integrals of chain transfer agent **15** in $CDCl_3$.

| Designation | | Integral | Expected Integral |
|---|---|---|---|
| α | $H^4$ | 0.89 | 1.00 |
| | $H^3$ and $H^1$ | 2.18 | 2.00 |
| | b | 1.96 | 2.00 |
| | c | 2.00 | 2.00 |
| ω | $H^5$ | 2.22 | 2.00 |
| | $H^7$ | 1.30 | 1.00 |
| | $H^6$ and $H^2$ | 3.36 | 3.00 |

To inquire if the polymers indeed lacked end group fidelity, the D1 recycle delay in the $^1H$ NMR experiment was altered to see if any variation arose (**Fig. 18**). Since polymer chains have many possible conformations and tumble in solution with long correlation times (the average time for a molecule to rotate through one radian) they have very short T1 relaxation times, on the order of <1 second.[92] However, the end groups despite being a part of the polymer, have more dynamic freedom and potentially might have slightly longer relaxation times.

**Table 6**. Altered D1 recycle delay $^1H$ NMR experiment for **18p.**

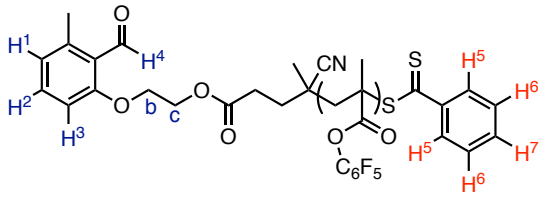


| Designation | | Integral Region | D1 Recycle delay (sec) | | | | Expected Integral |
|---|---|---|---|---|---|---|---|
| | | | 1 | 3 | 5 | 7 | |
| ω | $H^5$ | 8.03 .. 7.82 | 0.78 | 0.98 | 1.02 | 0.8 | 2 |
| | $H^7$ | 7.72 .. 7.57 | 1.52 | 1.52 | 2.18 | 1.62 | 1 |
| | $H^6 + H^2$ | 7.53 .. 7.36 | 3.12 | 3.44 | 3.52 | 3.04 | 3 |
| α | $H^1$ | 6.90 .. 6.79 | 1.12 | 1.26 | 1.62 | 1.2 | 1 |
| | $H^3$ | 7.08 .. 6.97 | 1.24 | 1.44 | 1.50 | 1.26 | 1 |
| | $H^4$ | 10.62 .. 10.55 | 1.34 | 1.46 | 1.56 | 1.36 | 1 |
| | b | 4.54 .. 4.48 | 2.00 | 2.00 | 2.00 | 2.00 | 2 |
| | c | 4.41 .. 4.34 | 2.08 | 2.4 | 2.08 | 2.04 | 2 |

In **Table 6** the D1 recycle delay was increased from 1 second to 3, 5 and 7 seconds. The protons part of a single end group still had incongruent integrals and results closest to the expected values occured at 7 seconds. Using integration in determining end group fidelity is limited because the peaks are broad with considerable overlap and were impacted by variations in the baseline in different parts of the spectrum. A T1 inversion recovery experiment was performed to determine the spin-lattice relaxation times and the results are summarized in **Table 7**.

**Figure 17**. Structure of proposed radical initiator **20**.

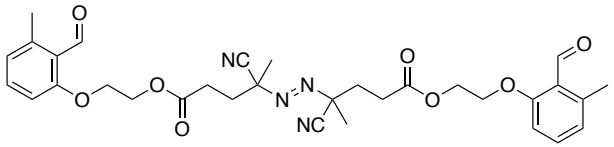


**20**

A consequence of using a radical initiator in RAFT is that a small number of chains at the α end will contain the 2-cyanopropanoic acid group. To overcome this, a potential approach would be to prepare the transesterification of 4, 4'-azobis(4-cyanopentanoic acid) with **11** to generate **20**. This approach[7] can be implemented with a Steglich Esterification and can help achieve greater end group fidelity in general for RAFT polymerization.

**Table 7**. T1 inversion recovery results for **18l**.

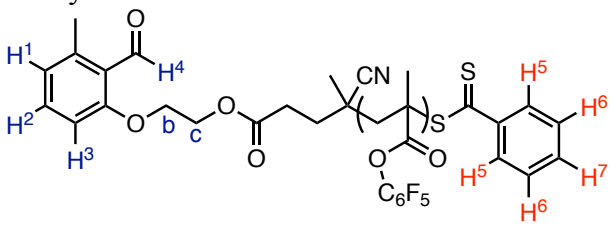


| Designation | Integral Region (ppm to ppm) | Spin-lattice relaxation time (T1) |
|---|---|---|
| $H^4$ | 10.624 to 10.574 | 3.5 s |
| $H^5$ | 8.051 to 7.860 | 2.2 s |
| $H^7$ | 7.730 to 7.609 | 2.1 s |
| $H^2$ + $H^6$ | 7.556 to 7.396 | 2.1 s |
| $H^3$ | 7.101 to 7.007 | 1.7 s |
| $H^1$ | 6.935 to 6.807 | 2.0 s |
| b | 4.580 to 4.498 | 875 ms |
| c | 4.441 to 4.359 | 701 ms |
| methylene backbone | 2.749 to 2.457 | 504 ms |
| methyl backbone | 1.763 to 1.378 | 298 ms |

The aldehyde peak has a very long relaxation time in comparison to the backbone signals but also in comparison to the methylene and aromatic signals of the same α end. For accurate integrals, the recycle delay was set to 5x the length of the longest T1 value to ensure all the nuclei have relaxed. When the D1 was optimized to 20 seconds the integrals of the end groups indicated that the polymerizations were occurring with end group fidelity.

**Figure 18**. $^{19}F$ NMR of **a**) **18o** in $(CD_3)_2CO$, **b**) **18** in $CDCl_3$, **c**) **1** in $CDCl_3$

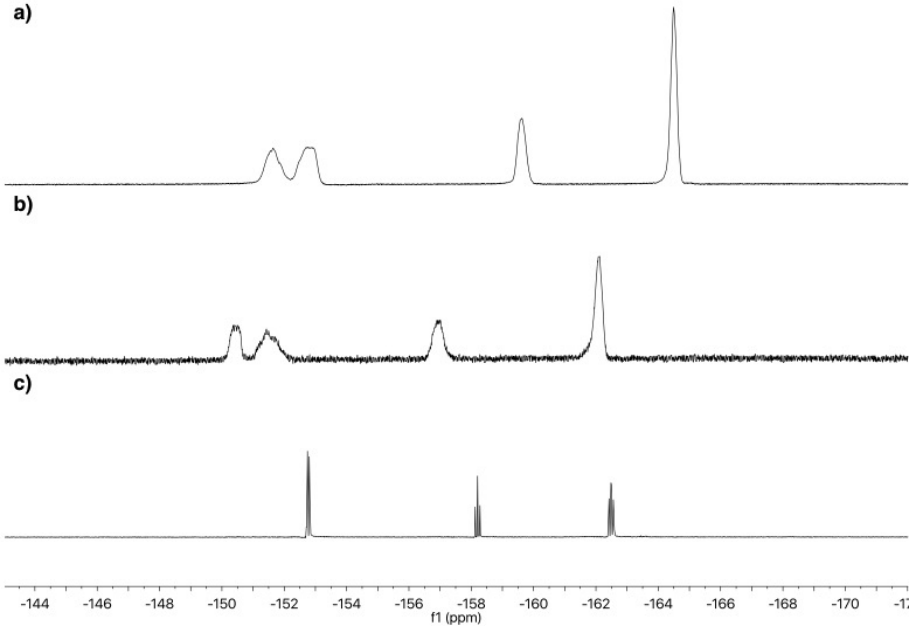


$^{19}F$ NMR was used to characterize the side groups of **18** and can be used to conveniently monitor substitution of the side groups. Upon polymerization, the three multiplets attributed to **1**, are shifted downfield and broaden out into four major peaks. (**Figure 18a, b**). The most downfield peaks at -150.90 ppm have additional splitting that was not expected but was presumed to appear similar in shape and breadth to the peak at -160.06 ppm.

**Figure 19**. **a)** different configurations indicating the chemical environments on **18 b**) **1**, **c**) pentafluorophenyl acrylate, **d**) pentafluorophenyl vinyl benzoate.

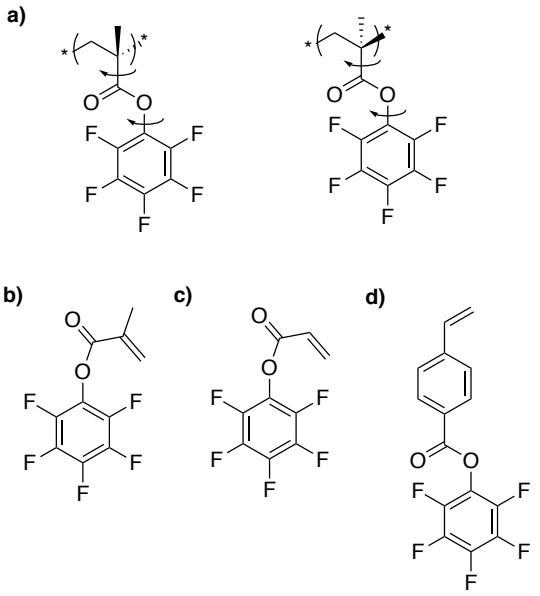


Other polymers bearing the pentafluorophenyl side group, such as poly(pentafluorophenyl acrylate) and poly(pentafluorophenyl 4-vinyl-benzoate) do not show this type of splitting pattern for the *ortho*-fluorine but a single broad peak.[81–85] It was suggested[83] that differences in the chemical environment for the *ortho*- fluorine atoms is due to the methyl group of the methacrylate backbone. When comparing the structure of the three monomers (**Fig. 19**) pentafluorophenyl methacrylate is best reflective of the compactness since the methyl group demonstrates the steric restriction imposed onto the rotation of the pentafluorophenol group about the $C_{Ar}$ - O bond. The chemical shift and splitting of this conformational effect can be probed by changing the NMR solvent. When the solvent was changed from $CDCl_3$ to $(CD_3)_2CO$ the two peaks had a slight change in shape, chemical shift, and integration. (**Fig. 18a)**. Relief of this steric strain might be an additional rationale for the reactivity of this active ester or conversely the sterics might make approach of the Bürgi – Dunitz angle more difficult during

nucleophilic acyl substitution and explain why **18** is less reactive than poly(pentafluorophenyl acrylate) towards primary amines.[79]

A VT NMR experiment was performed on **18l** from 263.0 K to 323.0 K in $CDCl_3$. As the temperature was lowered a downfield shift and peak broadening occurred for all the fluorine environments. The *meta*- peak appeared as two peaks that were significantly overlapping each other at lower temperature. As cooling occurred in this range, it appeared that a transition was occurring since the *ortho*- peaks were either coalescing or de-coalescing. The integral of this entire multiplet is 2 relative to the *para*- and *meta*- peaks, which were 1 and 2, respectively. Increasing the temperature range might give more insight into the transition occurring. Restriction of rotation was the cause of signal splitting since it could be probed by a VT experiment.

**Figure 20**. VT $^{19}F$ NMR of **18l** probing *ortho*- fluorine signal splitting.

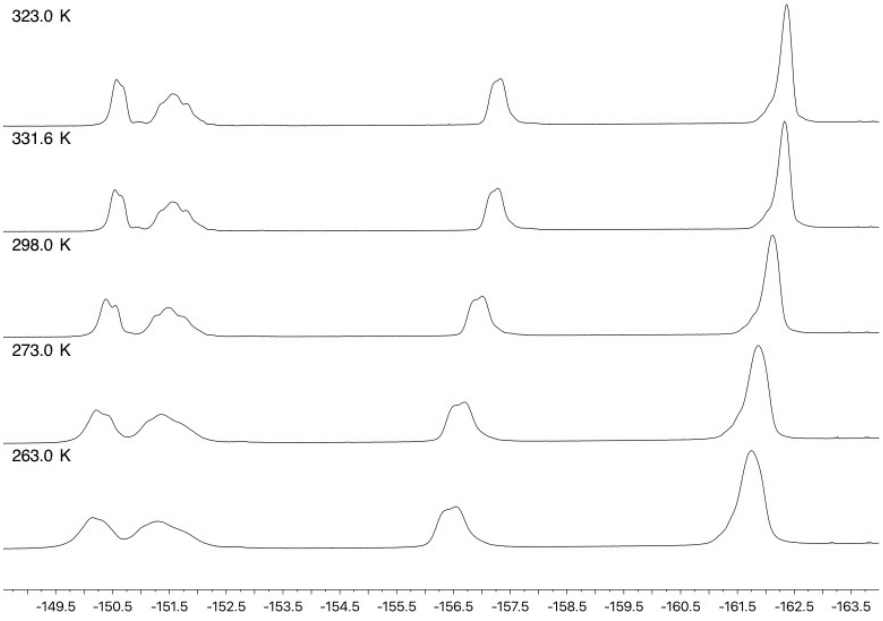

## 2.4 Synthesis of linear telechelic polymers of polystyrene and poly(methyl methacrylate)

**Scheme 5**. Synthesis of linear telechelic poly(methyl methacrylate) **21** and polystyrene **23**.

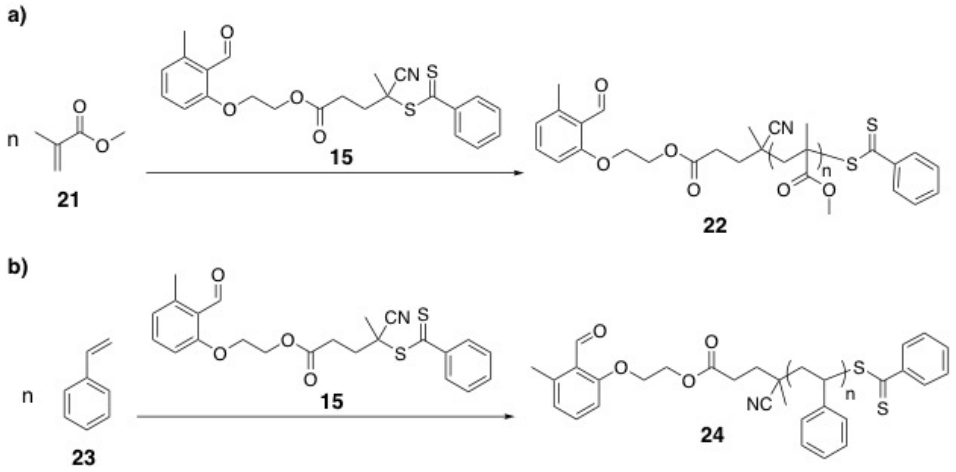


Linear telechelic polymers of polystyrene and poly(methyl methacrylate) bearing the same end groups and their cyclic counterparts have been previously reported.[46,47] They were prepared again in this work to aid as a template for the synthesis of cyclic poly(pentafluorophenyl methacrylate) (**Scheme 5**). The results are summarized in **Table 8**. These polymers were characterized by $^{1}$H NMR, UV-Vis spectroscopy, and GPC.

**Table 8**. Linear RAFT polymers of polystyrene and poly(methyl methacrylate) with varied molecular weights.

| Name | Expected (n) | $n_{NMR}$ ($CDCl_3$) | $n_{GPC}$ | % Yield (m/m) |
|---|---|---|---|---|
| **21a** | 28 | 28 | 16 | 27 |
| **21b** | 128 | 74 | 39 | 11 |
| **21c** | 40 | 92 | 47 | 30 |
| **21d** | 167 | 104 | 52 | 18 |
| **21e** | 90 | 114 | 97 | 27 |
| **21f** | 198 | 384 | 259 | 53 |
| **21g** | 221 | 696 | 274 | 44 |
| **23a** | 298 | 74 | 75 | 11 |
| **23b** | 297 | 27 | - | 1 |

The end groups of **18o** and **21** were very similar to each other's chemical shifts in $(CD_3)_2CO$ and $CDCl_3$. The only difference was in the *ortho*- proton peaks in PMMA it appeared as a singlet. See **Figure 21**. The polymer distributions were monomodal and the UV-Vis spectra contained a peak at 310 nm corroborating the end groups. The differences in the number of repeat units between techniques differ significantly but the most accurate value is obtained from the GPC since it was calibrated against a set of standards.

**Figure 21**. Stacked $^1H$ NMR spectrum in $(CD_3)_2CO$ of the **18o** (top) and **22c** (bottom) highlighting end group similarity between poly(pentafluorophenyl methacrylate) and poly(methyl methacrylate).

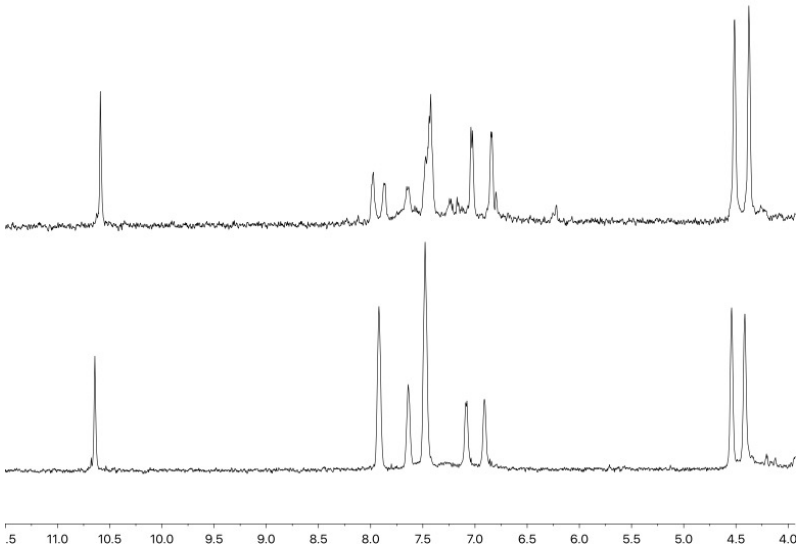


Following the synthesis and characterization of the linear telechelic polymers the materials were carried forward to cyclization with a UV source. The attempts, successful synthesis, and characterization of the cyclic polymers bearing active ester side groups is explored in the following chapter.

## 2.5 Experimental

### 2.5.1 Materials and Methods

All air sensitive compounds were handled using standard Schlenk line techniques (Ar) or in a $N_2$ filled glovebox (MBraun). $^1$H NMR spectra were collected on a 300 MHz Bruker Avance spectrometer with spectra referenced to residual solvent peaks.[93] UV-Vis spectra were collected using quartz cuvettes on a Helios Zeta UV-vis Thermo Scientific spectrophotometer from 190-600 nm, 2 nm bandwidth, 240 nm/min scan speed, and 1 nm data intervals using VISIONpro software. Gel permeation chromatography was performed on an Agilent 1100 Series with an Agilent PLgel 5μm MIXED-C column elution profiles were generated with THF or DCM (Sigma, HPLC grade) at 1 mL/min using ChemStation online and ChemStation offline software. A series of polystyrene standards were used to generate a 10-point calibration plot (Agilent). Solvents were removed using a rotoevaporator.

### 2.5.2 Syntheses

**Preparation of pentafluorophenyl methacrylate (PFMA) (1)**

PFMA was synthesized from pentafluorophenol (**17**) and methacryloyl chloride (**16**). To a 500 mL Schlenk flask 30 mL of anhydrous THF, pentafluorophenol (10.0 g, 0.054 mol), and triethyl amine (9.1 mL, 0.068 mol) were added and cooled to 0°C using an ice bath. While stirring, methacryloyl chloride (6.0 mL, 0.061 mol) in 30 mL anhydrous THF was added drop-wise over 1 h using a dropping funnel. After addition, the ice bath was removed and the contents were stirred overnight. The contents were filtered to remove the solid TEA•HCl salt and the THF solvent was removed. A slurry was made using silica and the contents were placed onto a silica column using dry loading. ca. 50 g of silica were used for 10 g of product with pentane eluent. $R_f$ = 0.45. The product was a clear to light yellow liquid. Yield 8.2 mL (60%). The NMR

characterization matched previous reports.[89] $^{1}$H NMR ($CDCl_3$, 300 MHz, 25°C) δ: 6.45 (s, 1H), 5.91 (s, 1H), 2.09 ppm (s, 3H); $^{19}$F NMR ($CDCl_3$, 282 MHz, 25°C) δ: -152.76 (d, 2F, $J_{FF}$ = 16.8 Hz, *ortho*-), -158.19 (d, 1F, $J_{FF}$ = 21.6 Hz, *para*-), -162.47 ppm (dd, 2F, $J_{FF}$ = 21.6 Hz, *meta*-).

**Preparation of prop-2-yn-1-yl-2-bromo-2-methyl-propanoate (PBIP) (2)**

The synthesis of **2** was adapted from Luedtke et al.[62] α-Bromo-isobutyryl bromide (1.25 mL, 0.01 mol) and anhydrous ether (4.5 mL, 0.04 mol) were added to a 50 mL Schlenk flask in the glove box. The flask was removed, placed on the Schlenk line, and cooled to 0°C using an ice bath. Propargyl alcohol (0.70 mL, 0.01 mol) in anhydrous ether (30 mL) and pyridine (0.97 mL, 0.01 mmol) was added and the ice bath was removed. The contents were stirred overnight. The resulting solution was washed with water, 5% sodium bicarbonate(aq), 10% HCl(aq), and brine. The remaining solvent was removed using a rotoevaporator and the product was stored at 10°C in a glass vial. $^{1}$H NMR ($CDCl_3$, 300 MHz, 25°C) δ: 4.76 (d, 2H, $J_{HH}$ = 2.4 Hz, -$CH_2$-), 2.51 (t, 1H, $J_{HH}$ = 2.3 Hz, $C_{sp}$-H), 1.97 ppm (s, 6H, -$(CH_3)_2$); $^{13}$C{$^{1}$H} NMR ($CDCl_3$, 75 MHz, 25°C) δ: 170.9 (-C(O)O-), 76.9 ($C_{sp}$), 75.5 (H-$C_{sp}$), 54.9 ($C_{4o}$), 53.5 ($CH_2$), 30.7 ppm ($(CH_3)_2$). FTIR (ATR) Abs: 3295 (≡C-H str), 2979 (C-H str), 2131 (C≡C str), 1737 cm$^{-1}$ (C=O str).

**Preparation of linear poly(pentafluorophenyl methacrylate) (4) via Atom Transfer Radical Polymerization (ATRP) with PMDETA and 2,2'-Bipyridine ligand**

To a 25 mL Teflon stoppered flask CuBr (0.02 g, 0.14 mmol), PMDETA (68 μL, 0.33 mmol), 1 (0.20 mL, 1.1 mmol), anhydrous anisole (0.40 mL, 3.7 mmol), and **2** (16 μL, 0.11 mmol) were added. The contents were subject to three freeze-pump-thaw cycles using liquid $N_2$ and the flask was placed into a preheated oil bath at 90°C for 5 h. The reaction was terminated by cooling in a liquid $N_2$ bath and exposed to oxygen. The contents were diluted with THF and filtered over a plug of neutral alumina to remove the copper catalyst. The THF was removed and

then diluted into 20 mL of methanol to precipitate the product. The entire mixture was centrifuged and the supernatant was decanted. The pellet was dissolved in THF, added drop-wise into a stirring solution of methanol (20 mL), centrifuged, and the supernatant decanted (this was repeated twice). The pellet was dried using a Schlenk vacuum overnight at room temperature. The stoichiometric amounts, temperature, and reaction times differ for other polymerizations. See **Table 9a-b**. Order of addition and work up remain the same. The same procedure is followed for the polymerizations with the addition of $CuBr_2$ with 2,2'-bipyridine. $^1$H NMR ($CDCl_3$, 300 MHz, 25°C) δ: 4.66 (s, 2H, $CH_2$), 2.36 (m, 2H, $CH_2$), 1.38 ppm (m, 2H, $CH_2$); $^{19}$F NMR ($CDCl_3$, 282 MHz, 25°C) δ: -150.4 to -151.5 (m, *ortho*-), -156.9 (br, *para*-), -162.0 ppm (br, *meta*-); FTIR (KBr pellet) Abs: 3316 (H-$C_{sp}$), 2991 (CH str), 2958 (CH str), 1778 (CO str), 1518 $cm^{-1}$ (C=C str).

**Table 9a**. Preparation of varied molecular weight poly(pentafluorophenyl methacrylate) 4 via ATRP with PMDETA and Cu(I)Br.

| Entry | Monomer: Initiator Ratio | Reagent Amounts | | | | | Time | Yield (m/m)% |
|---|---|---|---|---|---|---|---|---|
| | | **1**, mL | **2**, μL | Cu(I)Br, g | PMDETA, μL | Anisole, mL | | |
| 1 | 10:1 | 0.72 | 60.0 | 0.10 | 150 | 2.00 | 25 m | - |
| 2 | 10:1 | 0.20 | 16.1 | 0.048 | 68.8 | 0.40 | 5 h | 4 |
| 3 | 10:1 | 0.20 | 16.1 | 0.016 | 68.8 | 0.40 | 6 h | 20 |
| 4 | 10:1 | 0.20 | 16.1 | 0.016 | 68.8 | 0.40 | 48 h | 81 |
| 5 | 10:1 | 0.60 | 48.3 | 0.048 | 206 | 1.20 | 5 h | 20 |
| 6 | 10:1 | 0.60 | 48.3 | 0.048 | 206 | 1.20 | 14 h | 23 |
| 7 | 25:1 | 1.00 | 30.0 | 0.030 | 138 | 2.00 | 18 h | - |

Entries 1 and 7 were performed at 60°C. All other reactions were performed at 90°C

**Table 9b**. Preparation of varied molecular weight poly(pentafluorophenyl methacrylate) **4** via ATRP with 2,2'-bipyridine, Cu(I)Br, and Cu(II)$Br_2$

| Entry | Monomer: Initiator Ratio | Reagent Amounts | | | | | | Yield (m/m)% |
|---|---|---|---|---|---|---|---|---|
| | | **1**, mL | **2**, μL | Cu(I)Br, mg | $CuBr_2$, mg | Bipy, g | Anisole, mL | |
| 8 | 5:1 | 0.4 | 32 | 32 | - | 0.10 | 0.8 | 57 |
| 9 | 5:1 | 0.4 | 65 | 63 | 44 | 0.21 | 0.8 | 27 |
| 10 | 5:1 | 1.0 | 161 | 160 | 25 | 0.52 | 2.0 | 41 |
| 11 | 10:1 | 0.4 | 32 | 32 | - | 0.10 | 0.8 | 22 |
| 12 | 10:1 | 0.4 | 32 | 32 | 5 | 0.10 | 0.8 | 58 |
| 13 | 10:1 | 0.4 | 32 | 32 | - | 0.10 | 0.8 | 24 |
| 14 | 10:1 | 1.0 | 161 | 80 | 12 | 0.26 | 2.0 | 60 |
| 15 | 25:1 | 0.4 | 13 | 13 | 2 | 0.04 | 0.8 | 63 |

Entries 1 and 7 were performed at 60°C. All other reactions were performed at 90°C

**Preparation of azide substituted poly(pentafluorophenyl methacrylate) 7**

Poly(pentafluorophenyl methacrylate) **4** (43 mg, 2.1 mmol) was added with sodium azide (10 mg, 0.15 mmol) in DMF (1 mL) into a 20 mL scintillation vial. The contents were stirred overnight at room temperature. The DMF solution was added into a stirring solution of water (15 mL) to precipitate the product, the solid was centrifuged, the supernatant decanted, and dissolved into THF. The THF solution was added into a stirring solution of methanol (15 mL) to precipitate the product. The mixture was centrifuged followed by decanting of the supernatant. The purification with methanol solvent was repeated three times. The final product was dried on a Schlenk vacuum at room temperature overnight. Several sets of conditions for this reaction were tested and are summarized in **Table 10**. FTIR (KBr pellet) Abs: 2253 (R-$N_3$ str), 2137 (R-$N_3$ str), and 1700$cm^{-1}$ (C=O str).

**Table 10**. Azide substitution reaction

| Entry (**Table 9a-b**) | **4** : $NaN_3$ Molar Ratio | **4**, mg | $NaN_3$, mg | DMF, mL |
|---|---|---|---|---|
| 2 | 10:1 | 20 | 4450 | 1 |
| 8 | 14:1 | 43 | 10 | 1 |
| 9 | 5.0:1 | 110 | 10 | 1 |
| 10 | 6.4:1 | 115 | 10 | 1 |
| 12 | 5.0:1 | 91 | 5 | 1 |
| 13 | 22:1 | 21 | 10 | 1 |
| 15 | 5.0:1 | 100 | 10 | 1 |

**Preparation of 2-methoxy-6-methyl-benzaldehyde (9)**

The synthesis of **9** was adapted from Barner-Kowollik et al.[45] A 500 mL round bottom flask was charged with an acetonitrile/water mixture (1:1, 144 mL) and in the following order: 2, 3-dimethyl anisole **8** (2.0 g, 14 mmol), anhydrous copper sulfate (2.34 g, 14.7 mmol), and potassium peroxodisulfate (11.68 g, 63.20 mmol). The flask was equipped with a condenser and placed onto a preheated oil bath at 90°C. The contents were stirred for 1h, cooled to room temperature, and filtered over a plug of Celite to remove excess copper. Additional water (50 mL) was added and the mixture was extracted with dichloromethane (3 x 25 mL). The combined dichloromethane layers were dried ($Na_2SO_4$) and the solvent was evaporated to yield a dark yellow, viscous oil. Yield 2.0 g (93%). $^1$H NMR ($CDCl_3$, 300 MHz, 25 °C) δ: 10.64 (s, 1H), 7.38 (t, 1H, $J_{HH}$ = 8 Hz), 6.82 (dd, 2H, $J_{HH}$ = 9.2 Hz), 3.90 (s, 3H), 2.57 ppm (s, 3H).

**Preparation of 2-hydroxy-6-methylbenzaldehyde (10)**

In a 50 mL Schlenk flask, 10 mL of anhydrous dichloromethane and 6-methoxy-2-methylbenzaldehyde **9** (2.00 g, 13.8 mmol) were added and cooled to 0 °C. In a Teflon-plunger syringe $BBr_3$ (4.00 mL, 41.5 mmol) in 10 mL of anhydrous dichloromethane was cooled to 0°C and added drop-wise with careful venting of methylbromide. The ice bath was removed and the contents were stirred overnight. An excess of water (relative to $BBr_3$) was added to the mixture and allowed to stir for 20 min. The contents were filtered over Celite and stirred with $Na_2S_2O_3$ to

reduce any $Br_2$(l) generated. The mixture was dried ($Na_2SO_4$). The solvent was reduced and adark yellow viscous oil was recovered. Several sets of conditions for this reaction were tested, and these results are summarized in **Table 11** below. Yield 1.5 g (80%). $^1$H NMR ($CDCl_3$, 300 MHz, 25°C) δ: 11.90 (s, 1H), 10.33 (s, 1H), 7.38 (t, 1H, $J_{HH}$ = 8 Hz), 6.82 (d, 1H, $J_{HH}$ = 8 Hz), 6.72 (d, 1H, $J_{HH}$ = 7.1 Hz), 2.61 ppm (s, 3H).

**Table 11**. Preparation of 2-hydroxy-6-methylbenzaldehyde (**10**)

| Entry | mass of **9**, g | $AlCl_3$ (g)/ $BBr_3$ (mL) | DCM, mL | recovered mass, g | % yield |
|---|---|---|---|---|---|
| 1 | 0.51 | 1.35 | 10.6 | - | - |
| 2 | 1.06 | 2.81 | 15.2 | 0.46 | 48 |
| 3 | 2.10 | 5.62 | 30.0 | - | - |
| 4 | 2.00 | 3.00 | 20.0 | 0.61 | 33 |
| 5 | 1.90 | 3.00 | 20.0 | - | - |
| 6 | 1.90 | 3.00 | 20.0 | 2.30 | 134 |
| 7 | 3.87 | 6.00 | 40.0 | - | - |
| 8 | 1.50 | 3.00 | 20.0 | 2.59 | - |
| 9 | 1.95 | 3.75 | 20.0 | 1.90 | 108 |
| 10 | 2.18 | 4.20 | 20.0 | 1.80 | 91 |
| 11 | 2.08 | 4.00 | 20.0 | 0.90 | 48 |
| 12 | 0.90 | 2.00 | 20.0 | 0.44 | 54 |

**Preparation of 2-(2-hydroxyethoxy)-6-methylbenzaldehyde (11)**

In a 50 mL Schlenk flask 2-hydroxy-6-methylbenzaldehyde **10** (1.00 g, 7.34 mmol), $K_2CO_3$, (1.37 g, 9.98 mmol), and DMF (5 mL) were added sequentially. 2-Bromoethanol (0.42 mL, 5.9 mmol) was dissolved in DMF (2.2 mL) and added slowly drop-wise into the Schlenk flask. The flask was placed under static vacuum and then into a preheated oil bath at 95°C. The contents were stirred overnight. The reaction was quenched by adding water (8 mL) and stirring the reactions contents. The reaction mixture was transferred to a separatory funnel and extracted (20 mL x 5) with diethyl ether. The fractions were dried over $Na_2SO_4$ and the solvent was removed. Several sets of conditions for this reaction were tested, and these results are summarized in **Table 12** below. A bright yellow liquid was generated and purified by column

chromatography, dry loaded, (silica gel, petroleum ether/ethyl acetate 10:1 v/v). Yield = 0.66 g (50 %). $^1$H NMR ($CDCl_3$, 300 MHz, 25°C) δ: 10.64 (s, 1H), 7.35 (t, 1H, $J_{HH}$ = 9.2 Hz), 6.82 (m, 2H), 4.16 (t, 2H, $J_{HH}$ = 4.5 Hz), 3.99 (t, 2H, $J_{HH}$ = 4.9 Hz), 2.55 ppm (s, 3H).

**Table 12**. Preparation of 2-(2-hydroxyethoxy)-6-methylbenzaldehyde (**11**)

| Entry | **10**, g | 2-bromoethanol, mL | DMF, mL | mass of $K_2CO_3$, g | Time, h | Temp. (°C) | % yield |
|---|---|---|---|---|---|---|---|
| 1 | 1.30 | 0.55 | 7.0 | 1.80 | 71 | 25 | - |
| 2 | 2.00 | 1.22 | 10.3 | 8.20 | 48 | 70 | - |
| 3 | 0.50 | 0.24 | 20.0 | 1.60 | 22 | 70 | >99 |
| 4 | 0.50 | 0.211 | 4.0 | 0.70 | 41 | 25 | 76 |
| 5 | 0.36 | 0.15 | 3.0 | 0.50 | 18 | 90 | 87 |
| 6 | 1.80 | 0.76 | 14.4 | 9.48 | 22 | 90 | 66 |
| 7 | 0.34 | 0.16 | 3.0 | 0.46 | 27 | 105 | - |
| 8 | 0.90 | 0.38 | 7.1 | 1.24 | 18 | 90 | - |
| 9 | 0.43 | 0.21 | 14.0 | 0.60 | 18 | 95 | - |

**Preparation of 4-cyano-4-((thiobenzoyl)sulfanyl)pentanoic Acid (14)**

The synthesis of the chain transfer agent was adapted from Rizzardo et al.[75] To a Schlenk flask equipped with a condenser, bis(thiobenzoyl) disulfide (BTDS) (0.400 g, 0.131 mol) and anhydrous ethyl acetate (25 mL) was added. To the stirring solution 4,4'-azobis(4-cyanopentanoic acid) (ACPA) (0.549 g, 0.196 mol) was added and the contents were refluxed overnight for 19h. The reaction vessel was cooled and the solvent was removed. A red oil was recovered and dry loaded for purification by column chromatography (silica gel, ethyl acetate/hexanes 2:3 v/v). The fractions containing product were combined, the solvent was removed, and the oil was recrystallized from toluene at -10°C. Yield 0.71 g (93%). The product was a red solid. Several sets of conditions for this reaction were tested, and these results are summarized in **Table 13** below. $^1$H NMR ($CDCl_3$, 300 MHz, 25°C) δ: 7.91 (d, 2H $J_{HH}$ = 8.4 Hz), 7.57 (m, 1H), 7.40 (m, 2H), 2.73 (m, 4H), 1.94 ppm (s, 3H).

**Table 13**. Preparation of 4-cyano-4-((thiobenzoyl)sulfanyl)pentanoic Acid (**14**)

| Entry | BTDS, g | ACPA, g | ethyl acetate, mL |
|---|---|---|---|
| 1 | 0.21 | 0.28 | 4.00 |
| 2 | 0.38 | 0.50 | 8.00 |
| 3 | 0.30 | 0.55 | 8.00 |
| 4 | 0.40 | 0.55 | 25.00 |

**Preparation of 2-(2-hydroxythyl)-6-methylbenzaldehyde-4-cyano-4-((thiobenzoyl) sulfanyl) pentanoate (15)**

The synthesis of the chain transfer agent was adapted from Tang et al.[46] 2-(2-hydroxyethoxy)-6-methylbenzaldehyde **11** (83 mg, 0.508 mmol), 4-Cyano-4-((thiobenzoyl)sulfanyl) pentanoic acid **14** (120 mg, 0.430 mmol) were dissolved in anhydrous dichloromethane (4 mL) and cooled to 0 °C. *N*, *N*'-Dicyclohexylcarbodiimide DCC (180 mg, 0.860 mmol) and 4 – dimethylaminopyridine DMAP (11 mg, 0.086 mmol) were added in sequence. The ice bath was removed and the contents were stirred overnight at room temperature. The contents were further diluted with dichloromethane and washed with water (15 mL x 3). The organic layer was dried with $Na_2SO_4$ and the solvent was reduced to generate a bright red oil. The contents were purified by column chromatography (silica gel, first petroleum ether/ ethyl acetate 10:1 v/v to remove starting material, followed by petroleum ether/ ethyl acetate 1:1 v/v). Yield 0.19 g (12%). The product was a red oil. Several sets of conditions for this reaction were tested, and these results are summarized in **Table 14** below. $^1$H NMR ($CDCl_3$, 300 MHz, 25°C) δ: 10.65 (s, 1H, aldehyde), 7.91 (d, 2H, $J_{HH}$ = 7.7 Hz), 7.57 (m, 1H), 7.39 (m, 2H), 6.83 (t, 3H, $J_{HH}$ = 9 Hz), 4.52 (t, 2H, $J_{HH}$ = 4.6 Hz), 4.38 (t, 2H, $J_{HH}$ = 5.2 Hz), 2.69 (m, 4H), 2.57 (s, 3H), 1.94 ppm (s, 3H).

**Table 14**. Preparation of 2-(2-hydroxythyl)-6-methylbenzaldehyde-4-cyano-4-((thiobenzoyl) sulfanyl) pentanoate (**15**)

| Entry | **11**, mg | **14**, mg | DMAP, mg | DCC / EDC, mg | DCM, mL | Time, h | %, yield |
|---|---|---|---|---|---|---|---|
| 1 | 250 | 103 | 2.25 | 171 | 10 | 26 | - |
| 2 | 328 | 465 | 42 | 526 | 9 | 22 | - |
| 3 | 34.6 | 50.0 | 4.4 | 55.6 | 1.5 | 29 | 33 |
| 4 | 34.6 | 50.0 | 4.4 | 74.0 | 1 | 19 | 46 |
| 5 | 110 | 158 | 13.8 | 234 | 3.2 | 26 | 52 |
| 6 | 139 | 200 | 17.5 | 295 | 4 | 22 | 25 |
| 7 | 680 | 786 | 63 | 1140 | 7 | 18 | - |
| 8 | 83.0 | 120 | 11 | 860 | 9 | 21 | 12 |
| 9 | 24.0 | 113 | 5 | 846 | 10 | 18 | - |
| 10 | 321 | 432 | 38 | 640 | 10 | 19 | - |

DCC - *N*, *N*'-dicyclohexylocarbodiimide
EDC - 1-ethyl-3-(3-dimethylaminopropyl)carbodiimide

**Preparation of linear RAFT polymers (18)**

To a Schlenk flask monomer **1** (0.2 mL, 1.1 mmol), 1,4 – dioxane (0.15 mL, 1.7 mmol), and 2, 2'-azobis(isobutyronitrile) (AIBN) (1.0 mg, 6.0 mmol), and **15** (26 mg, 0.06 mmol) were added in sequence. The contents were subject to 4x freeze-pump-thaw cycles using liquid $N_2$. The flask was placed into a preheated oil bath and stirred for the specified time. The reaction flask was cooled to room temperature and the solvent was removed. The contents were dissolved in a minimal amount of THF and added drop-wise into a stirring solution of hexanes (15 mL) to precipitate the product. The mixture was centrifuged and the supernatant was decanted to isolate the product pellet. The purification steps were repeated for a total of three times and each time a minimal amount of THF was used to dissolve the pellet. The pellet was dried on a Schlenk line vacuum overnight at room temperature. Several sets of conditions for this reaction were tested, and these results are summarized in **Table 15** below.

**Table 15**. Preparation of telechelic RAFT polymers (**18**)

| Name | $n_{expected}$ | **1**, mL | **15**, mg | AIBN, mg | solvent, mL | Temp. (°C) | % Yield |
|---|---|---|---|---|---|---|---|
| **18a** | 5 | 0.05 | 24.9 | 1.8 | 0.50 | 105 | 16 |
| **18b** | 10 | 0.06 | 15.6 | 1.2 | - | 110 | 87 |
| **18c** | 12 | 0.11 | 22.5 | 1.7 | 0.50 | 110 | - |
| **18d** | 12 | 0.06 | 11.5 | 0.5 | 0.50 | 110 | 23 |
| **18e** | 17 | 0.15 | 15.3 | 1.0 | 0.50 | 110 | 44 |
| **18f** | 19 | 0.20 | 26.4 | 0.6 | 0.15 | 105 | 26 |
| **18g** | 20 | 0.28 | 35.2 | 2.6 | 0.30 | 105 | 64 |
| **18h** | 20 | 0.10 | 12.2 | 0.7 | 0.50 | 110 | 59 |
| **18i** | 22 | 0.30 | 33.1 | 0.4 | 0.10 | 110 | 54 |
| **18j** | 24 | 0.28 | 28.5 | 1.7 | - | 105 | 53 |
| **18k** | 26 | 0.25 | 23.7 | 2.5 | 0.30 | 105 | 82 |
| **18l** | 27 | 0.29 | 26.1 | 0.4 | 0.22 | 105 | 29 |
| **18m** | 29 | 0.46 | 24.2 | 2.8 | 0.50 | 110 | 51 |
| **18n** | 31 | 0.30 | 23.8 | 1.4 | 0.40 | 105 | - |
| **18o** | 33 | 0.20 | 14.7 | 0.3 | 0.50 | 110 | 70 |
| **18p** | 37 | 0.40 | 26.6 | 1.0 | 0.30 | 105 | 43 |
| **18q** | 98 | 0.52 | 13.1 | 1.0 | - | 110 | 63 |
| **18r** | 133 | 1.36 | 25.1 | 1.9 | - | 90 | 83 |
| **18s** | 133 | 1.36 | 25.1 | 1.9 | - | 90 | 112 |

# 3. Synthesis of cyclic polymers

## 3.1 Introduction

This chapter will explore the attempts, synthesis, and characterization of cyclic polymers. Amongst the methods available to synthesize cyclic polymers the α, ω ring closing method by means of a selective 'click' reaction of the end groups was attempted.[5] The difficulty in synthesizing cyclic polymers comes down to overcoming entropy to achieve intramolecular ring-closure with a relatively large distance between the reacting functional groups. This is achieved through large dilutions, on the order of $10^{-8}$ to $10^{-6}$ M, which minimizes intermolecular reactivity between chains and can be performed either through diluting with large amounts of solvent or through a continuous addition method.[94] The next arising obstacle is in characterization of the cyclic species to confirm its cyclic topology. Compared to other polymeric nanomaterials, such as micelles, vesicles and colloids, cyclic homopolymers are mono-molecular entities and require both small molecule and macromolecular characterization techniques.

$^{1}H$, $^{19}F$ NMR, diffusion-ordered NMR spectroscopy, gel permeation chromatography (GPC), UV-Vis spectroscopy, and fluorescence spectrometry were used to characterize the attempted and synthesized cyclic polymers. Any one piece of data collected on its own is insufficient to draw the conclusion that ring closure occurred but data taken together can corroborate the assignment of cyclic structure.

The UV-catalyzed hetero Diels-Alder (HDA) 'click' reaction was chosen to close off the ring because it did not require additional reagents, is fast, has a precedent for making block copolymers[43] and other cyclic polymers[46–48], and the product can be conclusively characterized by $^{1}H$ NMR spectroscopy. The HDA occurs between the carbon sulfur double bond dienophile (ω, **Fig. 1**) and the orthoquinodimethane (α*, **Fig. 1**) generated by irradiation of the *ortho*-

methylbenzaldehyde (α, **Fig. 1**).[42,43,45,95] The success of this reaction is based on the favourable orbital overlap between reactants as a result of a small frontier molecular orbital gap.[45] The electronic requirements are met for the diene because the electron withdrawing phenyl group lowers the HOMO of the dithioester and allows the reaction within a practical laboratory time period.[45] The isothiochroman group is the product of this reaction.

**Figure 1**. Hetero Diels-Alder (HDA) 'click' reaction mechanism.

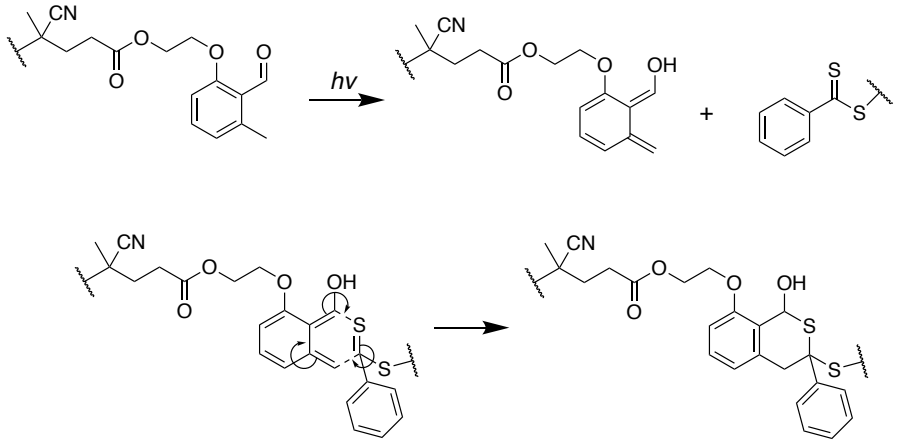


The $^{1}$H NMR spectra of cyclic polymers are expected to show an upfield shift of the aromatic protons, which can be compared to previous reports for this reaction.[45] The methylene peaks are expected to show a broadening because of incorporation into the ring. The methylenyl protons are part of the end groups, which possess more dynamic freedom compared to the rest of the polymer. Upon incorporation, their freedom is limited compared to that of the rest of the polymer chain which results in broader peaks. The aldehyde peak at 10.64 ppm and the methyl at 2.56 ppm are expected to disappear and two new peaks are expected for the tertiary carbon and alcohol protons of the isothiochroman group.[45,46] The methylene and methyl backbone peaks along with the broad fluorine peaks in the side group of the $^{19}$F NMR spectroscopy are expected to remain unchanged.

In the UV-Vis spectrum, disappearance of the peak at 315 nm is expected, which would indicate that both α and ω end groups have been consumed.[46] The consumption of the peak at 506 nm attributed only to the carbon sulfur double bond is expected and visually the colour of the polymeric solid is expected to transform from a light pink to white. The GPC trace is expected to show a shift towards longer retention time as the apparent size in solution will decrease.[46–48,65,96] The distribution of molecular weights is expected to remain unchanged as the polymers are reacting only with themselves. Diffusion NMR spectroscopy is expected to show an increase in the diffusion coefficient (d, [$m^2/s$]) since the particles are moving more quickly through solution because of their decreased size. The change in diffusion coefficient and apparent molecular weight, based on retention time, is expected to be on the order of 10 - 20% based on previous reports[97,98] and computational models[99,100].

Following the synthesis of the cyclic polymers they were modified with a fluorescent phenanthridyl reporter molecule from which emission can be seen in solution. The emission spectrum is expected to show a larger intensity compared to a similarly modified linear polymer because the restricted motion has fewer non-radiative modes of decay and the fluorophores are more isolated due to the rigidity of the cycle leading to less aggregation-caused self-quenching.[10] Additionally, this confirms cyclic integrity following Post polymerization modification (PPM).[101]

The following sections will explore how the HDA reaction was optimized using different emitting light sources starting with a broadband UV low-pressure mercury lamp, UV lamp with $\lambda_{max}$ = 365 nm, and finally the UVB Comedico Arimed B6 $\lambda_{max}$ = 320 nm.

## 3.2 Irradiation Experiments using a broadband UV low-pressure mercury lamp

Once the linear polymers were synthesized, initial attempts at the HDA were made in a fused silica quartz vessel using a broadband spectrum UV low-pressure mercury lamp. The solutions were degassed and both linear poly(methyl methacrylate) (PMMA) and poly(pentafluorophenyl methacrylate) (pPFMA) cyclization reactions were attempted. The attempts were performed on small scales and characterized either with $^{1}H$ and $^{19}F$ NMR or GPC. Cyclic PMMA was previously reported using the end groups in this work and since both polymers have methacrylate backbones it was presumed that both would require similar irradiation conditions.[46] If the conditions using the mercury lamp for PMMA were uncovered first then they could be used as a guide for pPFMA.

**Table 1.** Hetero Diels-Alder reaction using a broadband UV low-pressure mercury lamp

| Polymer | Entry | Linear, n | | Conc. (mg/L) | Irradiation Time (h) | Vessel | Solvent |
|---|---|---|---|---|---|---|---|
| | | $n_{nmr}$ | $n_{GPC}$ | | | | |
| pPFMA | **1** | 22 | - | 156 | 3 | quartz | AN/$CHCl_3$ |
| pPFMA | **2** | 35 | 38 | 145 | 3 | quartz | AN/$CHCl_3$ |
| pPFMA | **3** | 35 | 38 | 433 | 3 | quartz | AN |
| PMMA | **4** | 43 | 16 | 219 | 2 | quartz | DCM |
| PMMA | **5** | 43 | 16 | 189 | 2 | quartz | DCM |
| PMMA | **6** | 43 | 16 | 131 | 23.5 | quartz | DCM |
| pPFMA | **7** | 161 | 155 | 120 | 1 | quartz | DCM |
| PMMA | **8** | 30 | - | 44 | 27 | Pyrex | AN:DCM(2:1) |
| PMMA | **9** | 30 | - | 47 | 18 | Pyrex | AN:DCM(2:1) |
| PMMA | **10** | - | 2 | 500 | 20 | Pyrex | DCM |
| pPFMA | **11** | 52 | 73 | 102 | 20 | Pyrex | DCM |
| PS | **12** | 36 | 76 | 50 | 3 | Pyrex | AN:DCM(2:1) |

Dichloromethane eluent at 1 mL/min. Number average molecular weight was determined with a five point polystyrene calibration standard. Distance from lamp: 5.5 cm. DCM - dichloromethane, AN - acetonitrile, $CHCl_3$ - chloroform.

After irradiation of the quartz glassware the initial material collected was yellow and odorous indicating that parts of the macromolecules were breaking down and were most likely

arising from the end groups. The $^{1}$H NMR of **Entries 1-3** showed lots of unidentified impurities, residual solvent peaks, and the disappearance of the end groups (**Fig. 2**).

**Figure 2.** $^{1}$H NMR spectra of three pPFMA polymers following irradiation with a broadband UV low-pressure mercury lamp.

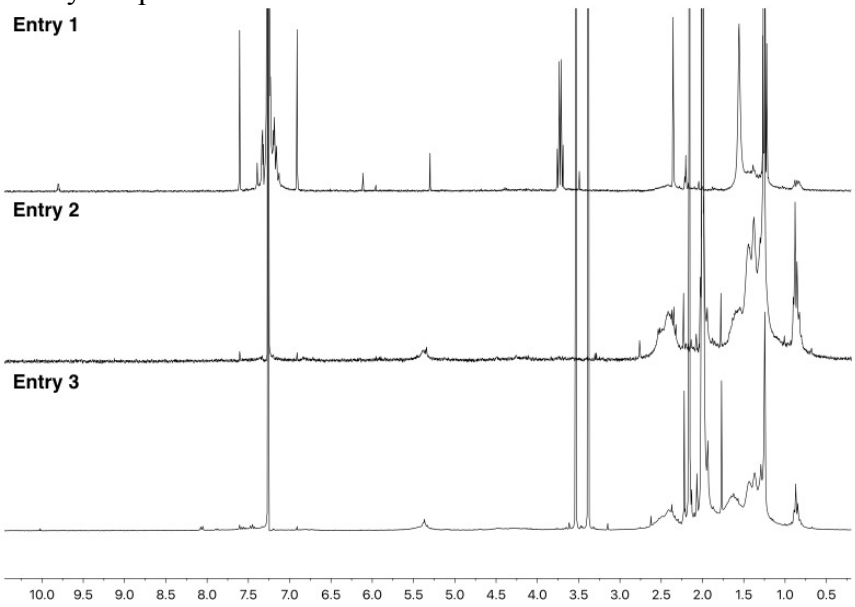


**Figure 3.** Stacked GPC trace of an n = 16-mer PMMA telechelic polymer, **Entry 6**, and decomposition products after irradiation with a mercury lamp in a quartz vessel.

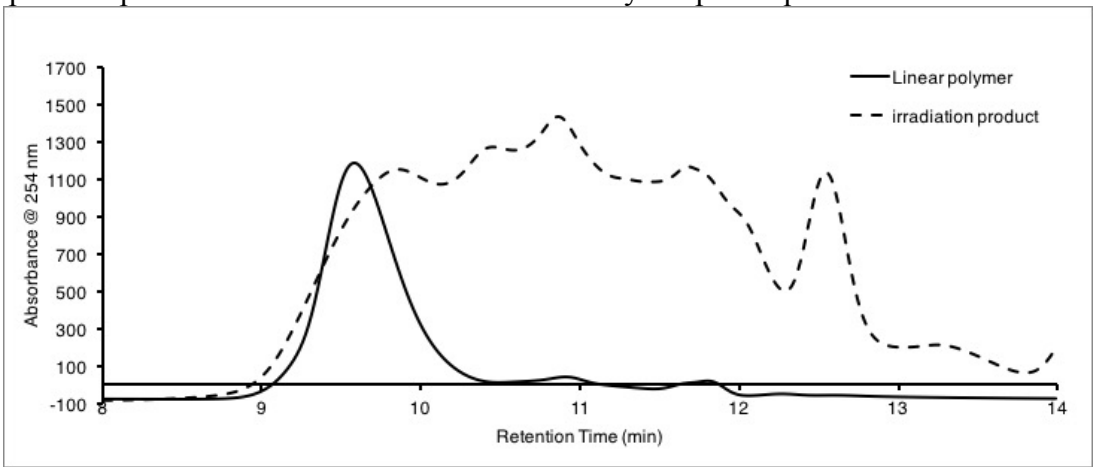


The GPC traces showed multiple peaks at longer retention time indicating breakdown of the polymer (**Fig. 3**). The short wavelengths of the UV mercury lamp were suspected to provide sufficiently high energy (200 nm) to break the carbon-carbon bonds of the backbone. To mitigate

this the irradiation vessel was switched from quartz to Pyrex to filter the high energy wavelengths.

**Figure 4**. Stacked GPC trace of an n = 30-mer telechelic PMMA polymer, **Entry 8**, and decomposition products after irradiation with a mercury lamp in a Pyrex vessel showing linear polymer and irradiation product.

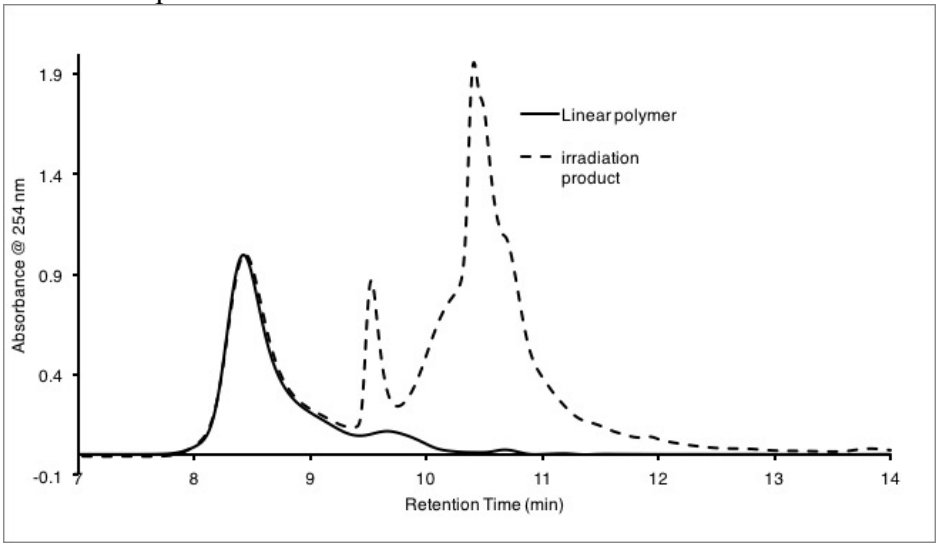


The GPC traces showed improvement but small molecular weight impurities were still present. The first peak belonging to the polymer showed no change in retention and only side reactions were occurring because of the reaction conditions (**Fig. 4**, dotted trace). The $^{1}$H NMR spectrum showed consumption of the end groups along with many unidentified broad and narrow peak impurities (**Fig. 5**).

**Figure 5**. $^{1}H$ NMR of telechelic PMMA polymer after irradiation in a Pyrex vessel with a low-pressure mercury lamp of **Entry 10** ($CDCl_3$, 300 MHz).

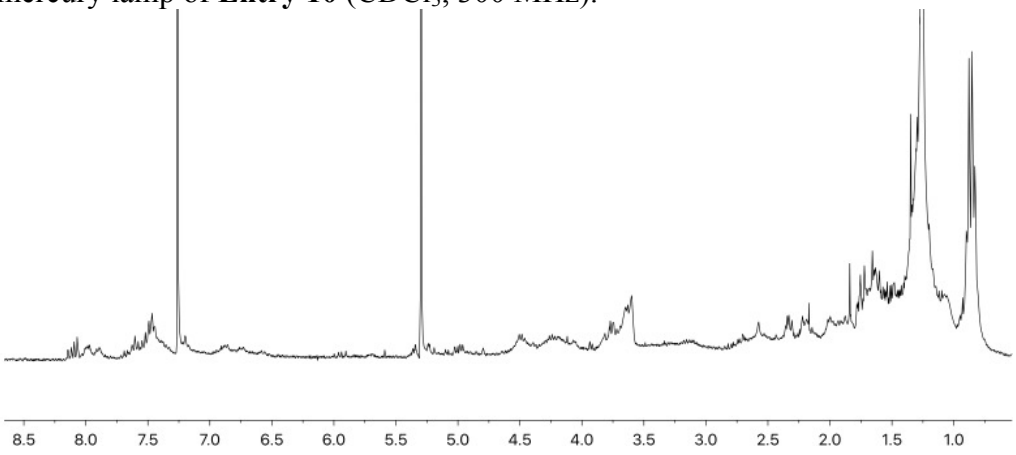


The pPFMA $^{19}F$ NMR of the irradiation products in quartz were unchanged from the linear polymer (**Fig. 6**) indicating preservation of the active ester. The $^{1}H$ and $^{19}F$ NMR of lone monomer was unchanged after irradiation as well.

**Figure 6**. $^{19}F$ NMR spectra of an n = 38-mer pPFMA telechelic polymer after irradiation with a low-pressure mercury lamp in a quartz vessel. **Entry 2, Table 1** in ($CDCl_3$, 300 MHz).

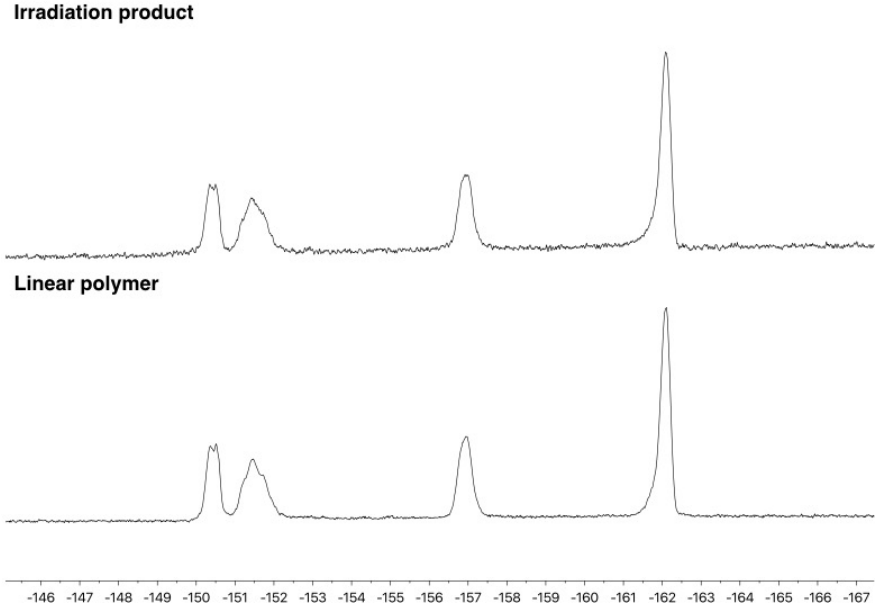


Similarly, telechelic polystyrene **Entry 12** was irradiated using the broadband UV mercury lamp source. The end groups appeared to be largely unchanged and unidentifiable impurities started to appear throughout the $^{1}H$ NMR spectrum. From the three different

polymers, it was determined that the broadband UV low-pressure mercury lamp causes undesirable side reactions and was incapable of driving the HDA reaction forward. A UVA lamp emitting at a maximum wavelength of 365 nm was used as the next light source and the reactions performed are summarized in **Table 2**. All reactions were degassed by bubbling with argon, and monitored by GPC.

**Figure 7**. Photoactive polystyrene **2** irradiated with a low-pressure mercury lamp in a Pyrex vessel. Stacked $^{1}$H NMR spectra linear polymer (top) and irradiation product (bottom) **Entry 12**. ***** unidentified impurities.

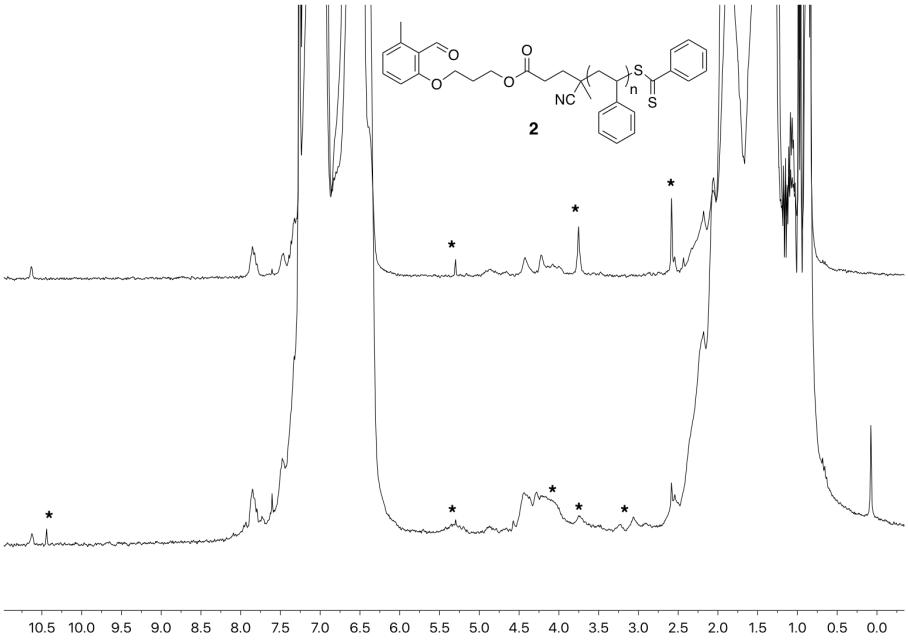

## 3.3 Irradiation experiments using a UVA lamp source with $\lambda_{max}$ = 365 nm

**Table 2**. Irradiation reactions involving light source at $\lambda_{max}$ = 365 nm.

| Entry | Linear, n | | Concentration (mg/L) | Irradiation Time (min) | $MW_{n,cyclic}/MW_{n,linear}$ | Solvent |
|---|---|---|---|---|---|---|
| | $n_{nmr}$ | $n_{GPC}$ | | | | |
| 1 | 240 | 195 | 34 | 30 | 1.08 | DCM |
| 2 | 240 | 195 | 34 | 30 | 0.97 | DCM |
| 3 | 240 | 195 | 34 | 15 | - | DCM |
| 4 | 240 | 195 | 34 | 30 | - | AN:DCM(2:1) |
| 5 | 240 | 195 | 34 | 30 | - | DCM |
| 6 | 240 | 195 | 34 | 30 | - | DCM |
| 7 | 240 | 195 | 34 | 30 | - | AN:DCM(2:1) |
| 8 | 240 | 195 | 850 | 30 | 1.04 | DCM |
| 9 | 35 | 38 | 74 | 30 | 1.43 | DCM |
| 10 | 70 | 73 | 92 | 30 | 1.31 | DCM |
| 11 | 161 | 155 | 93 | 30 | 1.14 | DCM |
| 12 | 240 | 195 | 33 | 45 | 1.99 | AN:DCM(3:1) |
| 13 | 240 | 195 | 33 | 45 | 2.09 | AN:DCM(7:1) |
| 14 | 240 | 195 | 8 | 45 | 1.98 | AN:DCM(7:1) |

Dichloromethane eluent at 1 mL/min. Number average molecular weight was determined with a five point polystyrene calibration standard. DCM - dichloromethane, AN - acetonitrile. Distance from lamp: 13 cm. All Entries are pPFMA.

A ratio above 1.00 of the number average molecular weights indicates that a reaction did occur. Ratios equal to 2 indicate condensations (linking between two polymers), ratios lower than 2 and greater than 0.90 indicate that the polymers were altered but $^{1}$H NMR did not reveal any information that might hint at what changes occurred because of insufficient amounts of polymer available for the NMR experiments, and because of the large size of the polymer, the end groups were in significantly smaller molar amounts than the side groups. Additionally, it was found that running the columns with dichloromethane solvent led to the same samples eluting at different retention times. Significant impurities comparable in amount to the polymer were found in all the entry traces (**Figure 9**).

**Figure 8**. GPC trace of an n = 200 pPFMA telechelic polymer showing significant lower molecular weight impurity (*) after irradiation of **Entry 5** with a UV lamp ($\lambda_{max}$ = 365 nm) in a Pyrex vessel

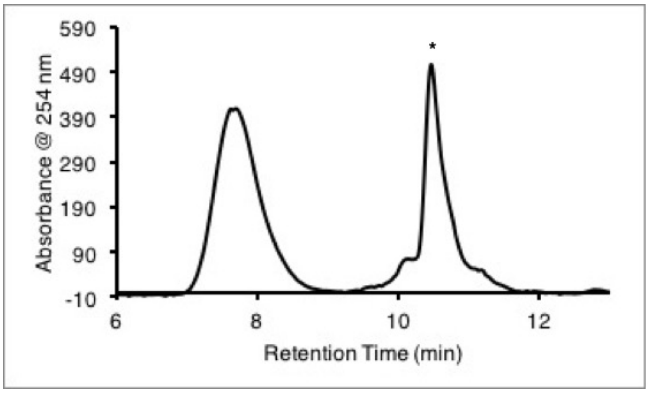


It was determined in **Entries 4**, **7**, **12 – 14** that a reaction was occurring at the end groups since shouldering peaks were forming (**Fig. 9**). Compared to the other entries **4**, **7**, **12-14** contained acetonitrile solvent and this agreed with previous reports of solvent choice for the HDA.[46–48] Linear pPFMA had poor solubility in acetonitrile and it was avoided as much as possible but this was overcome by adding dichloromethane to aid in the solubility.

**Figure 9**. GPC trace of **Entry 10** an n = 73-mer pPFMA telechelic polymer showing significant lower molecular weight impurity (*) and higher molecular weight shoulder peak (arrow) after irradiation with a UV lamp ($\lambda_{max}$ = 365 nm) in a Pyrex vessel.

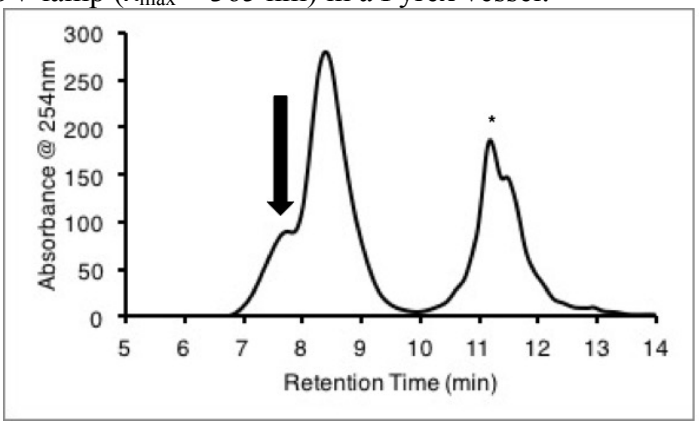


The experimental setup involving the light source with $\lambda_{max}$ = 365 nm was not capable of irradiating larger amounts of polymer or stirring the reaction contents. Despite some reactivity being achieved this reaction setup was surpassed with a UVB Comedico Arimed B6 lamp with

an emission maximum at 320 nm. This light source was previously reported and had significant overlap with the broad absorbance peak of the *ortho*-methylbenzaldehyde at 315 nm.[45]

## 3.4 Irradiation experiments using a UVB Comedico lamp with $\lambda_{max}$ = 320 nm

To confirm if the photoenol could be accessed with the Comedico lamp an irradiation experiment was performed to substitute the *ortho*-methyl with deuterium. In this experiment degassed solvent, *ortho*-methylbenzaldehyde **3**, and deuterium oxide were irradiated for 30 minutes.[50] After working up the reaction, an NMR of the material revealed that the *ortho*-methyl had become deuterated by its disappearance from the spectrum. See (**Fig. 10**). This reaction proved that the lamp could generate the photoactive diene.

**Figure 10**. Accessing the photoenol; deuterated *ortho*-methyl of *ortho*-methylbenzaldehyde after irradiation with Comedico lamp. $^1$H NMR of the starting material **3** (top) and deuterated product **4** (bottom). * residual solvent. ‡ indicates NMR solvent. Dotted box highlights the *ortho*-methyl peak.

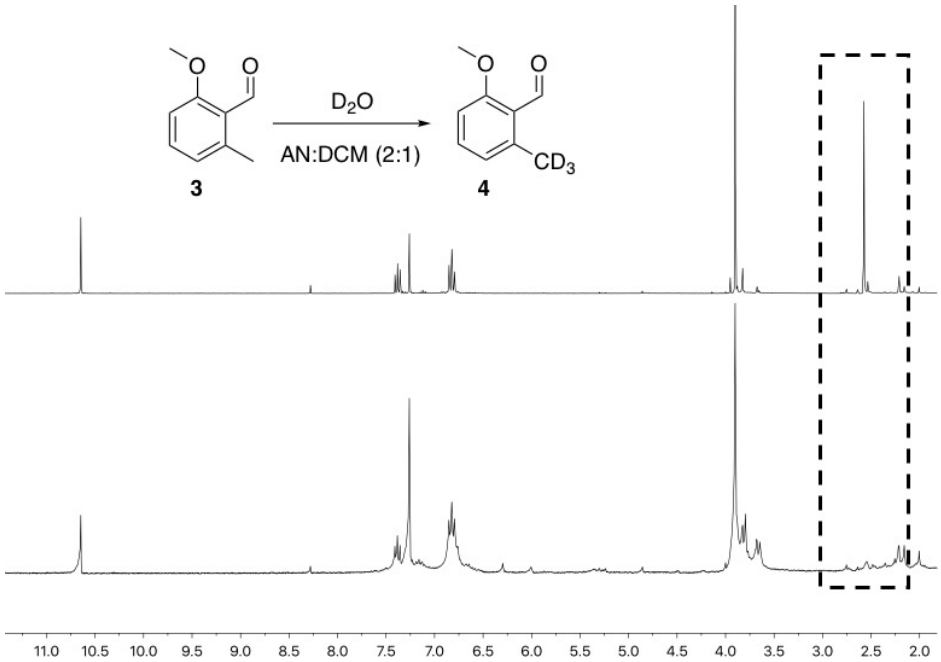

**Table 3**. Irradiation reactions with Comedico lamp.

| Entry | $n_{nmr}$ | $n_{GPC}$ | Concentration (mg/L) | Irradiation Time (min) | Solvent | $O_2$ present |
|---|---|---|---|---|---|---|
| 1 PS | 79 | 76 | 8 | 900 | AN:DCM(2:1) | yes |
| 2 PS | 30 | - | 700 | 180 | AN:DCM(2:1) | no |
| 3 PMMA | 43 | 16 | 700 | 180 | AN:DCM(2:1) | no |
| 4 PMMA | 43 | 16 | 26 | 360 | AN:DCM(2:1) | no |
| 5 pPFMA | 240 | 209 | 31 | 540 | AN:DCM(1:1) | no |
| 6 pPFMA | 240 | 209 | 30 | 540 | AN:DCM(2:1) | no |
| 7 pPFMA | 240 | 209 | 30 | 540 | AN:DCM(3:1) | no |
| 8 pPFMA | 240 | 209 | 683 | 180 | AN:DCM(2:1) | no |
| 9 pPFMA | 240 | 209 | 717 | 180 | DCM | no |
| 10 pPFMA | 240 | 209 | 700 | 180 | THF | no |
| 11 pPFMA | 35 | 38 | 104 | 30 | AN:DCM(2:1) | yes |
| 12 pPFMA | 35 | 38 | 132 | 30 | AN:DCM(2:1) | no |
| 13 pPFMA | 35 | 38 | 104 | 30 | AN:DCM(2:1) | yes |
| 14 pPFMA | 46 | 34 | 128 | 30 | AN:DCM(2:1) | yes |

Distance from lamp: < 5 mm

**Table 3** summarizes the initial reactions using the Comedico lamp as the light source. The $^1$H NMR spectra of polymers irradiated with this lamp indicated that reactivity was occurring as changes were taking place to the end groups in the spectra. The irradiation experiments were performed in the presence and absence of oxygen. From these preliminary results, more systematic investigation of the irradiation reaction was pursued. The first two entries were telechelic polystyrene polymer (PS) and after irradiation **Entry 1** had multiple peaks in the 10.5 ppm region indicating aldehyde was still present and aldehyde-type side products formed. A peak at 5.37 ppm appeared that was initially attributed to the protons belonging to the tertiary carbon and alcohol of the isothiochroman group and was later investigated. The methylene region contained a series of broadened out peaks and in the aromatic region the *ortho* peaks belonging to the dithiobenzoate were still present. The GPC traces had unchanged retention times indicating a lack of change in morphology.

**Figure 11**. $^1$H NMR of polystyrene telechelic polymer after irradiation with Comedico lamp for 900 minutes.

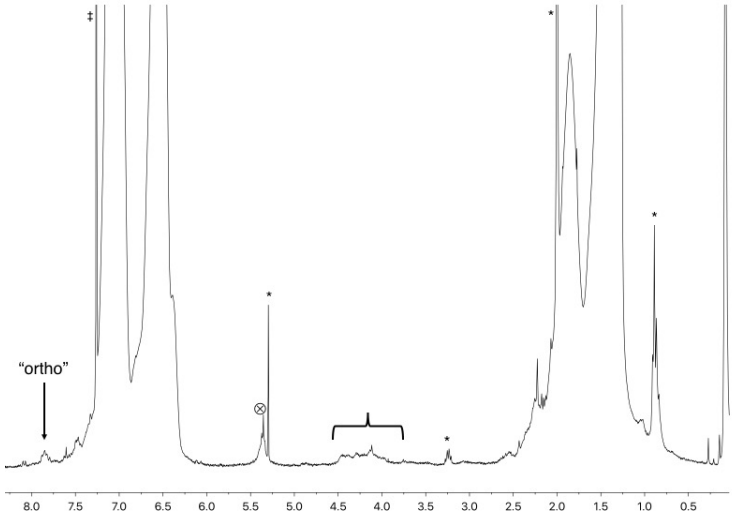


$^1$H NMR of polystyrene **Entry 1, Table 3**. Bracket indicates broadened methylene region, * residual solvent and impurities, ⊗ indicates the impurity at 5.37 ppm, "ortho" indicates the *ortho*- dithiobenzoate protons, and ‡ indicates NMR solvent.

**Entry 2** was degassed and irradiated for a shorter time. The $^1$H NMR indicated broadening of the methylene peaks, disappearance of the aldehyde peak, and disappearance of the *ortho*- dithiobenzoate peak possibly further upfield underneath the phenyl backbone signal. The peak at 5.37 ppm also appeared. Compared to **Entry 1**, this result was more promising.

**Figure 12**. Stacked $^1$H NMR of **Entry 2** (top) of polystyrene telechelic polymer after irradiation with Comedico lamp for 180 minutes and starting material (bottom). Bracket indicates broadened methylene region, * residual solvent and impurities, ⊗ indicates the impurity at 5.37 ppm, the box indicates the changes in the aromatic region of the *ortho*-dithiobenzoate peak.

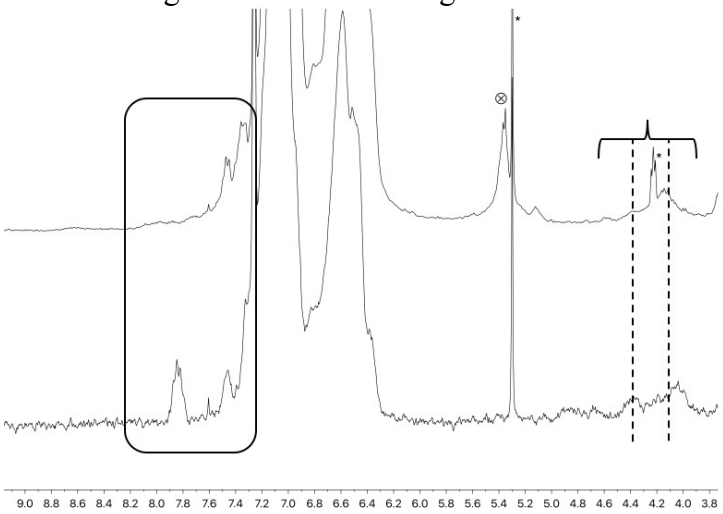

The $^{1}$H NMR spectrum of **Entry 3** indicated that the PMMA polymer had broadened methylene groups and completely consumed aldehyde and disappearance of the *ortho*-methylbenzaldehyde methyl peak at 2.58 ppm. The peak at 5.37 ppm also appeared, however, despite the upfield shift of the *ortho*-dithiobenzoate peaks, there appeared to be more than one set of aromatic peaks in the region between 6.6 – 8.2 ppm. There was residual solvent and unidentified impurities present in the sample. **Entry 4** was followed by GPC and the trace displayed an increase in peak breadth compared to the starting material.

**Figure 13**. **A)** $^{1}$H NMR spectrum of PMMA telechelic polymer after irradiation with Comedico lamp; characterization of **Entry 3** and **4.** Stacked $^{1}$H NMR of **Entry 3** (top) and linear starting material (bottom); bracket indicates broadened methylene region, * residual solvent and impurities, ⊗ indicates the impurity at 5.37 ppm, circle indicates the methyl of the *ortho*-methylbenzaldehyde at 2.54 ppm, and ‡ indicates NMR solvent. **B)** stacked GPC trace of **Entry 4** in dichloromethane at 1 mL/min. * indicates unidentified small molecular weight impurities.

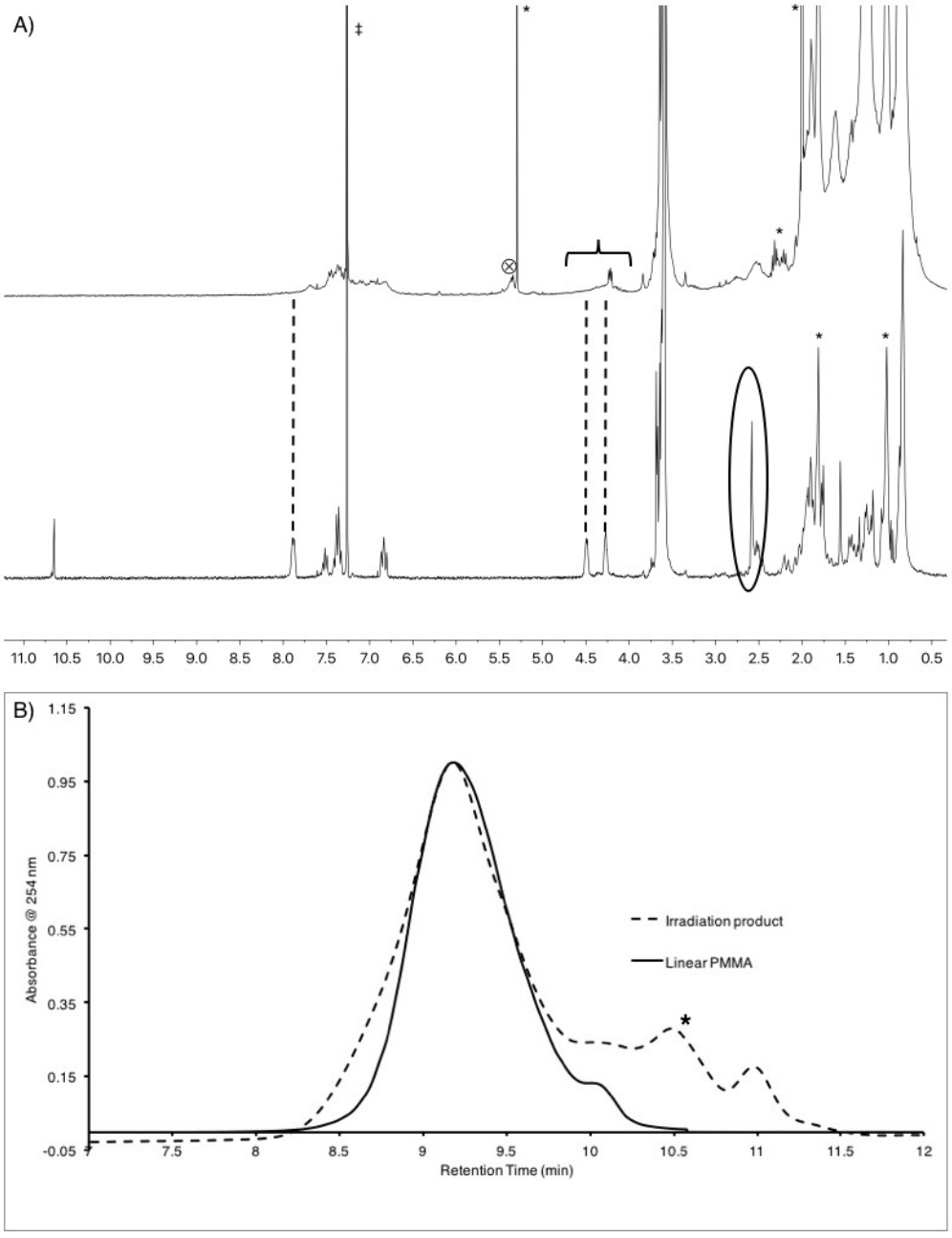


The starting material for **Entries 5 – 11** was a large polymer of n = 200 repeat units and it was used to compare the impact of solvent. **Entries 5** to **7** had similar concentrations and

irradiation times but the relative amount of acetonitrile was increased. The results were followed by GPC, accurate retention times were not acquired, but a new peak most likely attributed to intermolecular chain extension products appeared at higher molecular weight. A large distribution of impurities also appeared at later retention times.

**Figure 14**. Stacked GPC traces of irradiated n = 200-mer pPFMA telechelic polymer with increasing relative acetonitrile solvent content Stacked GPC traces of **Entries 5 – 7** in dichloromethane at 1 mL/min. * indicates lower molecular weight impurities starting at 10.2 to 12 min. Dotted vertical grey line indicates the linear polymer. Solid vertical grey line denoted by ‡ indicates potential condensation product for the same irradiation time with increasing amount of acetonitrile.

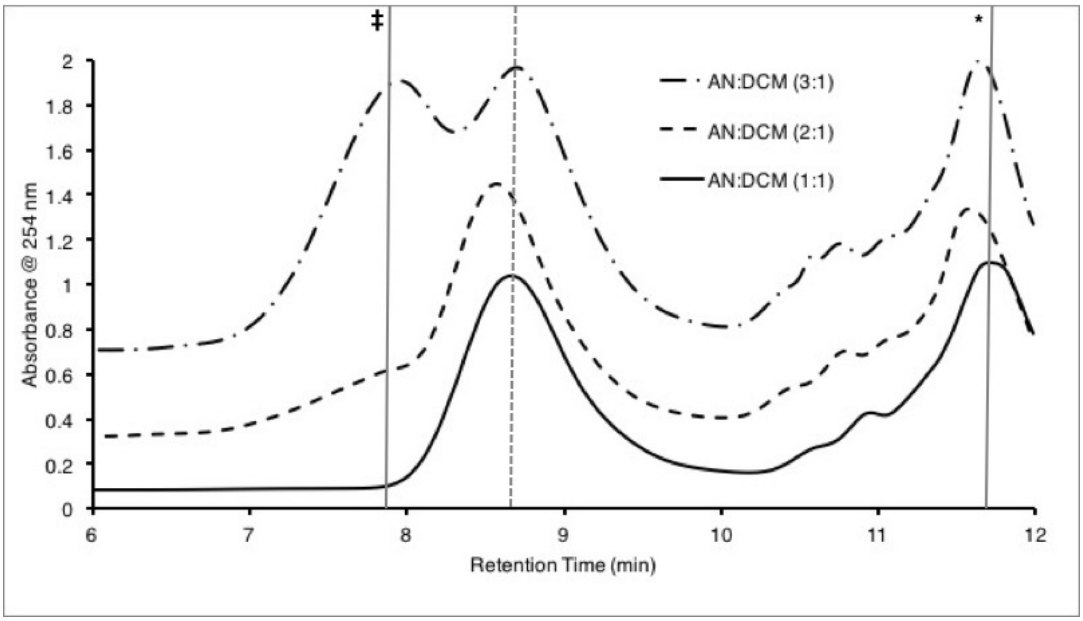


**Entries 8** to **10** were followed by $^{1}$H NMR as the solvent was altered from AN:DCM mixture, to DCM, and THF, respectively. In each case, identical reaction times were used with similar concentration ranges. The peak at 5.37 ppm appeared with integrals differing from the backbone signal indicating that it is most likely an impurity and not attributed to the isothiochroman group.

The first 10 entries of **Table 3** followed longer reaction times from a literature precedent from Tang et al.[46] but then were shortened to 30 minutes[47] for **Entries 11** to **14** which might minimize the amount of side products generated.

**Entries 11** to **14** were characterized with $^{1}$H NMR and GPC. The impurity peak at 5.37 ppm appeared for all four polymers but the aldehyde was completely consumed along with the *ortho*-methylbenzaldehyde methyl peak, the methylene peaks were broadened, and when observable the *ortho*- aromatic peaks were shifted upfield. The backbone signals and $^{19}$F NMR remained unchanged after irradiation. The GPC traces showed unaltered distributions and changes towards longer retention compared to the linear polymers. A UV-Vis spectrum indicated disappearance of the peak at 315 nm. These were the first promising results of cyclization that were further pursued in the following section for a collection of different molecular weights. See **Figure 15a - c**.

**Figure 15a-c)**. Promising sample characterization data set of an n = 38-mer pPFMA telechelic polymer. **A)** Stacked $^{1}$H NMR spectrum of **Entry 12** (top) and linear starting material (bottom); bracket indicates broadened methylene region, * residual solvent and impurities, ⊗ indicates the impurity at 5.37 ppm, circle indicates the methyl of the *ortho*-methylbenzaldehyde at 2.54 ppm, and ‡ indicates NMR solvent. **B)** Overlaid GPC traces of **Entry 12** and linear polymer in dichloromethane at 1 mL/min. Small molecular weight impurities were not present in the traces. **C)** Overlaid UV-Vis spectrum of **Entry 12** and linear polymer in dichloromethane. Solid arrow indicates the disappearance of the end group peak at 315 nm.

**A)**

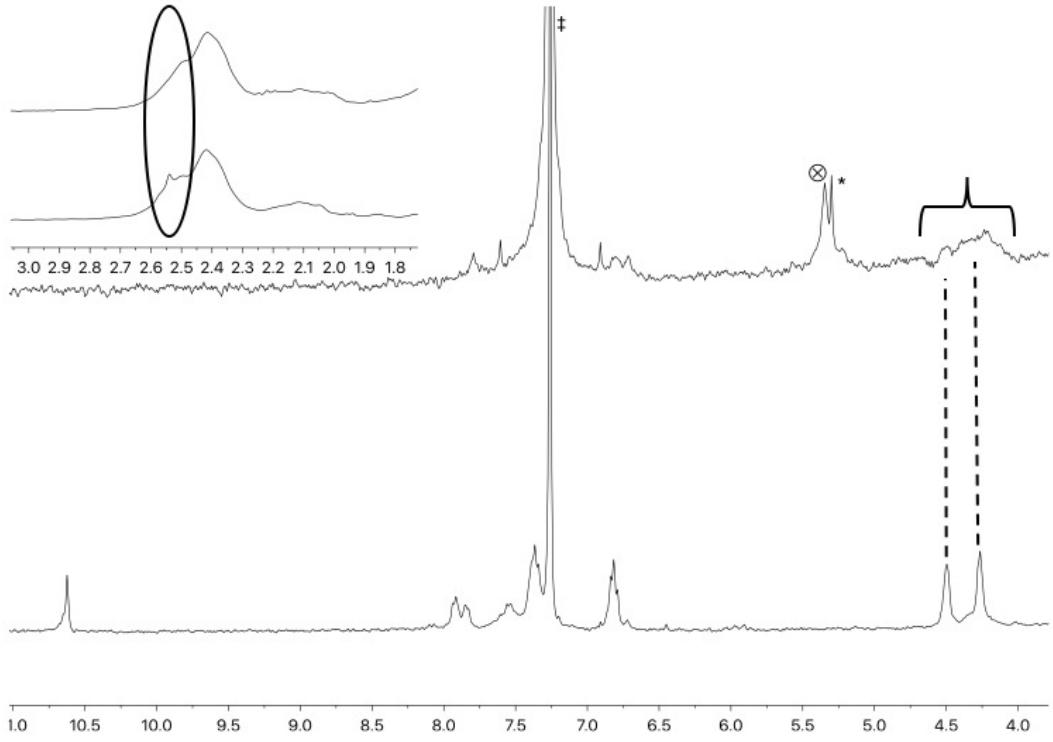


**B)**

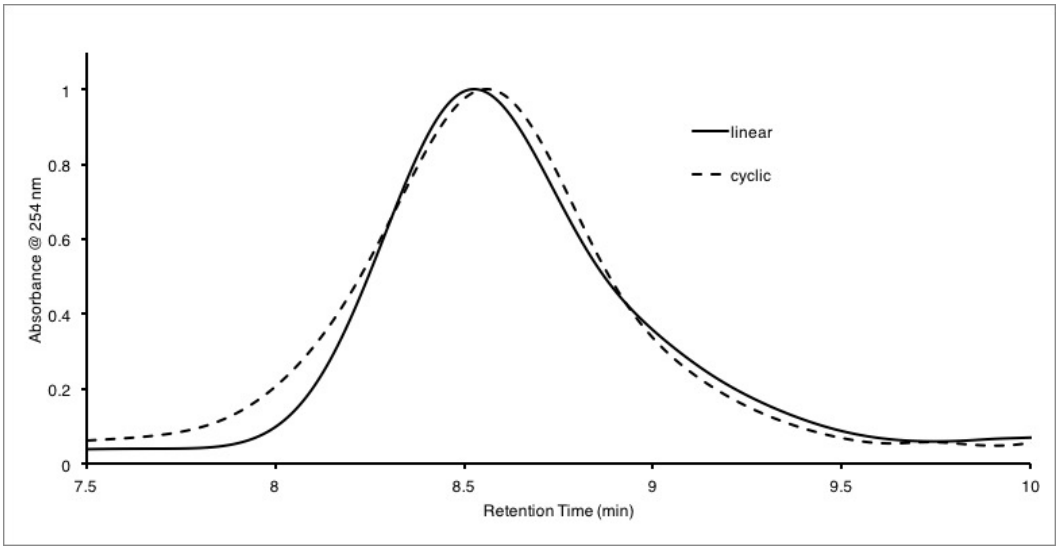

**C)**

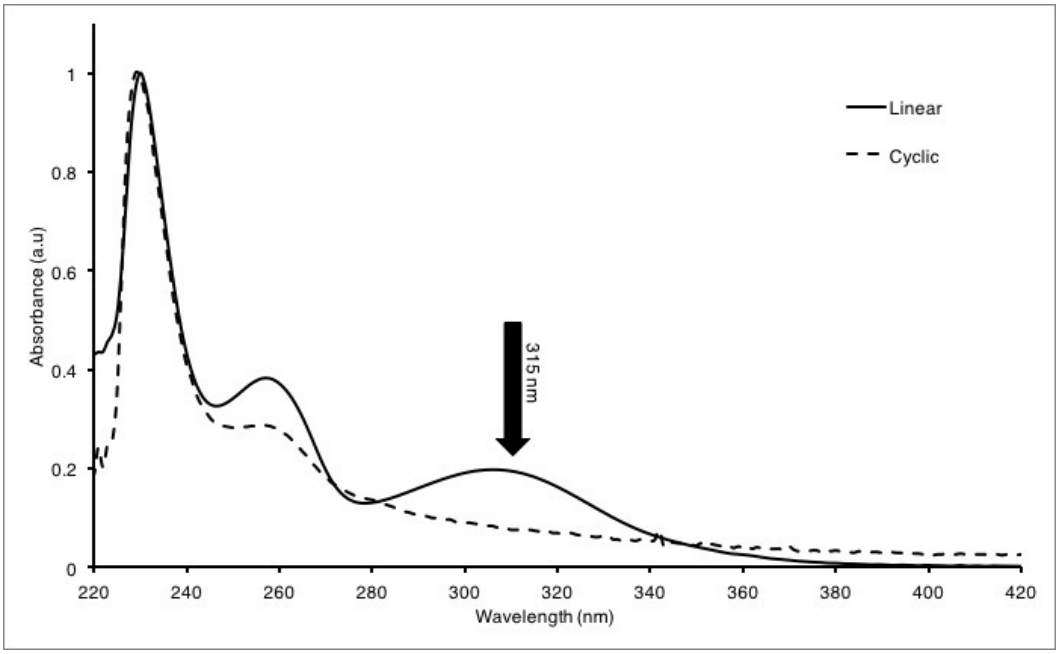


## 3.5 Irradiation experiments using UVB lamp at shorter reaction times

**Table 4.** Irradiation reactions with Comedico lamp at shorter reaction times without degassing.

| Entry | Linear, n | | Concentration (mg/L) | Irradiation Time (min) | $MW_{n,cyclic}/MW_{n,linear}$ |
|---|---|---|---|---|---|
| | $n_{nmr}$ | $n_{GPC}$ | | | |
| 1 | 5 | 9 | 62 | 30 | 2.46 |
| 2 | 5 | 9 | 42 | 15 | 4.63 |
| 3 | 15 | 14 | 87 | 30 | 1.20 |
| 4 | 15 | 14 | 74 | 15 | 1.20 |
| 5 | 21 | 26 | 71 | 30 | 1.13 |
| 6 | 21 | 26 | 111 | 30 | 1.11 |
| 7 | 27 | 34 | 109 | 30 | 0.83 |
| 8 | 32 | 37 | 109 | 30 | 0.69 |
| 9 | 33 | 34 | 112 | 30 | 0.95 |
| 10 | 35 | 38 | 107 | 30 | 0.99 |
| 11 | 51 | 51 | 114 | 30 | 1.03 |
| 12 | 51 | 51 | 93 | 30 | 1.02 |
| 13 | 51 | 51 | 98 | 30 | - |
| 14 | 65 | 63 | 94 | 30 | 0.75 |
| 15 | 65 | 63 | 100 | 30 | 0.96 |
| 16 | 65 | 63 | 112 | 30 | 1.00 |

All Entries are pPFMA. Distance from lamp: < 50 mm

**Table 4**. summarizes the shorter reaction time results where ACS grade acetonitrile and dichloromethane in a 2:1 ratio by volume was used without degassing. The contents were stirred and irradiated in Pyrex glassware vessels. Following the removal of solvent, NMR was acquired in $CDCl_3$ and then GPC traces were collected of the product and linear precursor in THF at 1 mL/min.

Oxygen was not removed because previously it was reported that the HDA, with the current orthoquinodimethane and dienophile, could occur in the presence of oxygen.[46] Despite being a photochemical reaction this seemed reasonable since the electronics were different for the $O_2$/ dithiobenzoate dienophile pair and the solution contained no additional photosensitizers. The HDA can occur in the presence of water since it was determined that hydrogen bonding could stabilize the photoenol.[52]

For smaller oligomeric polymers, **Entries 1-6**, irradiation resulted in a broadening of the distributions as determined by GPC. The $^1$H NMR indicated a broadening of the methylene region along with the introduction of extra peaks and consumption of the *ortho*-methylbenzaldehyde methyl and aldehyde groups, which was also confirmed with UV-Vis. It was possible that the HDA reaction did occur but it led to simultaneous condensation and ring closure morphology changes.

A small $MW_{n,cyclic}/MW_{n,linear}$ ratio of < 0.95 was used show an apparent molecular weight change which demonstrates a successful cyclization. All the entries had $^1$H NMR data that indicated consumption of the *ortho*-methylbenzaldehyde end group, broadening of the methylene region, no changes to the methylene and methyl backbone, and no changes in the $^{19}$F NMR side group signals. As well, all the UV-Vis spectra indicated consumption of the end group. See (**Fig. 16**)

Cyclization requires complete consumption of the end groups, which is the case for **Table 4 Entries 1 – 14,** however, there might be error attributed to the GPC experiment. All the other data indicates a promising result but the conflicting GPC experiment 1) might not have a large enough resolution to consistently show a retention time change or 2) there can be a small amount of linear impurity, below NMR detection levels, which can offset the physical properties of a cyclic polymer considerably and lead to only minor changes in the retention time. A mixture of linear and cyclic polymer of the same distribution does not provide a trace with two individual peaks but a single peak at an intermediate retention time.[46] Polymers with a $MW_{n,cyclic}/MW_{n,linear}$ ratio close to 1.0 might be successful results but were most likely subject to these errors.

**Figure 16**. Data set of an n = 34-mer pPFMA telechelic polymer after irradiation with Comedico lamp at shorter reaction times **A)** Stacked $^{1}$H NMR of **Entry 9** (top) and linear starting material (bottom); dotted vertical lines indicate broadened methylene region, * residual solvent and impurities, ⊗ indicates the impurity at 5.37 ppm, circle indicates the methyl of the *ortho*-methylbenzaldehyde at 2.54 ppm, and ‡ indicates NMR solvent. **B)** Overlaid UV-Vis spectrum of **Entry 9** and linear polymer.

**A)**

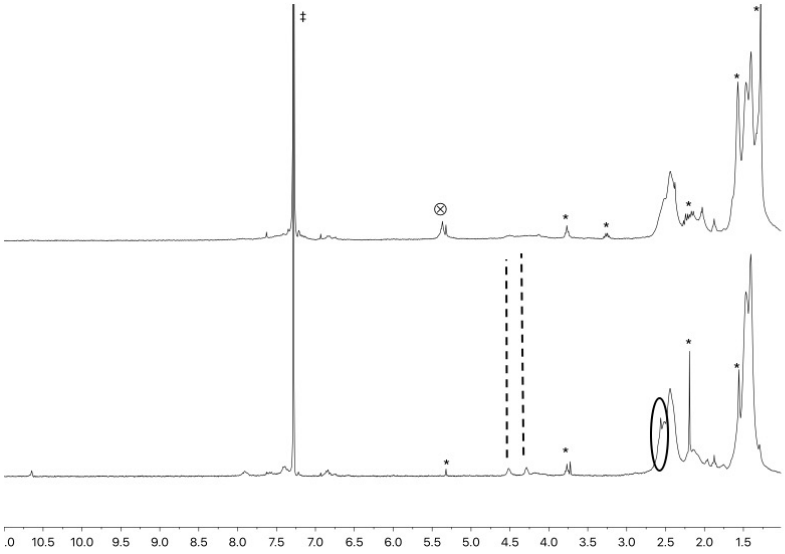

**B)**

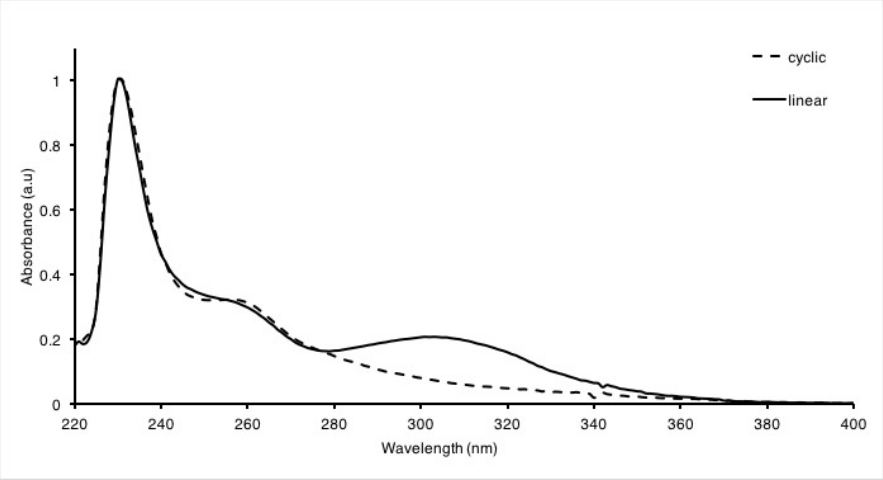


All NMR entries were acquired in $CDCl_3$ and since small amounts of material were used it was difficult to obtain information about changes to the ω end group. Subsequent HDA reactions were monitored in $d_6$-acetone.

Successful cyclization reactions were obtained for **Entries 7 – 9**, and **14**. In the next section the aim was to try to consolidate this reaction to obtain it reproducibly for a range of molecular weight polymers.

**Table 5.** Irradiation reactions with Comedico lamp; 30 min reaction times.

| Entry | Linear, n | | Concentration (mg/L) | $MW_{n,cyclic}/MW_{n,linear}$ | $O_2$ Present |
|---|---|---|---|---|---|
| | $n_{nmr}$ | $n_{GPC}$ | | | |
| 1 | 27 | 34 | 110 | 1.14 | No |
| 2 | 30 | - | 108 | - | No |
| 3 | 43 | 16 | 94 | 0.95 | Yes |
| 4 | 43 | 16 | 116 | 0.91 | Yes |
| 5 | 43 | 16 | 106 | 0.90 | Yes |
| 6 | 43 | 16 | 104 | 0.89 | No |
| 7 | 46 | 34 | 112 | 0.94 | No |
| 8 | 51 | 51 | 130 | - | No |
| 9 | 52 | 73 | 116 | - | No |
| 10 | 52 | 73 | 120 | 0.93 | No |
| 11 | 89 | 63 | 114 | - | Yes |
| 12 | 89 | 63 | 110 | - | Yes |
| 13 | 89 | 63 | 102 | 1.12 | No |
| 14 | 89 | 63 | 104 | - | Yes |
| 15 | 89 | 63 | 108 | - | Yes |
| 16 | 89 | 63 | 119 | 0.99 | No |
| 17 | 89 | 63 | 122 | 1.03 | No |
| 18 | 240 | 209 | 147 | 0.62 | No |

Entries 2, 3, 4, 5, and 6 are PMMA. Rest of the entries are pPFMA. Irradiation time: 30 m. Distance from lamp: < 50 mm.

All entries in **Table 5** were irradiated for 30 minutes except for **Entry 14** which was irradiated for 15 minutes. When oxygen was present ACS grade acetonitrile and dichloromethane in a 2:1 ratio by volume was used. When oxygen was absent distilled and degassed solvent stored in the glove box was used. The contents were irradiated in Pyrex glassware vessels while stirring. Following the removal of solvent NMRs were acquired in $d_6$-acetone and then GPC traces were collected of the product and linear precursor in THF at 1 mL/min. It was found that oxygen did not have a large impact on the results and that there might be some irreproducibility to the HDA that maybe due to factors not controlled for or considered in these experiments. Again, a small $MW_{n,cyclic}/MW_{n,linear}$ ratio of < 0.95 was used as an approximate indicator towards successful cyclization. The error considerations for GPC

mentioned for **Table 4** are still relevant for **Table 5**. Successful cyclization reactions were obtained for **Entries 3 - 7**, **10** and **18**.

**Entries 1** to **18** had $^{1}H$ NMR data that indicated consumption of the *ortho*-methylbenzaldehyde, end group, broadening of the methylene region, no changes to the methylene and methyl backbone protons, rearrangement of the ω end, and no changes in the $^{19}F$ NMR side group signals. As well, UV-Vis spectra indicated consumption of the end groups. Entries lacking a molecular weight ratio were analyzed exclusively with NMR. To investigate the peak at 5.37 ppm **Entries 14** and **15** were prepared and irradiated at 15 and 30 minutes, respectively. The integral values between the broadened methylene peaks and the peak at 5.37 ppm were compared and the **Entry 15** ratio was found to be larger (**Table 6**). It was concluded that the peak was an impurity with the amount formed depending on irradiation time. Additionally, precipitation of the polymers from pentane and methanol removed this peak (**Fig. 18**).

**Table 6.** Integral ratios for suspected isothiochroman peaks

| Entry | Integral Ratio | Irradiation Time (minutes) |
|---|---|---|
| **14** | 0.31 | 15 |
| **15** | 0.42 | 30 |

Integral ratio was calculated as the quotient of the integral between 4.58 – 4.07 ppm and 5.38 – 5.31 ppm.

The aromatic region was unobstructed when the NMR solvent was switched from $CDCl_3$ to $d_6$-acetone and the expected rearrangement of the aryl protons could be visualized more clearly. See **Figure 17**. The peaks previously reported for the proton of tertiary carbon and the alcohol of the isothiochroman could not be visualized and might be buried under the backbone signal or methylene peaks.

**Figure 17**. $^{1}$H NMR spectrum of **Entry 16** n = 63-mer pPFMA after precipitation from methanol and pentane. Inset: stacked $^{1}$H NMR of **Entry 16** (top) and linear precursor (bottom). * residual solvent and impurities. ‡ indicates NMR solvent.

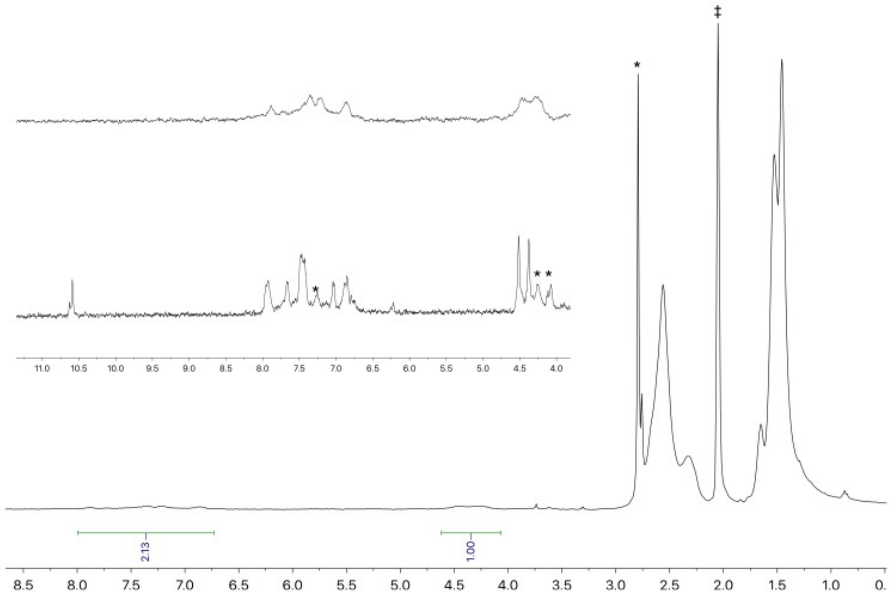


According to Stockmeyer-Jacobson ring closure occurs more readily for shorter polymer chains than for longer ones for the same amount of time. The SJ Theory explains why both cyclization and condensation reactions occurred for **Entry 18** suggesting more dilute conditions were required for an n = ~200 pPFMA. A longer reaction time might additionally be necessary to allow for all the polymers to completely react. The evidence for the condensation product appears as a shoulder on the GPC trace for **Entry 18** (See **Fig. 18**).

**Figure 18**. Stacked GPC trace of **Entry 18**. Traces were collected in THF (1 mL/min). Solid line - linear polymer, dotted line – irradiation product. * denotes the condensation product impurity.

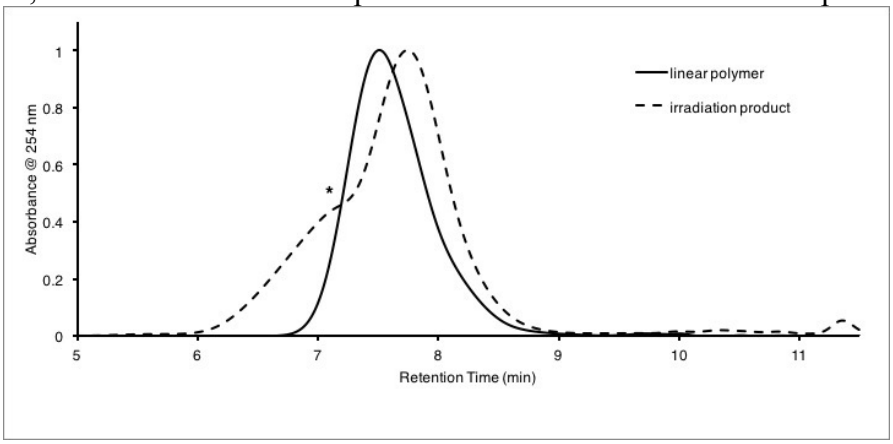


To simplify the reaction conditions acetonitrile was removed and irradiation was attempted in lone dichloromethane. **Table 7** summarizes these results.

All entries in **Table 7** used dried and degassed dichloromethane solvent. The contents were stirred and irradiated in Pyrex glassware. Following the removal of solvent NMRs were acquired in $d_6$-acetone and then GPC traces were collected of the product and linear precursor in THF at 1 mL/min. A small $MW_{n,cyclic}/MW_{n,linear}$ ratio of < 0.95 was used an approximate indicator towards successful cyclization. The error considerations for GPC mentioned above for **Table 4** and **5** are still relevant for **Table 7**. Successful cyclization reactions were obtained for **Entry 9** only.

**Table 7**. Irradiation with Comedico lamp in lone dichloromethane solvent.

| Entry | Linear, n | | Concentration (mg/L) | Irradiation Time (min) | $MW_{n,cyclic}/MW_{n,linear}$ |
|---|---|---|---|---|---|
| | $n_{nmr}$ | $n_{GPC}$ | | | |
| 1 | 43 | 41 | 54 | 30 | 1.02 |
| 2 | 43 | 41 | 44 | 30 | 1.09 |
| 3 | 43 | 41 | 55 | 30 | 1.02 |
| 4 | 46 | 34 | 87 | 30 | 1.03 |
| 5 | 46 | 34 | 0.8 | 396 | 0.99 |
| 6 | 51 | 51 | 90 | 30 | 1.12 |
| 7 | 51 | 51 | 89 | 30 | - |
| 8 | 51 | 51 | 61 | 30 | 1.06 |
| 9 | 52 | 73 | 103 | 30 | 0.95 |
| 10 | 89 | 63 | 108 | 30 | 1.20 |
| 11 | 161 | 155 | 93 | 30 | 1.09 |
| 12 | 166 | 87 | 100 | 30 | - |
| 13 | 240 | 209 | 76 | 30 | 1.04 |
| 14 | 240 | 209 | 76 | 90 | 1.02 |

All entries are pPFMA. Distance from lamp < 50 mm.

The UV-Vis spectra indicated consumption of the end groups and the light pink linear polymer generated a white or yellow solid product after irradiation. In the $^{1}H$ NMR asymmetric peaks consistently appeared in the methylene region and the aromatic protons did not rearrange upfield as expected but remained broad and at times adulterated with sharp peaks after precipitation. Since the irradiation products' $MW_{n,cyclic}/MW_{n,linear}$ ratios were 1.00 and superimposed the linear traces it was assumed that the polymers remained linear. Both $^{1}H$ NMR and UV-Vis show the end groups were being consumed but it was difficult to ascribe the nature of the change.

**Figure 19**. $^{1}$H NMR of irradiation products highlighting asymmetry in the methylene region (B). $^{1}$H NMR stack of **Entries 4**, **6**, **7** and **10** (top to bottom). **A** denotes the aromatic region, **B** denotes the asymmetric methylene region, and * denotes residual solvent and unidentified impurities.

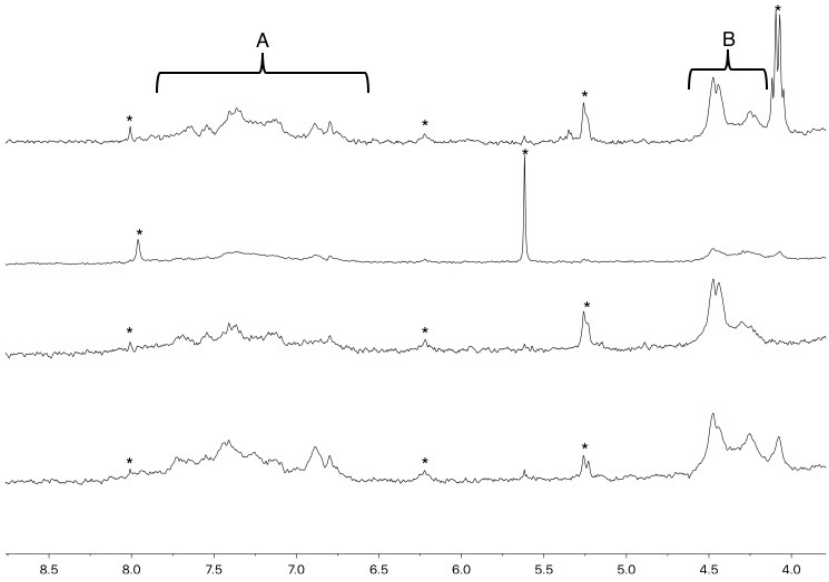


Despite the use of dichloromethane in previous HDA reactions, it was used as an accompaniment to acetonitrile. Acetonitrile makes it possible to achieve the photoenol excited triplet state with higher quantum efficiencies and subsequent reactions maintained the acetonitrile and dichloromethane (2:1 v/v) solution.[52] The following irradiation experiments (**Table 8**) were performed on larger scales and at lower concentrations than before and successful results were carried forward with PPM.

**Table 8**. Large scale HDA reactions for post polymerization modification.

| Entry | Linear, n | | Concentration (mg/L) | Irradiation Time (min) | $MW_{n,cyclic}/MW_{n,linear}$ |
|---|---|---|---|---|---|
| | $n_{nmr}$ | $n_{GPC}$ | | | |
| 1 | 17 | - | 46 | 30 | - |
| 2 | 26 | 29 | 44 | 30 | 1.12 |
| 3 | 43 | 41 | 50 | 30 | - |
| 4 | 43 | 41 | 68 | 30 | 0.93 |
| 5 | 43 | 41 | 49 | 30 | 0.91 |
| 6 | 43 | 41 | 57 | 30 | 0.9 |
| 7 | 43 | 41 | 56 | 30 | 0.9 |
| 8 | 43 | 41 | 56 | 30 | 0.79 |
| 9 | 58 | 52 | 52 | 45 | 0.9 |

All entries were pPFMA. Distance from lamp: < 50 mm.

All entries in **Table 8** used distilled and degassed acetonitrile and dichloromethane solvent in a 2:1 v/v. The contents were stirred and irradiated in Pyrex glassware vessels. Following the removal of solvent NMRs were acquired in $d_6$-acetone and then GPC traces were collected of the product and linear precursor in THF at 1 mL/min. A small $MW_{n,cyclic}/MW_{n,linear}$ ratio of < 0.95 was used as an approximate indicator towards successful cyclization. The error considerations for GPC mentioned above for the above tables are still relevant for **Table 8**. Successful cyclization reactions were obtained for **Entries 4-9**. Once the cyclic polymers were synthesized they were further characterized with Diffusion NMR. The following section explores the results for a small assortment of cyclic polymers.

## 3.6 Confirmation of the cyclic polymer structure by Diffusion NMR

Comparing polymer topologies, rings are expected to have more compact structures in solution. The incorporation of the chain ends into the ring restricts their motion resulting in an overall reduction in size, for the same length and distribution, which is reflected in a smaller hydrodynamic radius. The compact structure of cyclic polymers results in fewer interactions with the surroundings than a corresponding linear macromolecule. Molecules diffuse through solution and diffusion NMR spectroscopy can be used to extract the diffusion coefficient, $D_e$, from such

motion. The diffusion coefficient for similarly sized cyclic and liner molecules can be used to confirm their different topologies.[98]

The diffusion coefficient, $D_e$, is described the Stokes-Einstein equation which assumes a spherical shape in solution

$$D_e = \frac{kT}{6\pi\eta r} \quad (1)$$

where k is the Boltzmann constant, T is the temperature, $\eta$ is the viscosity of the solvent, and r is the hydrodynamic radius of the molecule.

The polymer samples were dissolved in $d_6$ - acetone and placed into a 1.7 mm NMR tube to reduce effects of convection that can arise from temperatures differences in the probe. The sample was subjected to a series of magnetic field gradients that locates the molecule's position. Any change in position due to the Brownian motion of the molecules was encoded into another magnetic field gradient and the difference in the molecules position appears as a change in intensity.[102] A magnetic field gradient, in contrast to a homogenous magnetic field such as in a typical 1D $^1$H NMR experiment, is a field that changes with respect to position and reflects any changes in position of a molecule more clearly.[102]

In the diffusion NMR experiment, a dephasing pulsed field gradient is applied that cancels out the bulk magnetization and then a refocusing pulsed field gradient is applied to return that vector.[102] In the time span between those two pulses the molecules could diffuse and not be fully refocused thus weakening their signal intensity.[102] This pulse sequence is repeated and the gradient magnetic field strength is gradually increased for subsequent pulses.[102]

The change in the magnetic field gradient strength and duration is important because of the impact it has on the intensity of the signal.[102] The longer and more intense the gradient pulse

the more spatial selectivity is encoded but at the cost of signal intensity. The final information that is generated is either in the form of an intensity versus gradient Strength gaussian decay plot or a 2D plot called a DOSY. The diffusion constant, $D_e$, can then be extracted from this Gaussian decay plot. Since different molecules have different diffusion coefficients this technique can resolve different components in a mixture based on the rates of intensity decay. The diffusion constant is reported in units of [$m^2$ /s] and is larger for smaller molecules and less viscous solvents.

The change in signal intensity used to calculate $D_e$ is described by

$$I = I_0 e^{-D_e \gamma^2 g^2 \delta^2 (\Delta - \delta/3)} \quad (2)$$

where I is the observed intensity, $I_0$ is the reference intensity, γ is the gyromagnetic ratio of the nucleus of the molecule of interest, g is the gradient strength, δ is the length of the gradient, and Δ is the diffusion time.

The $D_e$ is reflective of the solute's interaction with the solvent. A larger value for the coefficient represents coverage of a greater amount of area by the molecule for a given period of time, meaning that the particles move faster and to do so they must be smaller according to the Stokes-Einstein equation. Cyclic polymers are expected to have a larger $D_e$ than their linear counterparts and this has been confirmed with a diffusion NMR experiment for a set of linear and cyclic poly(pentafluorophenyl methacrylate)s.

In preparing the samples the concentrations were kept as close to one another between linear and cyclic species to ensure that a legitimate comparison between the $D_e$'s was made. It has been demonstrated for linear and cyclic polystyrene that the $D_e$ is concentration dependent.[99] However, despite weighing the samples as accurately as possible concentration differences arose

as revealed by $^{1}H$ NMR. The methyl backbone proton was integrated from 1.60 to 1.40 ppm in all the spectra and the $D_e$ was extracted by fitting the decay in that region in MestRe Nova.

**Table 9**. Comparison of linear and cyclic polymers by Diffusion NMR at 1.60 – 1.40 ppm.

| Entry | Linear, n | | Cyclic Location | $D_{e,linear}$ ($m^2/s$) | $D_{e,cyclic}$ ($m^2/s$) | $D_{e,linear}/D_{e,cyclic}$ |
|---|---|---|---|---|---|---|
| | $n_{nmr}$ | $n_{GPC}$ | | | | |
| 1 | 46 | 34 | Table 5, Entry 7 | $2.66 \times 10^{-6}$ | $2.94 \times 10^{-6}$ | 0.91 |
| 2 | 43 | 41 | Table 8, Entry 6 | $2.60 \times 10^{-6}$ | $2.68 \times 10^{-6}$ | 0.97 |
| 3 | 51 | 51 | Table 7, Entry 7 | $2.66 \times 10^{-6}$ | $2.67 \times 10^{-6}$ | 1.00 |
| 4 | 89 | 63 | Table 7, Entry 10 | $2.37 \times 10^{-6}$ | $2.17 \times 10^{-6}$ | 1.09 |
| 6 | 52 | 73 | Table 5, Entry 10 | $1.81 \times 10^{-6}$ | $2.34 \times 10^{-6}$ | 0.77 |
| 7 | 240 | 209 | Table 5, Entry 18 | $1.11 \times 10^{-6}$ | $8.79 \times 10^{-7}$ | 1.26 |

The spectra reveal residual water from the NMR solvent and solvent impurities which might be responsible for concentration differences. Closer investigation of **Entries 2**-**4**, and **7**, **Table 9** reveal differences in concentration based on the relative areas of the NMR solvent peak to polymer peaks as well as due to additional solvent peaks. The other entries have comparable concentrations and are within the expected $D_{e,linear}/D_{e,cyclic}$ ratio range.

DOSY colloquially is referred to as 'NMR chromatography' as it can separate the contents of a mixture. This technique is ideal for confirming cyclic topology as changes in $D_e$ denote structural changes and the linear impurity from an incomplete reaction can be readily detected in the DOSY. No linear impurities were detected for the HDA reactions.

**Figure 20**. Gaussian fit to integral at 1.60 to 1.40 ppm of peak intensity using a mono-exponential fit of an $n_{nmr}$ = 52-mer linear and cyclic pPFMA. Decay plots for **Entry 6**, **Table 9** denote very good fit for 32 data points.

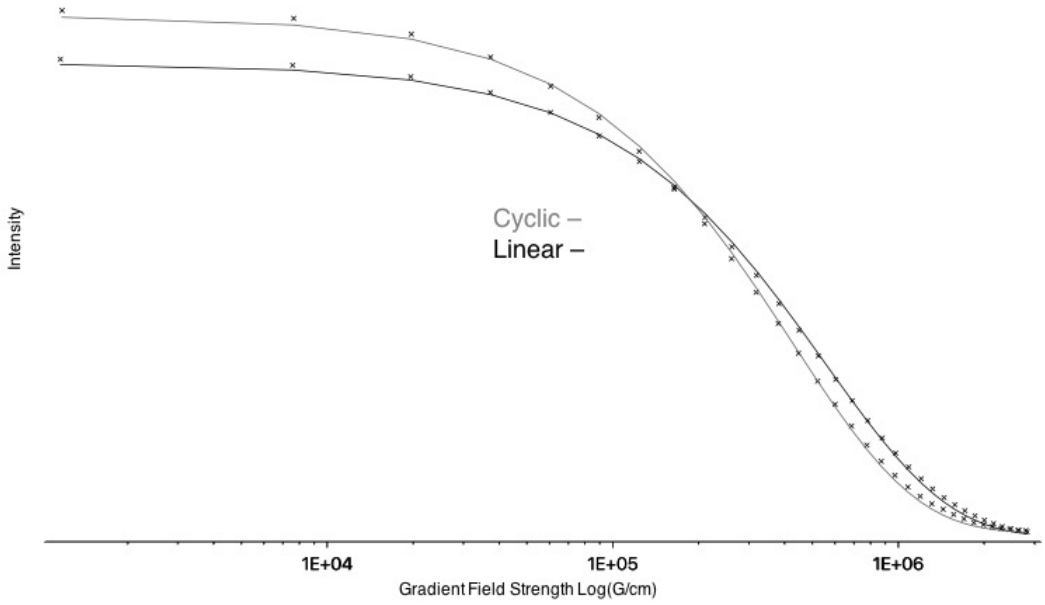


The polymers that were successfully cyclized and characterized were taken forward to PPM. PPM chemistry was investigated for both linear and cyclic systems and will be explored in the next chapter.

## 3.7 Experimental

### 3.7.1 Materials and Methods

All air sensitive compounds were handled using standard Schlenk line techniques (Ar) or in a $N_2$ filled glovebox (MBraun). $^1$H NMR spectra were collected on a 300 MHz Bruker Avance spectrometer with spectra referenced to residual solvent peaks.[93] UV-Vis spectra were collected using quartz cuvettes on a Helios Zeta UV-vis Thermo Scientific spectrophotometer from 190-600 nm, 2 nm bandwidth, 240 nm/min scan speed, and 1 nm data intervals using VISIONpro software. Gel permeation chromatography was performed on an Agilent 1100 Series with an Agilent PLgel 5μm MIXED-C column elution profiles were generated with THF or DCM

(Sigma, HPLC grade) at 1 mL/min using ChemStation (online) and (offline) software. A series of polystyrene standards were used to generate a 10-point calibration plot (Agilent). Fluorescence Spectra were collected using quartz cuvettes on a Fluorolog Horiba Jobin Yvon or a Photon Internal Technology QuantaMaster spectrofluorometer using FelixGX 4.1.2 software in ACS reagent grade chloroform (Sigma).

The following reagents were prepared for all reactions as follows: tetrahydrofuran (Sigma) and acetonitrile (Sigma) were dried over sodium metal and benzophenone and stored in the glovebox; dichloromethane (Sigma) was dried over $CaH_2$ and stored in the glovebox; dry dimethylformamide (Sigma), 1,4-dioxane (Sigma), pentane (Sigma), methanol (Sigma), and hexanes (Sigma) were used as received.

Contents were either degassed by bubbling of argon gas for the specified times, freeze-pump-thaw cycles using liquid $N_2$ until no bubbling occurred upon thawing, or repeated cycles of sonication and dynamic vacuum.

# 4. Post polymerization modification of linear and cyclic polymers

## 4.1 Introduction

Phenanthridine derivatives are used in emissive materials[103,104] and they can also be easily synthesized with functional groups[105,106] that can be modified to generate primary amines/alcohols appropriate for post polymerization modification (PPM)[2,86,107,108] of pentafluorophenylmethacrylate (pPFMA) polymers via nucleophilic acyl substitution. We therefore targeted phenanthridine-derived nucleophiles to append to cyclic pPFMA. Phenanthridine-substituted cyclic pPFMA can then be visualized by taking advantage of its new emissive properties, further modified to alter the solubility, and the extent of nucleophilic substitution can be determined through $^{1}H$, $^{19}F$ NMR, and UV-Vis spectroscopy. Cyclic integrity can be confirmed after PPM through fluorescence spectrometry as cyclic polymer topologies have been shown to exhibit enhanced emission compared to linear materials due to their more restricted topologies.[9,109]

## 4.2 Attempted syntheses of tethered phenanthridine pincer fluorophores

Initial phenanthridine-containing synthetic targets used pincer-type phenanthridine/quinolinyl amines[105] to prepare emissive reporters with pendant primary amines connected to the *N*-heterocyclic fragment by an alkyl tether (**Figure 1, Table 1**).

**Figure 1**. Phenanthridine-containing synthetic targets for emissive reporter pendants.

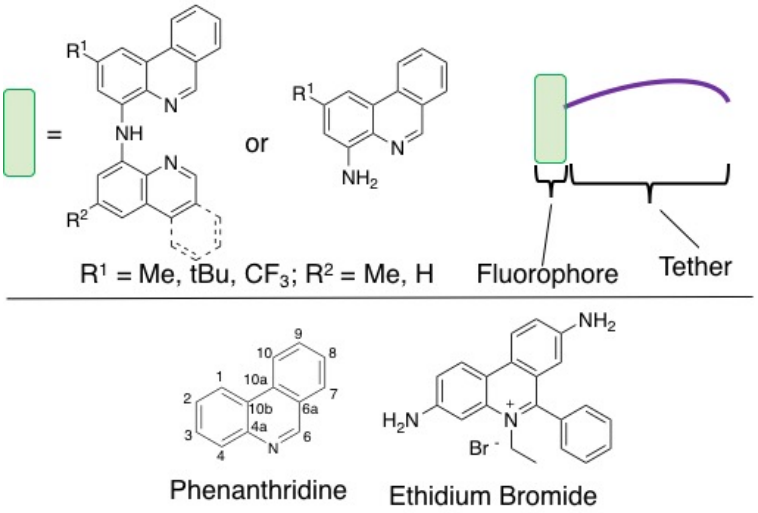


These molecules are also of interest in potentially acting as scavengers of metal ions or as hosts for phenanthridine metal complexes, due to the plausible tridentate coordination of the pincer-type side-chains to metal ions.[105] However, the amine alkylation reactions to generate these emissive reporters did not afford the intended pincer targets, nor the phenanthridine targets. $^1$H NMR spectra of the worked-up reactions only indicated either a mixture of starting materials or inefficient conversions of < 5%. The ineffectiveness of these reactions could arise from poor nitrogen nucleophilicity and steric bulk of the phenanthridine rings leading to low rates of alkylation at the N-H. Aromatic amines are weakly nucleophilic due the delocalization of the lone pairs into the conjugated π network and this effect is most likely greater in the pincers because of the second phenanthridine unit. Additionally, the sterics arising from rotation of the large rings about the C-N bond probably hinders the approach towards the electrophile.

These reactions were worth pursuing because it might be possible to push them forward with high temperatures as seen with the alkylation of aniline.[110] Various conditions were utilized to improve the nitrogen nucleophilicity or improve the leaving group capabilities of the tether

molecule. Initially, pincer frameworks **1** and **2** with a base were refluxed with **3** in either tetrahydrofuran (THF) or acetonitrile (AN) (**Scheme 1**).

**Scheme 1**. Attempted alkylation reactions of various phenanthridine pincer derivatives.

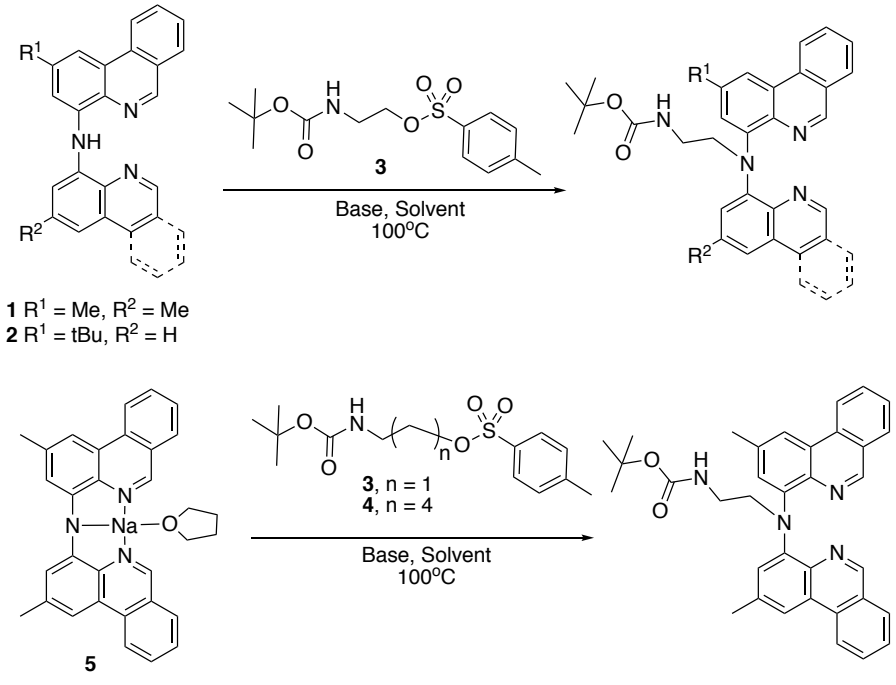


These reactions did not lead to alkylation so to increase the nucleophilicity of the central 2° amine a sodium salt **5** was prepared and reacted in THF but it did not yield any substitution of the tether. The chain length of the tether was also altered from two carbons to five which could lead to less steric hinderance from the tert-butyl protecting group and allow the amine a greater approach towards to the tosylate. However, only starting materials were isolated. The preparation of **3** and **4** were adapted from the literature.[111,112]

**Table 1.** Summary of Phenanthridine-Pincer Fluorophore Reactions (**Scheme 1**)

| Phenanthridine Species | Tether | solvent | Base |
|---|---|---|---|
| **1** | **3** | AN | NaOtBu |
| **2** | **3** | THF | TEA |
| **5** | **3** | THF | none |
| **1** | **4** | AN | $K_2CO_3$ |
| **5** | **4** | THF | none |

All reactions were performed at temperature 100°C.

## 4.3 Syntheses of tethered phenanthridine fluorophores

Compound **6** was refluxed under two different conditions initially in THF at 100°C and then in AN with potassium carbonate at 130°C (**Scheme 2**) with no products being isolated. The forcing conditions previously reported for the analogous aniline substitution of bromoethanol[110] did not drive the reaction forward.

**Scheme 2.** Attempted alkylation of 2-methyl-4-aminophenanthridine **6** derivative under forcing conditions.

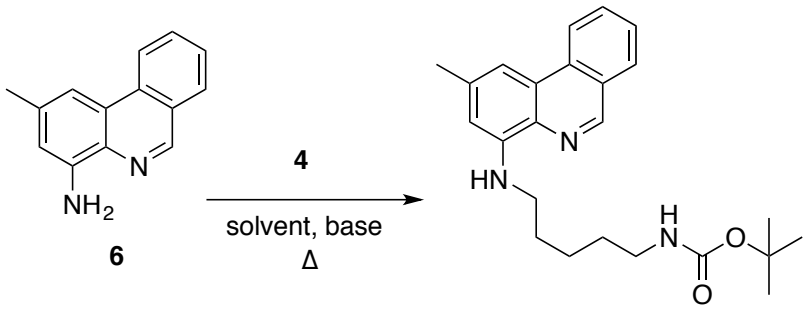


To improve the leaving group capacity of the alkyl halide the reactants were placed under Finkelstein reaction conditions (**Scheme 3**). In the reaction, use of NaI leads to substitution of bromide with the more polarizable iodide which is a better leaving group than bromide in acetone[113] and as a result the phenanthridinylamine **6** can more easily substitute the alkyl chain. Only sodium salts were used which led to the formation of insoluble sodium bromide thus driving conversion of **7** to the corresponding and more reactive 12-iodo-dodecanol.

Percentages in **Figure 2** indicate relative integral sizes; 20% belongs to the remaining terminal alkyl bromine and 80% belongs to the terminal alkyl iodine.

**Scheme 3**. Attempted Finkelstein conditions for the alkylation of aromatic amine **6**.

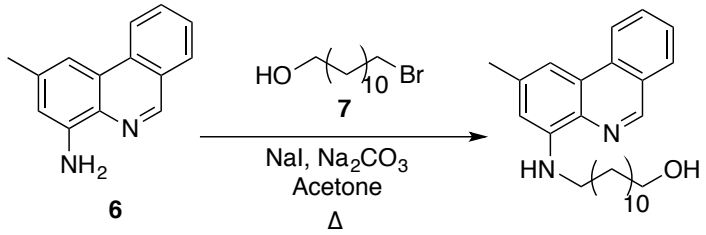

Unfortunately, amine alkylation did not result and **7** was converted by 80% to the iodo-species as observed by $^{1}$H NMR after 18 h of reflux. We next turned to Buchwald Hartwig cross-coupling reaction to form an aryl C-N bond between **8** and **9** (**Scheme 4**).

**Figure 2**. $^{1}$H NMR stack of Finkelstein (**Scheme 3**) crude reaction mixture (top) and **7** (bottom).

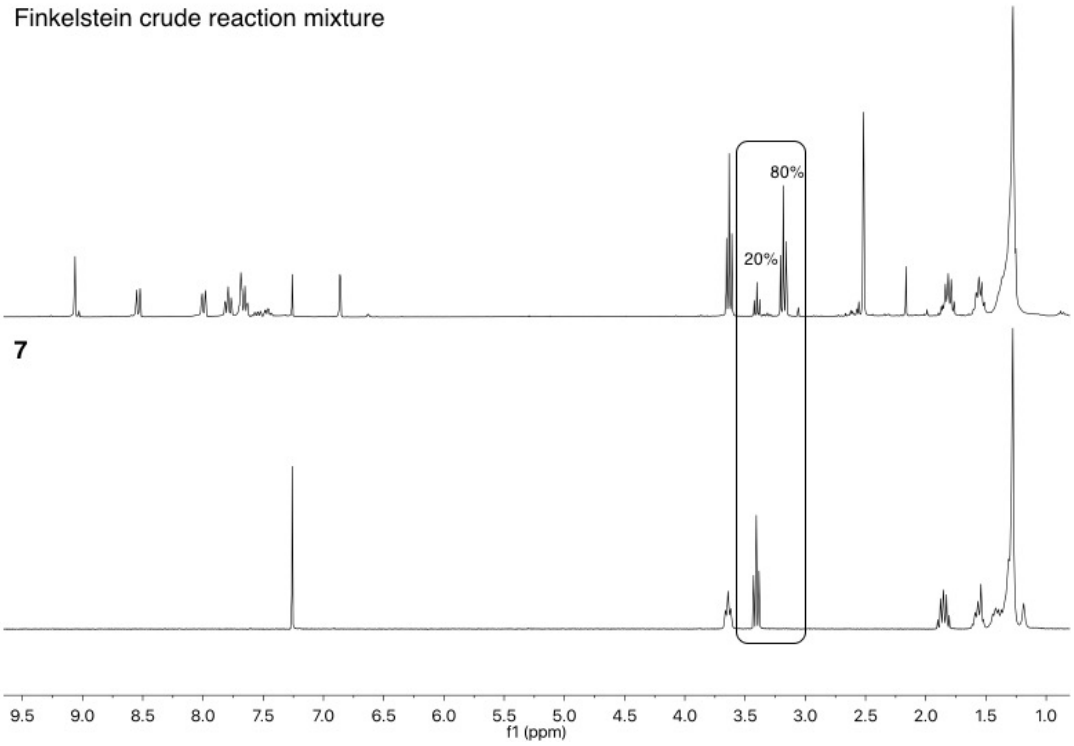


Given the previously reported successful cross-coupling of 4-bromoquinoline and **9**,[114] tris(dibenzylideneacetone)palladium(0) ($Pd_2dba_3$) was used as the palladium source, sodium tert-butoxide (NaOtBu) as the base, toluene solvent, and a reaction temperature of 150°C were applied for the Buchwald hartwig amination of **8** with **9** (**Scheme 4**).

**Figure 3**. Previously reported Buchwald Hartwig cross-coupling of 4-bromoquinoline and **9**.[114]

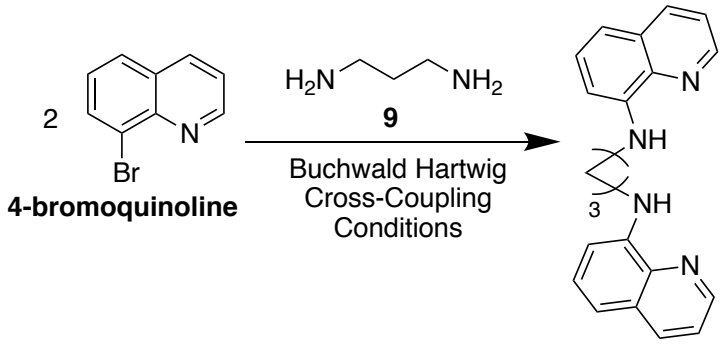


$Pd_2dba_3$ was used as the palladium source because of its solubility in toluene and it did not require further reducing agents to activate.[115] As well, compound **9** possesses α-hydrogens that could oxidize leading to their consumption to generate Pd(0) from other palladium sources, however, more importantly this could affect the stoichiometry between the substrates leading to the formation of more bis product, **11**. The 2-methyl derivative of **8**, as opposed to the 2-trifluoromethyl, had been subject to cross-coupling conditions of 130°C,[105] however due to the electron withdrawing $CF_3$- a higher temperature was chosen to encourage oxidative addition to palladium. Compound **9** has a boiling point of 140°C but refluxing in a sealed Teflon stoppered flask maintained it in the reaction mixture. Both the starting substrates were soluble in toluene.

**Scheme 4**. Buchwald Hartwig cross-coupling of 2-trifluoromethyl-4-bromophenanthridine **8** with 1,3-propyldiamine **9** for the formation of **10.**

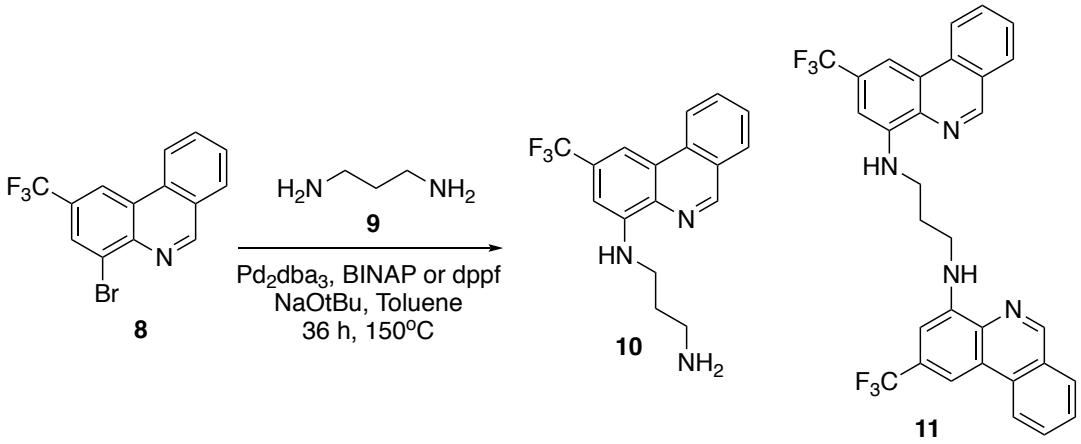

Of the cross-coupling reactions performed the most successful reaction utilized (±)-2,2′-bis(diphenylphosphino)-1,1′-binaphthalene (BINAP) instead of 1,1′-ferrocenediyl-bis(diphenylphosphine) (dppf). This was not surprising as Pd/BINAP is the most widely used and active catalyst for the coupling of aryl bromides with primary amines.[116] The reaction involving dppf was difficult to purify and isolate making it difficult to assess the results of the reaction. Compared to the harsh and ineffective conditions previously employed this catalytic process was a more efficient approach towards the synthesis of **10**.

The structure of BINAP, in the context of the catalytic cycle, is the reason for the success of this cross-coupling reaction. BINAP discourages catalytically inactive bis(amine)aryl halide complexes through chelation of both phosphine groups to the metal, the rigidity of the backbone and small bite angle of 92.7°, relative to dppf's 99.1°, leads to a tight chelate which prevents dissociation of one arm that could lead to β-hydride elimination, and its large size disfavours double arylation of the amine substrate promoting reductive elimination to the arylamine.[116]

Unlike the cross-couple with 4-bromoquinoline[114] only monosubstituted **9** was sought and an excess of 1.4 molar equivalents of primary amine to **8** was added to offset the formation of **11**. However, the crude $^{1}$H NMR indicates formation of 8% of **11** which could be readily removed with a silica plug. Confirmation of the structure of **10** was determined by $^{1}$H NMR spectroscopy. In the $^{1}$H NMR spectrum, the α-methylene groups (2.71 and 1.53 ppm) loose their symmetry resulting in three different chemical shifts (3.45, 2.96, and 1.98 ppm). The seven aromatic protons also resulted in an upfield shift and the singlet in the $^{19}$F NMR shifted from -61.97 ppm (**8**) to -62.39 ppm (**10**). In **Figure 3** the seven aromatic protons are rearranged slightly upfield.

**Figure 3a.** $^{1}$H NMR spectra of **8** and the Buchwald Hartwig cross-coupling product **10**.

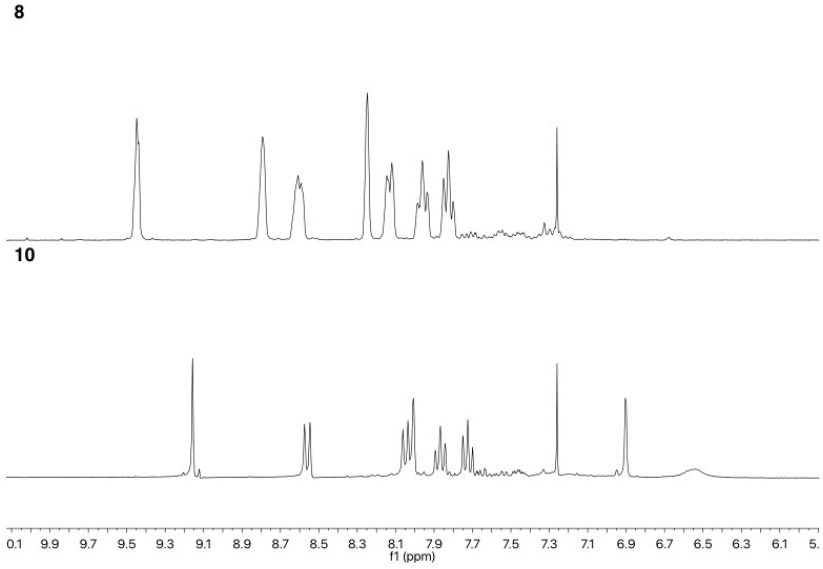


***

Post polymerization modification is an effective means of altering an already existing polymer. In this work, the conditions were demonstrated for primary amines and to extend poly(pentafluorophenyl methacrylate)'s scope alcohol nucleophiles were investigated. Utilizing reductive amination, a trifluoromethyl phenanthridine fluorophore was prepared with a primary alcohol tether. The first step involved formation of the aldehyde **13** with sec-butyl lithium and dimethyl formamide (DMF) in diethyl ether at -78 °C for 6 h. (See **Scheme 5**) The major product was the aldehyde along with unidentified impurities that broadened the baseline of the aromatic region in the $^{1}$H NMR. See **Figure 4**. After an ethanol washing step to remove some of the impurities the contents were carried forward to condensation.

**Scheme 5**. Reductive amination pathway for the synthesis of **16.**

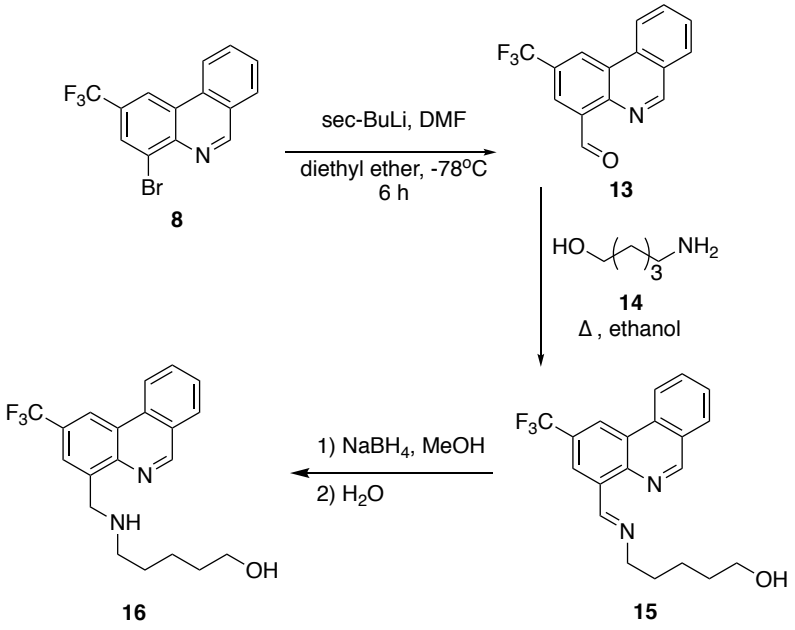


Refluxing **13** with 5-amino pentanol **14** in anhydrous ethanol for 4 h at 90 °C afforded complete conversion to the imine **15**. The imine was reduced with sodium borohydride and resulted in the formation of **16**.

**Figure 4**. $^{1}$H NMR stack of **8**, **13**, **15**, and **16** after each chemical conversion. Compound **15** and **16** contain considerable unidentified impurities that broaden the aromatic and aliphatic regions of the spectrum. * denotes the seven aromatic peaks of interest. The peak at 11.54 ppm belongs to the aldehyde of **13**.

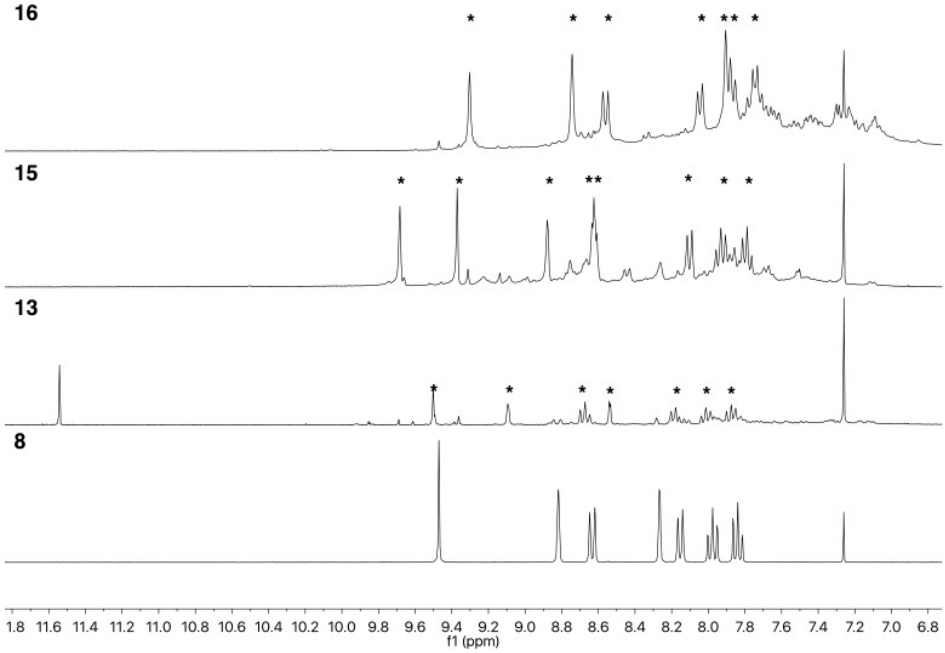


Compound **13** was validated with the appearance of the aldehyde peak at 11.54 ppm. The condensation step was confirmed with the disappearance of the aldehyde peak, formation of the vinylic proton at 9.68 ppm, and the shift in the aliphatic protons of **14**. Reduction was confirmed by the disappearance of the imine peak and appearance of the methylene group at 4.48 ppm.

**Table 2.** Summary of Phenanthridine Fluorophore Reactions

| Primary Amine Tethered Fluorophores | | | | |
|---|---|---|---|---|
| Scheme | Phenanthridine Species | Tether | Comment | Isolated Yield |
| 2 | **6** | **4** | THF reflux | - |
| 2 | **6** | **4** | AN reflux | - |
| 3 | **6** | **7** | Finkelstein Reaction | - |
| 4 | **8** | **9** | Buchwald Hartwig: dppf | - |
| 4 | **8** | **9** | Buchwald Hartwig: BINAP | 74%(m/m) |
| Primary Alcohol Tethered Fluorophores | | | | |
| Scheme | Phenanthridine Species | Tether | Comment | Isolated Yield |
| 5 | **12** | none | Lithiation reaction | quantitative |
| 5 | **13** | **14** | Condensation reaction | quantitative |
| 5 | **15** | none | $NaBH_4$ reduction | quantitative |

## 4.4 Attempted syntheses of tethered phenanthridine fluorophores

Amidst the pursuit for the N-heterocyclic fluorophores a quinonyl species containing a fluorine group for use as an NMR handle was pursued. A Skraup reaction using **17**, sodium iodide, concentrated sulfuric acid, and glycerol was performed to form the 2-trifluoromethyl-4-nitroquinolyl species **18** which was washed and purified by column chromatography. The preparation was adapted from the literature.[117,118]

**Scheme 6.** Alternative synthetic pathway to tethered trifluoromethyl quinolyl fluorophore.

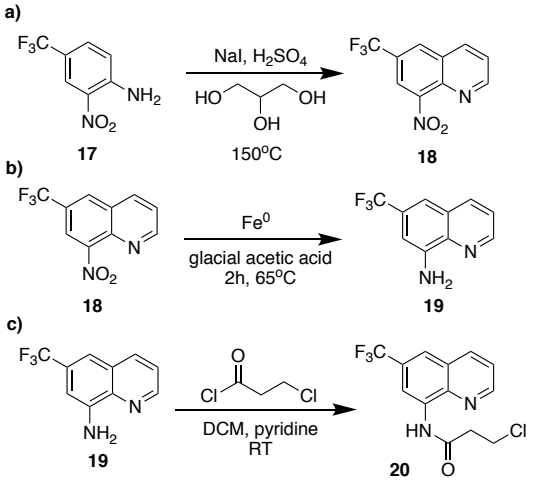


The product was confirmed with the appearance of the diagnostic conjugated imine proton (*) at 9.20 ppm. See **Figure 5**. Compound **18** was reduced with metallic $Fe^0$ to generate the amine species **19** which contains the $–NH_2$ group at 5.19 ppm and the aromatic peaks shifted upfield as a result of the transformation of the strongly electron withdrawing nitro-group.[118] The transformations were also followed by $^{19}F$ NMR where the singlet of **17** at -62.09 ppm shifted upfield to -62.40 ppm (**18**), and then to -62.84 ppm (**19**). Compound **19** was reacted with 3-chloropropionyl chloride.

**Figure 5**. $^{1}$H NMR stack of **17**, **18**, and **19** displaying the synthetic transformations at each step. * denotes the diagnostic conjugated imine proton, ‡ denotes $CDCl_3$ solvent. The green boxes highlight the broad primary amine groups.

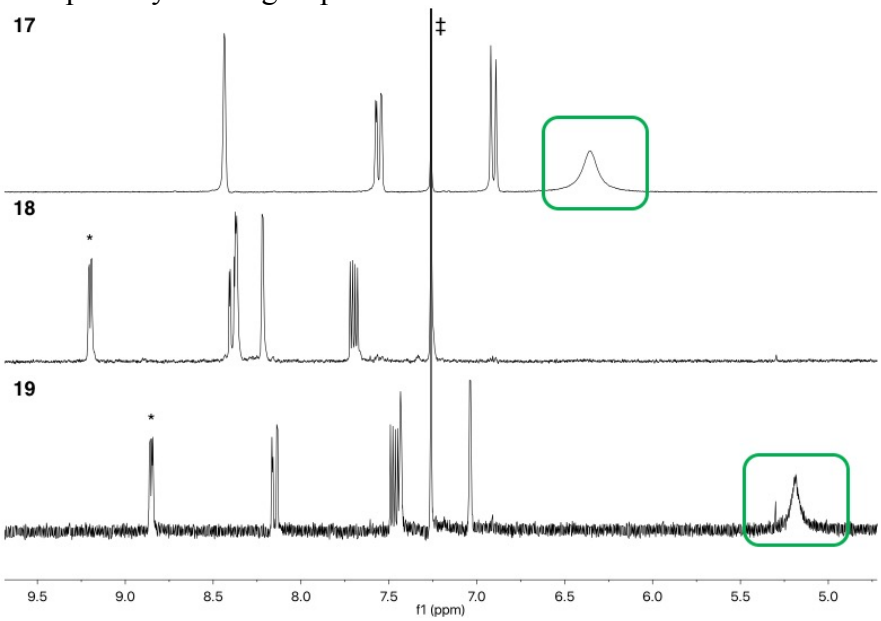


Compound **20** was confirmed (**Figure 7**) most notably with the downfield shift of the amine (2H, 5.19 ppm) to the amide (1H, 9.94 ppm) and was substituted with sodium azide in DMF at 70°C to eventually be reduced by the Staudinger reaction. Difficulty arose during substitution of the chloride since the crude $^{1}$H NMR indicated starting material and many unidentified impurity peaks scattered throughout. To try to augment this reaction step **20a** was used instead since it was cheaper and easier to prepare than **20**.

**Figure 6**. Alternative quinolyl species used to optimize the azide substitution.

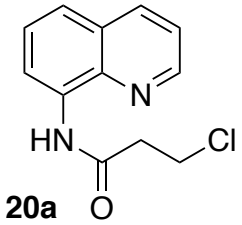


**20a**

The substitution reaction was promoted more cleanly with $Cu(OAc)_2$ additive[119] and the time was shortened to 2.5 h at 85°C to generate the azide substituted product where the

methylene triplets shifted upfield to 3.79 and 2.82 ppm. Coincidently, the successful synthesis of **10** (above) was achieved and this route was no longer pursued.

**Figure 7.** Substitution of 3-chloro-propionyl chloride with **19**. $^{1}$H NMR of **19** and **20**. The aliphatic region (not shown) shows downfield shifts of the methylene triplets from 3.78 and 2.99 ppm to 3.97 and 3.06 ppm. Substantial 3-chloropropanoic acid was present after work up. Inset: $^{19}$F NMR of **20** indicating a single peak at -62.79 ppm.

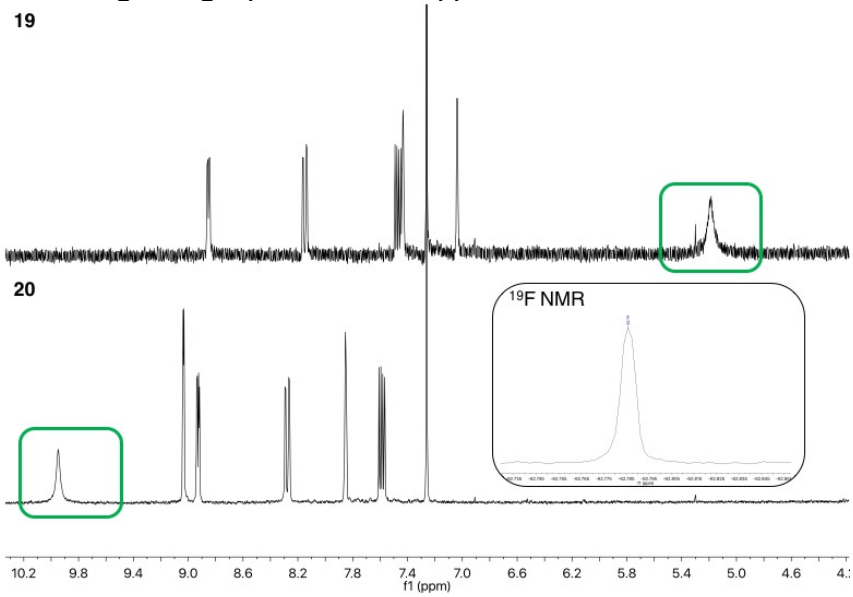


Other quinolyl and phenanthridyl based fluorophores were explored with some success. They are summarized in **Scheme 7** and **Table 3**.

**Scheme 7.** Summary of miscellaneous fluorophores

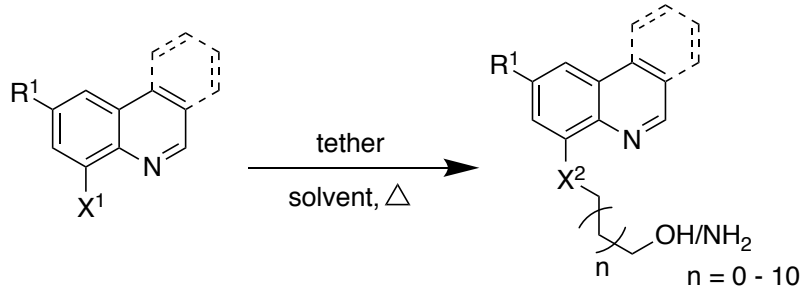


**Table 3.** Summary of quinolyl and phenanthridyl fluorophores

| Reaction No. | Phen. species | $R^1$ | $X^1/X^2$ | Tether | Solvent | Temp. (°C) |
|---|---|---|---|---|---|---|
| **1** | **21** 'quinolyl' | H | $NH_2$/NH | **7** | AN | 80 |
| **2** | **21** 'quinolyl' | H | $NH_2$/NH | **7** | AN/TEA | 120 |
| **3** | **22**'phenanthridyl' | tBu | $NH_2$/NH | **7** | AN | 70 |
| **4** | **23** 'quinolyl' | H | OH/O | 2-bromo-ethanol | DMF/$K_2CO_3$ | 80 |
| **5** | **23** 'quinolyl' | H | OH/O | 3-bromopropylamine hydrobromide | DMF/$K_2CO_3$ | 60 |

In **Table 3** reactions **1** and **2** involved placing **21** under similar reaction conditions to **6** whereby the reaction was intended to be driven forward by temperature. However only starting materials were recovered from the crude mixture. Similarly, **22** was used because of the electron donating character of the tert-butyl group on position 2, but only starting material was recovered. Reactions **4** and **5** used **23**, 4-quinolinol, to side step the use of the aromatic amine nucleophile for the substitution. Reaction **5** did not result in the intended product but reaction **4** generated the ethyl tethered quinolinol, **24** (**Figure 8**).

**Figure 8**. Synthesis of 2-hydroxyethyl-quinolinol **24**. Stacked $^{1}$H NMR spectra of 2-bromoethanol, **23**, and product **24**. The rearrangement of the aromatic protons and the downfield shift of the methylene protons at 4.34 and 4.05 ppm indicates that the substitution reaction took place. * indicates residual solvent.

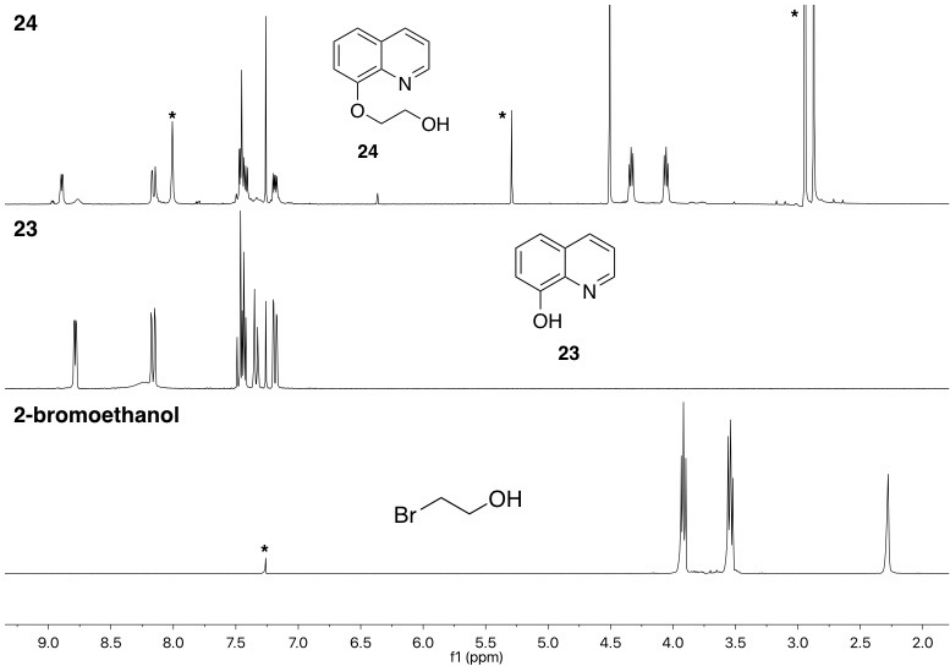


## 4.5 Post polymerization modification of linear poly(pentafluorophenyl methacrylate)

With fluorophore **10** in hand, we next set out to functionalize linear and cyclic pPFMA. The chief aim of synthesizing cyclic polymers with active ester side chains is to further explore the chemistry of various functional molecules or bring about functionality to small molecules by appending them readily onto the scaffold. This section surveys the conditions and small molecules that were explored in PPM.

**Figure 9.** Structure of poly(pentafluorophenyl methacrylate) **25**.

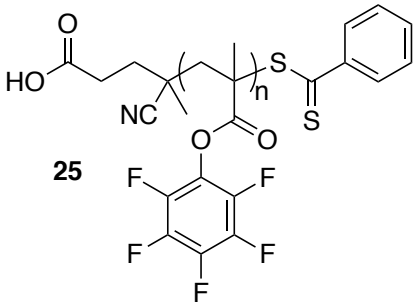


**25**

In the literature, post polymerization modification was attempted on linear polymers of poly(pentafluorophenyl methacrylate), **25**, to determine the conditions necessary for substitution. A library of water soluble polymers was prepared using **25** and those conditions were used as the starting point for optimization.[86] A consideration for nucleophilic acyl substitution for linear polymers prepared by RAFT is the substitution of the dithiobenzoate end group. The aminolysis is well known for small molecule dithioesters and the reactivity readily translates to the polymer. The chemistry of the ω-end group is incredibly rich for RAFT polymers[120,121] and its versatility is the basis for the ring closing reaction in this work. In the literature, it was observed in GPC and MALDI-MS that thiol terminated polystyrene doubles in molecular weight due oxidative coupling to the disulfide.[122] In the same study a collection of methacrylate backbone polymers were also investigated and found to form a back-biting thiolactone product by which the molecular weight remained unaltered (**Fig. 10**).[122]

**Figure 10**. Organic structure of the thiolactone (orange) terminated methacrylate polymer.

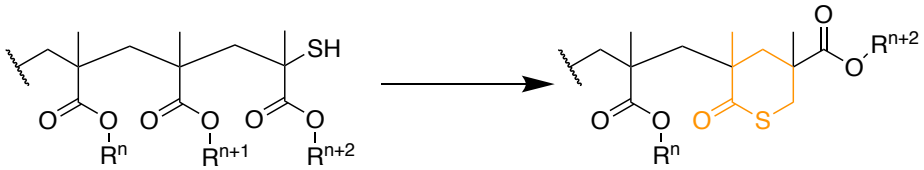


**generic methacrylate polymer** **thiolactone terminated polymer**

The standard reduction potential for the half reaction: RS-SR + $2e^-$ → $2RS^-$ is - 0.25 V and the reverse half reaction can be achieved under relatively mild conditions such as in the presence of oxygen.[121] However, the methacrylate polymers seemed to side step this when the thiol backbites the penultimate carbonyl and forms a stable five-membered ring. Interestingly, Klok et al. determined, with an Ellman's assay, that nearly 100% of the thiol end groups remain present in **25** after aminolysis.[86]

It is this literature precedent and a lack of larger molecular weight products in the GPC that suggest that linear PPM products of **25** potentially form a thiolactone but do not react further in cross-linking or oxidative coupling reactions. The PPM conditions are the main subject of investigation and since no complications arose from the thiol end group it was not further investigated. An asterisk at the ω end of the polymers in the following figures and schemes below denotes the unknown identity of the end group.

## 4.5.1 Post polymerization modification of linear poly(pentafluorophenyl methacrylate) with 4-aminoquinoline 27

**Scheme 8** Post polymerization modification of **26** with 4-aminoquinoline **27**.

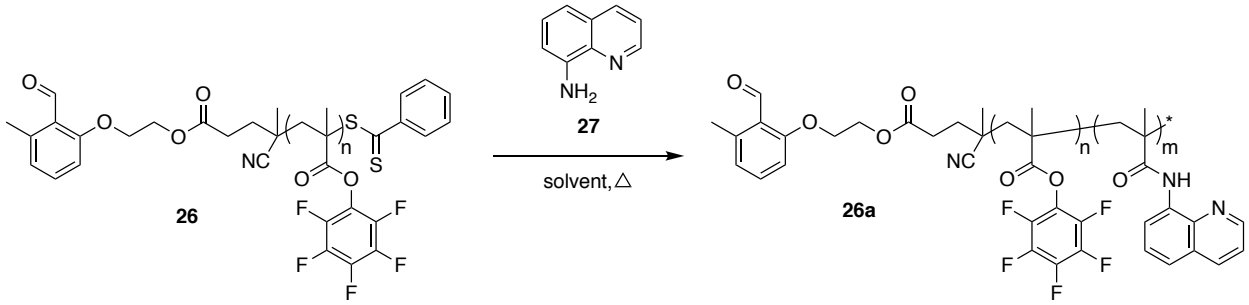


| Reaction No. | Equivalents[a] | Solvent | Temp. (°C) | Base |
|---|---|---|---|---|
| **1** | 24 | DCM | 50 | none |
| **2** | 26 | DCM | 50 | TEA |
| **3** | 100 | DCM | 60 | none |
| **4** | 190 | DCM | 60 | none |
| **5** | 100 | 1,4-dioxane | 60 | DMAP |
| **6** | 90 | 1,4-dioxane/DMF | 80 | DMAP |
| **7** | 90 | 1,4-dioxane/DMSO | 80 | none |

a – molar equivalents of amine to polymer repeat units, n. The number average molecular weight of the linear precursor was assumed to be 47900 g/mol as determined by GPC with a ten-point polystyrene calibration standard. All entries do not have conversion as determined by $^{1}$H NMR. Triethyl amine (TEA), 4-dimethyl aminopyridine (DMAP).

Compound **27** lacks a molecular tether (**Scheme 8**) and was initially used for PPM under various conditions to try to circumvent the steps needed to attach a tether onto an aromatic amine. It was thought that the pentafluorophenyl leaving group was more labile and that this would help overcome the sterics.

Substitution was not achieved as determined by $^{1}$H NMR since the material recovered did not contain any new broad aromatic peaks. The starting polymeric material was a light pink colour and was isolated as a white solid which indicated aminolysis of the dithiobenzoate. No peaks were present in the 2.3 – 3.0 ppm region indicative of thiolactone formation.[122] This set of reactions confirmed that a tether was necessary for substitution.

## 4.5.2 Post polymerization modification of linear poly(pentafluorophenyl methacrylate) with 2-amino-propanol 28

**Scheme 9.** Post polymerization modificationof **26** with 2-amino-propanol **28**.

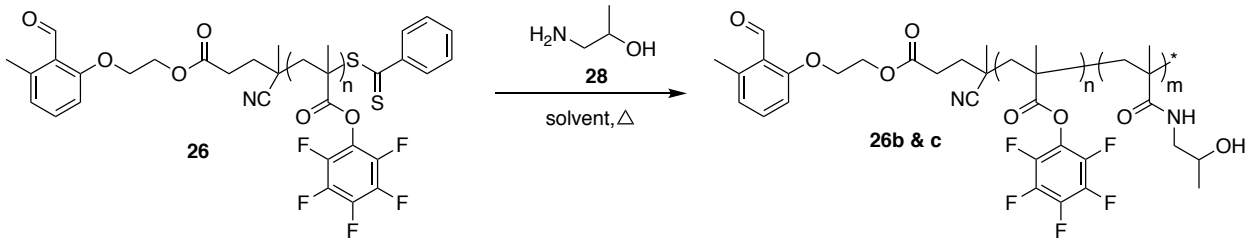


| Reaction No. | Solvent | Temp. (°C) | Base | Status |
|---|---|---|---|---|
| **1** | 1,4-dioxane / DMF (10:1)v/v | 70 | none | PPM observed |
| **2** | 1,4-dioxane / DMF (10:1)v/v | 60 | TEA | PPM observed |
| **3** | 1,4-dioxane / DMF (10:1)v/v | 60 | none | 100% conv. |
| **4** | 1,4-dioxane / DMF (10:1)v/v | 50 | TEA | PPM observed |
| **5** | 1,4-dioxane / DMF (1:1)v/v | 90 | none | could not isolate |
| **6** | 1,4-dioxane / DMF (5:1)v/v | 60 | none | 100% conv. |
| **7** | 1,4-dioxane / DMF (7:1)v/v | 60 | none | 100% conv. |

Post polymerization modification of polymer **26** using 2-aminopropanol (**28**) was carried out under neutral and basic conditions in a solution of 1,4-dioxane and DMF in the absence of water to synthesize poly(*N*-(2-hydroxypropyl)methacrylamide) (pHPMA) **26c** (where n = 0 %, m = 100 % in **Scheme 9**). Since **28** does not contain other useful nuclei NMR handles and due to the overlapping peaks in the $^{1}$H NMR spectrum partial conversion could be observed but not quantified without external standards. Full conversion could be ascertained by the complete disappearance of the side groups in the $^{19}$F NMR. The random copolymer **26b** (n = (1-m)) was soluble in $CDCl_3$ but **26c** was soluble only in $D_2O$ (**Figure 11)**. Similar reactions of **26c** report using basic conditions but neutral conditions were explored and shown to be possible.[107,123–126]

**Figure 11**. NMR of poly(*N*-(2-hydroxypropyl)methacrylamide) **26c**.

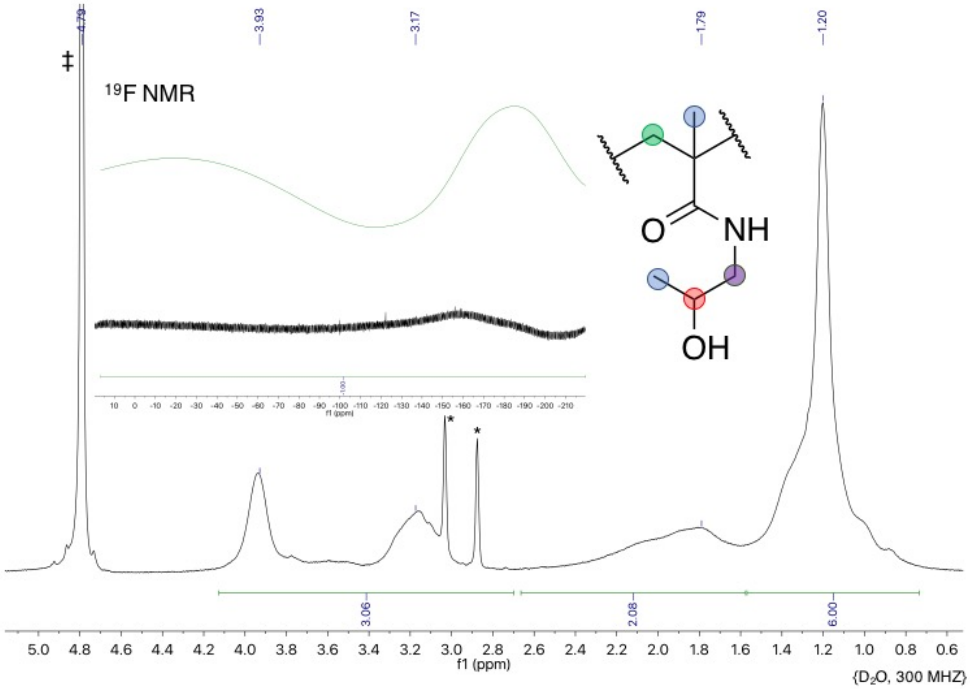


$^{1}$H NMR of pHPMA in $D_2O$. Highlighted protons: (Blue) methyl groups integrating for 6 protons, (green) backbone methylene integrating for 2 protons, (red) side group methane and (purple) side group methylene together integrating for 3 protons. Inset: $^{19}$F NMR confirming lack of side groups. Integral indicates no peaks present. Rolling character to baseline is due to the Teflon lining on the NMR probe. * indicates residual DMF present, ‡ indicates NMR solvent peak.

1,4-Dioxane was used to solubilize the **26** since it was partially or entirely insoluble in DMF and tended to precipitate out at 60°C. DMF is thought to behave as a catalyst in the nucleophilic acyl substitution (**Fig. 12**).[107]

**Figure 12**. Proposed catalytic mechanism of nucleophilic acyl substitution with DMF.

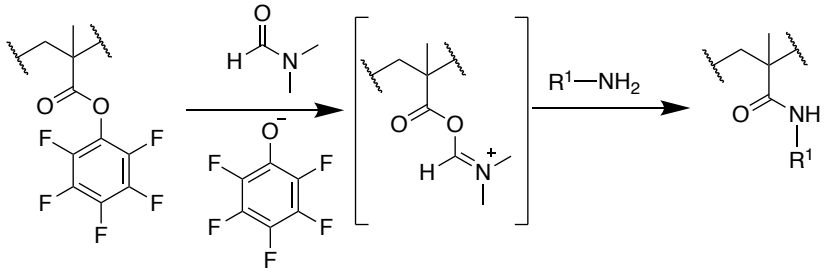


The random copolymers were isolated as a powdered precipitate formed after the reaction mixture was added drop-wise into a stirring solution of diethyl ether. They could not be isolated

as solids from hexanes, pentane, methanol or ethanol. The reaction conditions for **26b** and **c** were applied to the substitution of **26** using **10**. See **Scheme 10**.

## 4.5.3 Post polymerization modification of linear poly(pentafluorophenyl methacrylate) with phenanthridyl 10

**Scheme 10** Post polymerization modification of **26** with **10**.

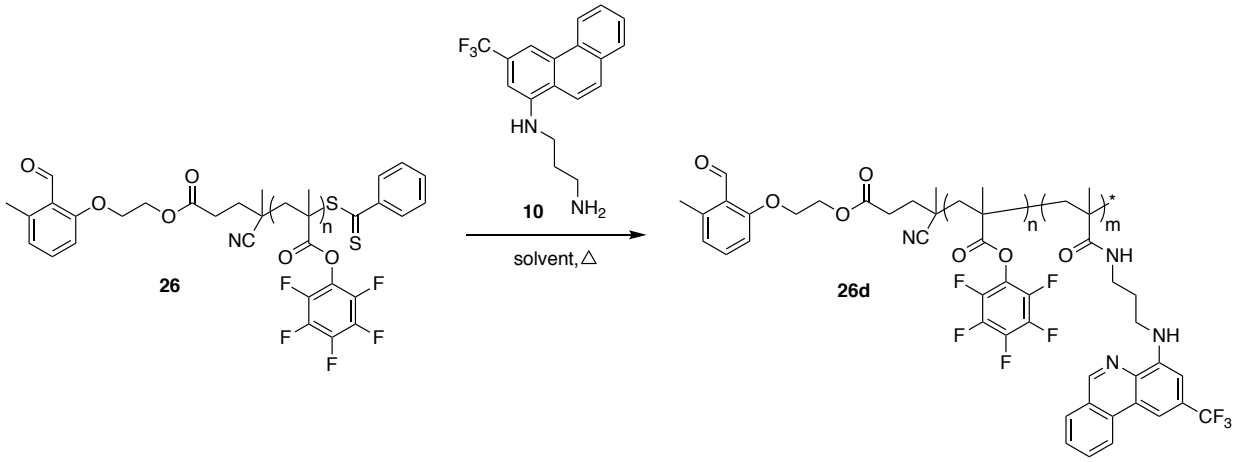


| Reaction No. | $n_{linear, NMR}$ | Equivalents[a] | Time (h) | Conc. **10** [M] | % Conv.[b] |
|---|---|---|---|---|---|
| **1** | 188 | 0.25 | 18 | 0.015 | 2.3 |
| **2** | 188 | 0.75 | 23 | 0.053 | 31 |
| **3** | 67 | 0.33 | 19.5 | 0.018 | 12.3 |
| **4** | 67 | 0.33 | 19.5 | 0.016 | 12.0 |

All reactions were performed at 60°C in 20% (v/v) DMF : 1,4 –dioxane
a - equivalents of fluorophore to n repeat units of polymer
b - % conversion was determined by $^{19}F$ NMR using the peak at -62.8 ppm

The mild conditions determined for the synthesis of **26b** and **c** were applied to fluorophore **10**. It was found that the higher the concentration of **10,** the higher the conversion for approximately a similar amount of hours See table in **Scheme 3**. The trifluoromethyl group in **10** was used as a $^{19}F$ NMR handle to quantify relative % conversion of the backbone. Polymers of **26d** were isolated as a powdered precipitate by dissolving the contents in THF and adding I

drop-wise to a stirring solution of methanol. The dark yellow solid was characterized $^{1}H$ and $^{19}F$ NMR spectroscopy (**Figure 13a-b**).

**Figure 13**. $^{1}H$ and $^{19}F$ NMR spectra of **26d** compared to **26** and **10**.

**a)**

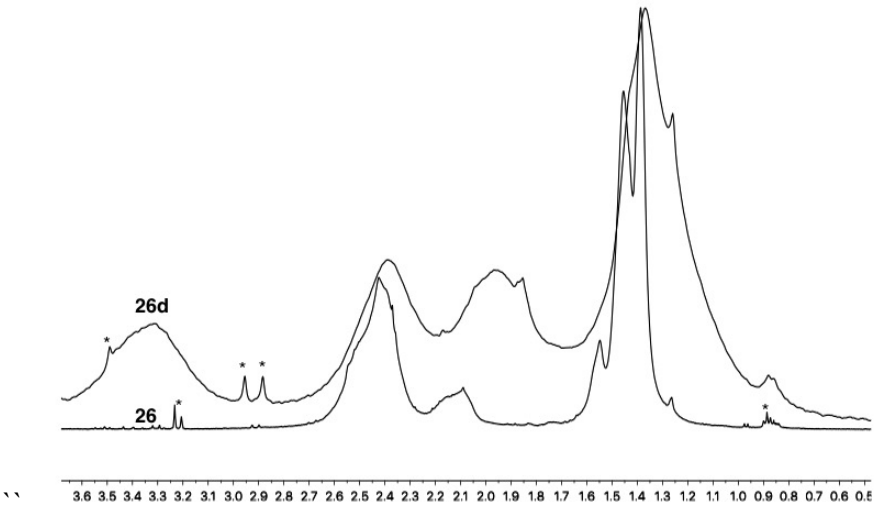


**b)**

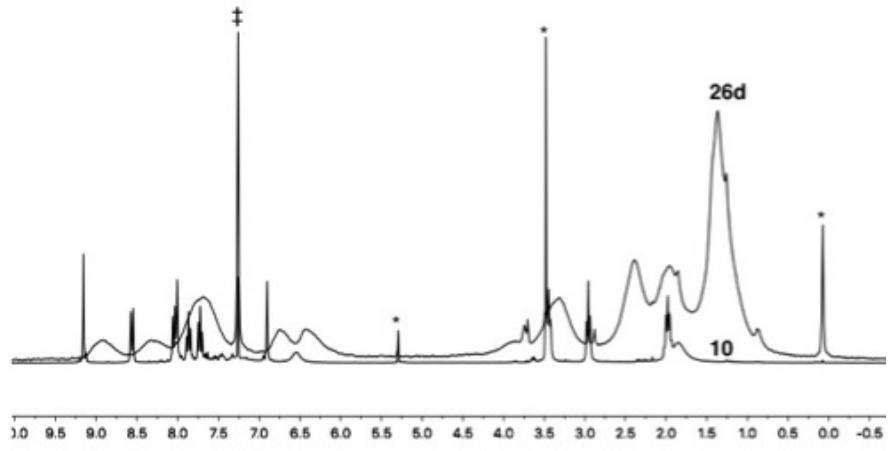

**c)**

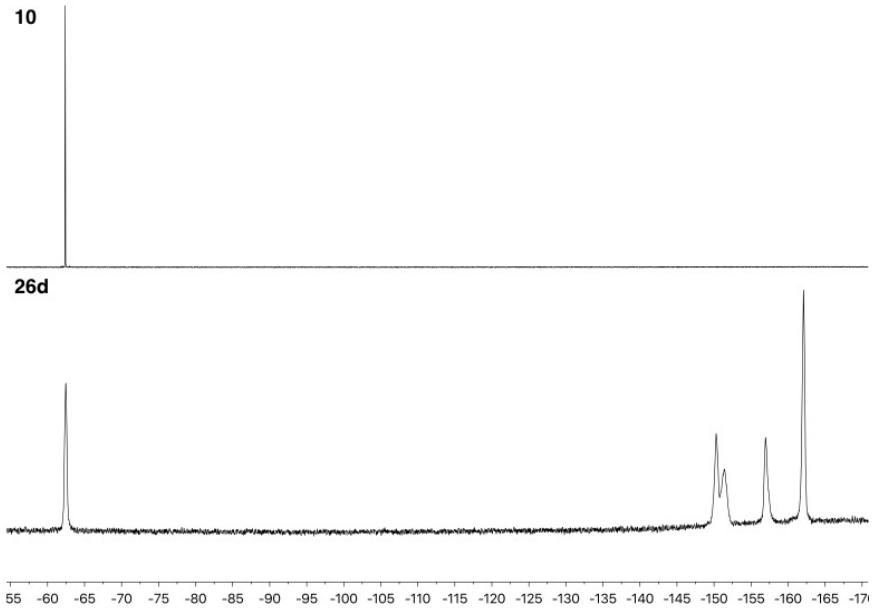


**a)** $^{1}$H NMR stack of **26** and **26d** in the aliphatic region denoting the change to the backbone upon incorporation of **10 b)** A broad view of the $^{1}$H NMR stack of **10** and **26d** indicating how the narrow peaks of the small molecule broaden upon incorporation onto the polymer **c)** $^{19}$F NMR stack of **10** and **26d** displaying a convenient NMR handle and broadening upon incorporation onto the chain. * indicates residual solvent. ‡ indicates NMR solvent peak.

To try to confer water soluble properties to the fluorescent substitution product **26d** the rest of the pentafluorophenyl side groups (from **Scheme 10**, Reaction No. 2) were substituted with **28** (**Scheme 11**).

The product isolated **26e** (m = 30%, n = 70%) was a yellow solid that was only soluble in DMF and partially soluble in $CDCl_3$. It was insoluble in $D_2O$ and diethylether. The solubility was qualitatively determined by observing the presence of a yellow colour change to the NMR solvents. The $^{19}$F NMR spectra indicated that **10** remained intact and $^{1}$H NMR indicated that the aliphatic region had been altered (**Figure 14**).

**Scheme 11** Post polymerization modification of **26d** with **28**; conferring water solubility to linear fluorescent polymer.

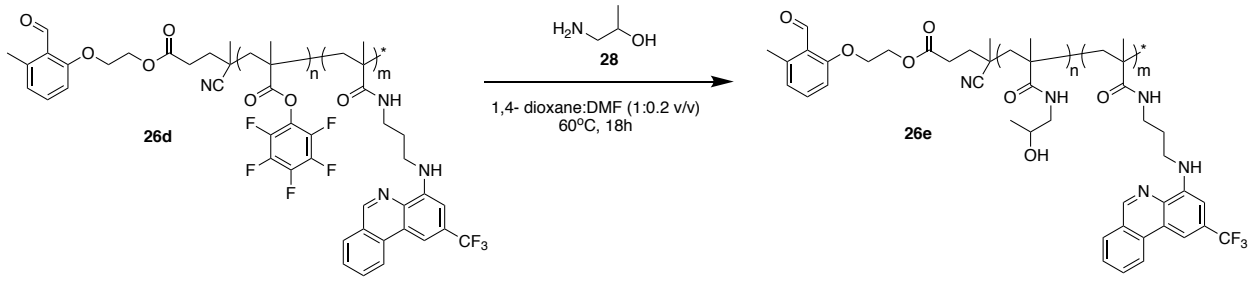


**Figure 14**. Post polymerization modification product **26e.** $^{1}$H NMR stack (top) of **10**, **26d**, and **26e**. * indicates residual solvent. ‡ indicates NMR solvent peak. The peak at 2.39 ppm in **26d** belongs to the methylene backbone of **26** and the broad methyl peak has an upfield shift from 1.36 to 1.15 ppm after incorporation of **28**. $^{19}$F NMR stack (bottom) of **10**, **26d**, and **26e**.

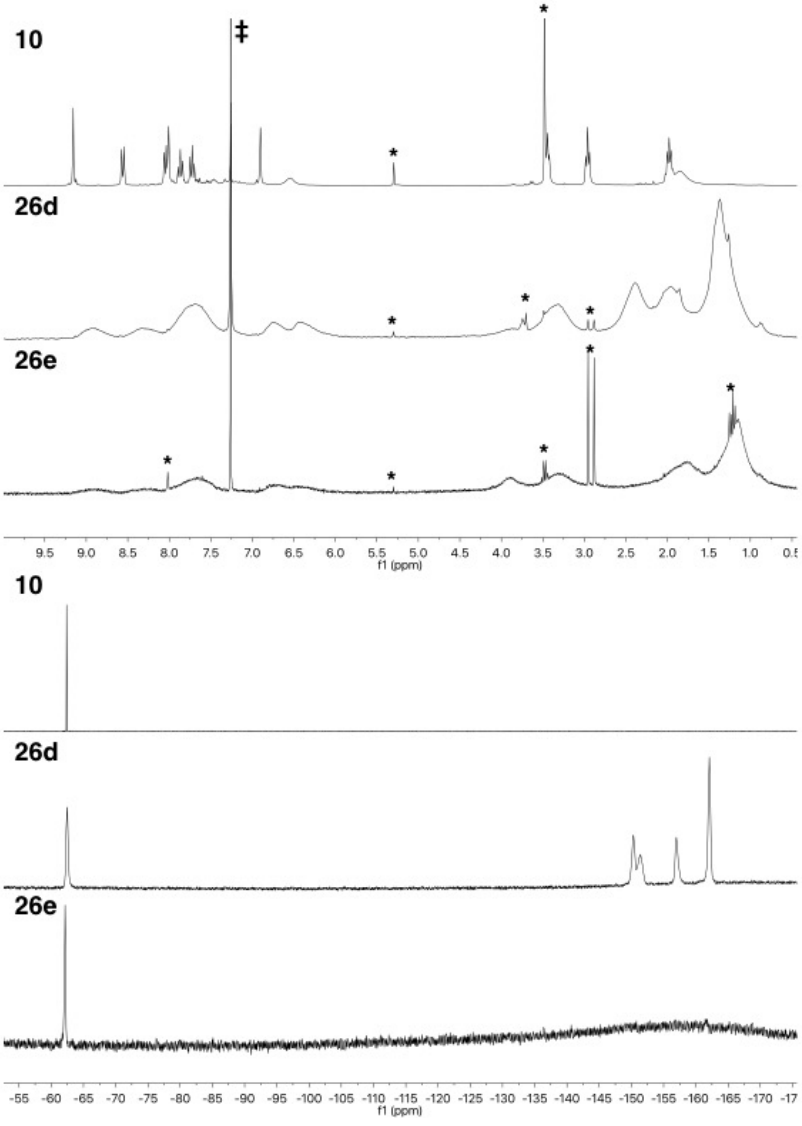

## 4.5.4 Post polymerization modification of linear poly(pentafluorophenyl methacrylate) with 2-amino-ethanol 29

**Scheme 12** Post polymerization modification with 2-amino-ethanol **29**.

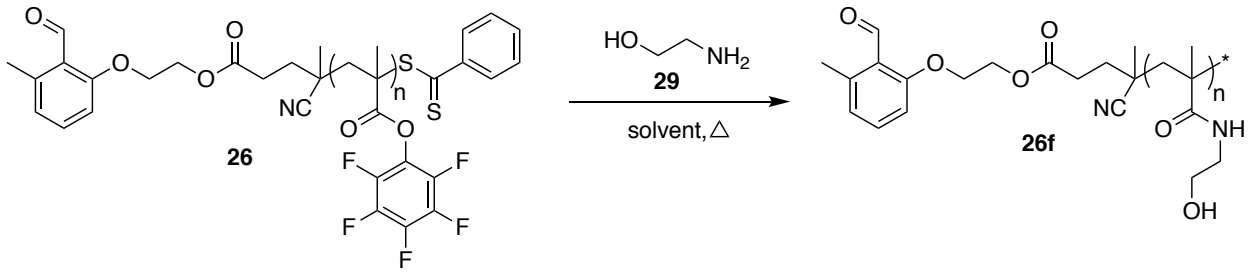


When **26** was dissolved in 20% (v/v) DMF:1,4-dioxane and heated to 60°C with an excess of **10** and **28** and allowed to compete the product was entirely pHPMA **26c**.

Compound **29** and **26** were subject to PPM conditions to synthesize poly(N-(2-hydroxyethyl) methacrylamide) **26f**. $^{1}H$ and $^{19}F$ NMR was used to characterize the white solid isolated (**Figure 15**). The polymer **26f** is an interesting material because it was tested for use as a soft contact lens material[127] and has been attached onto surfaces[128]. Herein a synthetic pathway has been explored that allows access of this material. No further analysis was performed.

**Figure 15**. $^{1}H$ NMR of poly(N-2-hydroxyethyl methacrylamide) **26f**. Inset: $^{19}F$ NMR indicating complete substitution. * residual THF solvent and unidentified impurity.

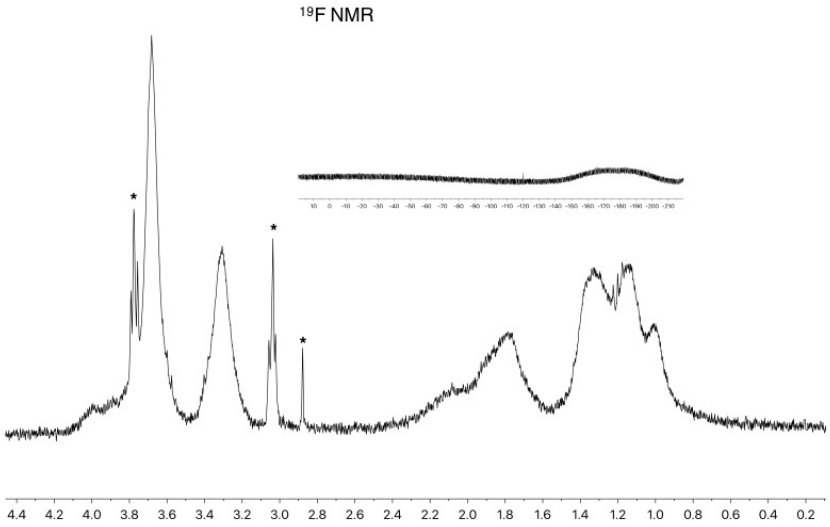


## 4.5.6 Post polymerization modification of linear poly(pentafluorophenyl methacrylate) with dodecanol 30

Transesterification was investigated for linear polymers of pPFMA. The attachment of various molecules via the formation of an ester onto a FDA approved polymer scaffold reveals another path to making these materials and can lead to materials that combine the effects of both the FDA polymer and small molecule.

**Scheme 13**. Post polymerization modification with dodecanol **30** under neutral, basic, and acidic.

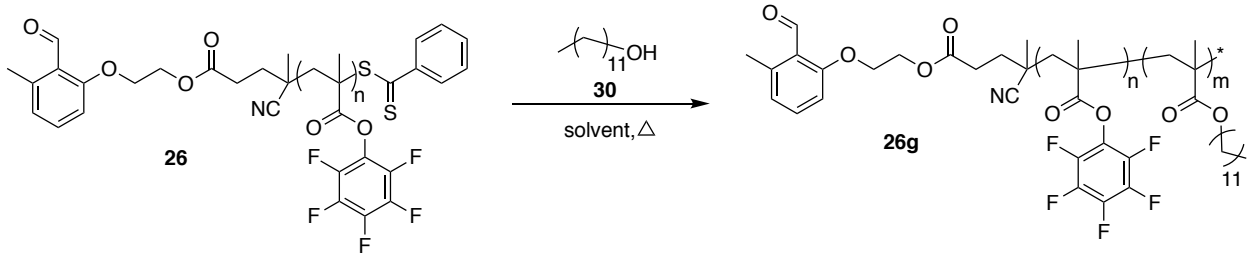


| Reaction No. | Equivalents | Catalyst | Time (h) | Status |
|---|---|---|---|---|
| **1** | 1 | - | 22 | no reaction |
| **2** | 0.5 | 1 eq DMAP | 19 | no reaction |
| **3** | 0.5 | 0.6 eq pTSA | 19 | observed |

Reactions were performed in 2:1 DMF:1,4-dioxane (v/v) and 90°C. pTSA: *para*-toluene sulfonic acid

The PPM of alcohols towards **26** was investigated under neutral, basic, and acidic conditions. It was found that, unlike the PPM of poly(pentafluorophenyl acrylate), substitution occured under acidic conditions.[107] The pentafluorophenyl methacrylate and acrylate have a reverse reactivity trend with regards to acid and base catalyzed transesterification.

**Table 4.** Transesterification Trend

| Pentafluorophenyl species | **Acid Catalyzed** | **Base Catalyzed** |
|---|---|---|
| **Methacrylate** | shows substitution | not observed |
| **Acrylate**[107] | negligible | shows substitution |

The main difference between the said polymers is the methyl group on the backbone and its influence on the equilibrium between the ester prior to substitution and the tetrahedral intermediate which eventually collapses to give back the starting ester or product. The evidence for substitution is the downfield shift of the penultimate 'b' and adjacent 'a' methylene groups of the alcohol[107] (**Fig. 16**). These peaks were referenced and determined not to be due to THF solvent. The peaks belonging to the nine methylene units 'c' composing the core of **30** retain their chemical shift and the terminal methyl 'd' is slightly broadened.

**Figure 16**. $^1$H NMR spectra indicating transesterification **26** with dodecanol **30** under acidic conditions.

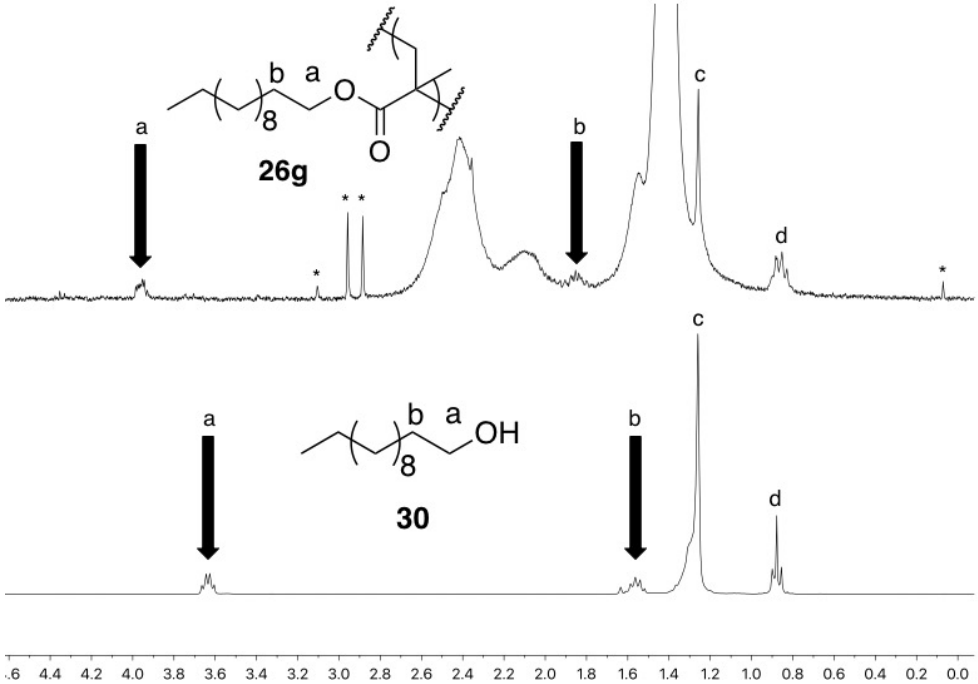


$^1$H NMR of **26g** and **30** (Reaction No. **3**) arrows indicate the shift in the methylene groups upon substitution.* indicates residual DMF solvent, an unidentified impurity, and stopcock grease.

**Scheme. 14** Attempted Post polymerization modification of **26** with **24**.

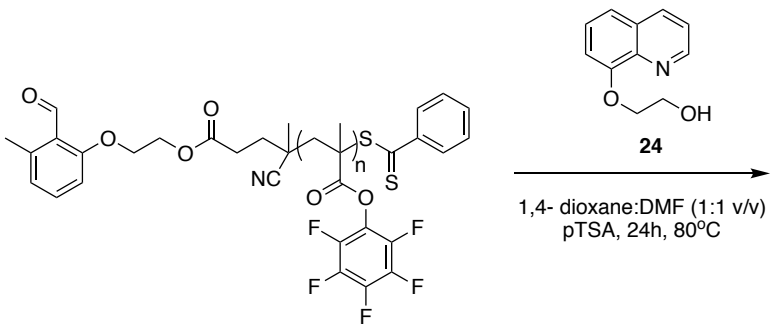


Nucleophilic acyl substitution with **24** was unsuccessful under acidic conditions where pTSA was used as the acid catalyst (**Scheme 14**). In the substitution reaction with dodecanol **30** (**Scheme 7**, **Reaction No. 3**) very little conversion resulted despite that it was a linear and minimally sterically hindered molecule. The reason that the reaction with **24** did not proceed comes down to the sterics of the aromatic rings and the weaker energetic incentive for

transesterification. Similarly, this is also why **16** (**Scheme 15**) did not substitute the pentafluorophenol group despite having a more extended tether length.

**Scheme 15** Attempted post polymerization modification of **26** with **16**.

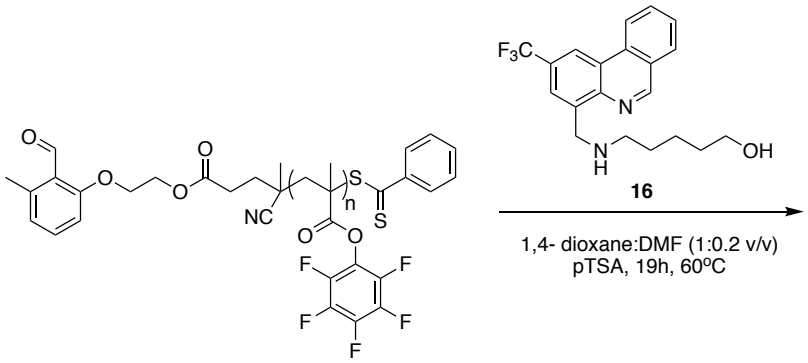


The formation of the ester could possibly be driven forward with more pTSA, longer reaction time, and a higher temperature.

## 4.6 Post polymerization modification of cyclic poly(pentafluorophenyl methacrylate) with phenanthridyl 10

Once the conditions for PPM were determined and explored for the linear polymeric species the conditions were used for cyclic polymers of poly(pentafluorophenyl methacrylate) **26**. After corroborating $^{1}$H NMR, GPC, and UV-Vis spectroscopy data was acquired indicating the successful synthesis of the cyclic polymers they were modified with a fluorescent phenanthridyl reporter molecule **10**. The modified cyclics generated are summarized in **Scheme 16**.

**Scheme 16**. Post polymerization modification of cyclic poly(pentafluorophenyl methacrylate) **31**

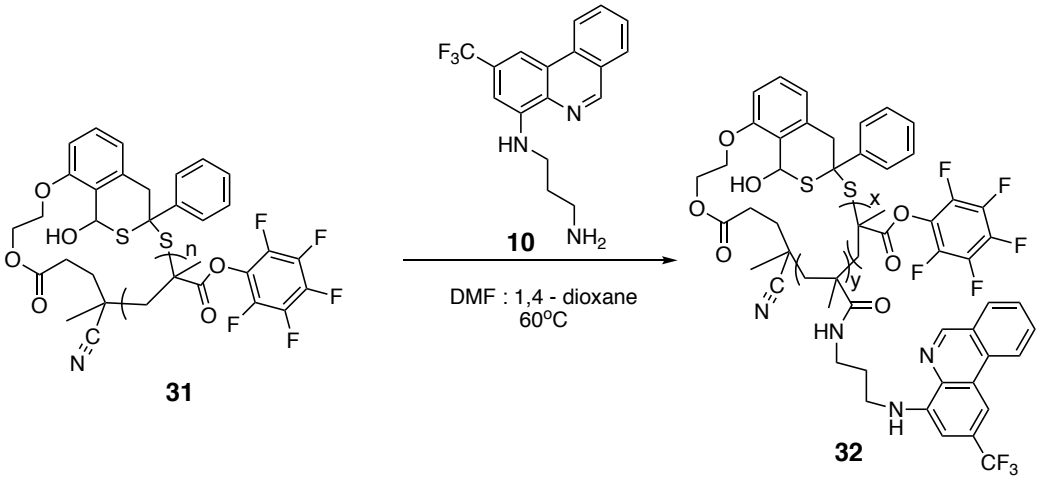


| Entry | Product | Cyclic Precursor | Linear, n | | % Conversion |
|---|---|---|---|---|---|
| | | | $n_{NMR}$ | $n_{GPC}$ | |
| 1 | **32** | Table 7, Entry 9 | 70 | 73 | 12 |
| 2 | **32a** | Table 7, Entry 4 | 33 | 34 | 17 |
| 3 | **32b** | Table 8, Entry 4 | 43 | 41 | 47 |
| 4 | **32c** | Table 8, Entry 3 | 43 | 41 | >99 |
| 5 | **32d** | Table 8, Entry 9 | 58 | 52 | 59 |

Cyclic precursor locations found in Chapter 3.
% conversion as determined by $^{19}F$ NMR

PPM was performed under Schlenk conditions with anhydrous solvent and the products were isolated by precipitation by adding the reaction mixture into a stirring solution of methanol. A $^{19}F$ NMR was collected of the yellow solid to determine the conversion of the side groups and GPC traces of these materials were monomodal (**Fig. 17**). To determine if cyclic integrity was maintained after PPM fluorescence emission spectra were collected. Cyclic polymers are expected to show a larger intensity compared to a similarly modified linear polymer.

In order to be able to compare the emission of the cyclic polymers the corresponding linear telechelic polymers **26** were modified to similar conversions. **Scheme 17** summarizes the results for PPM of the linear species.

**Figure 17**. Poly(pentafluorophenyl methacrylate) bearing a fluorescent side group phenanthridyl species **10.** Stacked $^{19}F$ NMR of **Entry 1** (top) and the cyclic precursor (bottom). Green dotted box highlights the phenanthridyl trifluoromethyl NMR handle. Inset: GPC trace collected in THF at 1 mL/min of **32**.

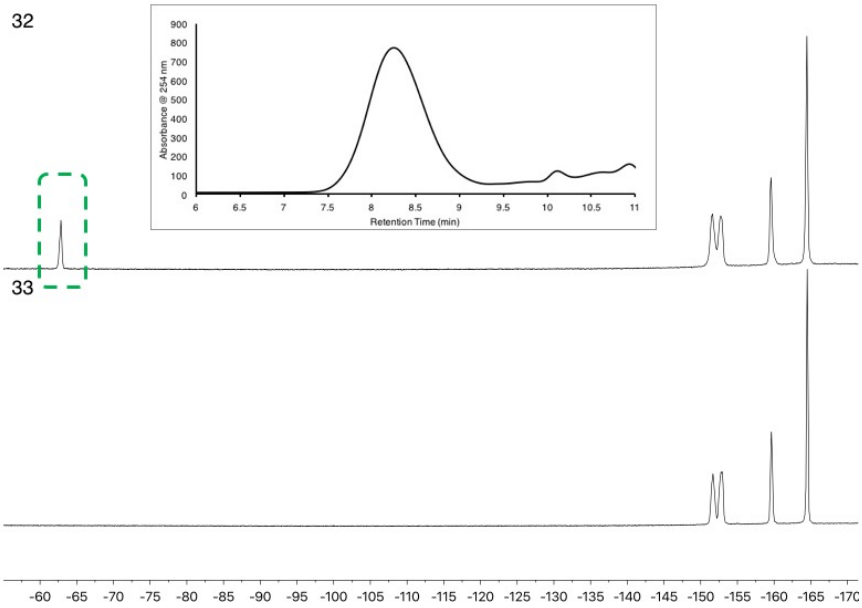


**Scheme 17**. Post polymerization modification of linear poly(pentafluorophenyl methacrylate) **26** for comparison to cyclic polymers.

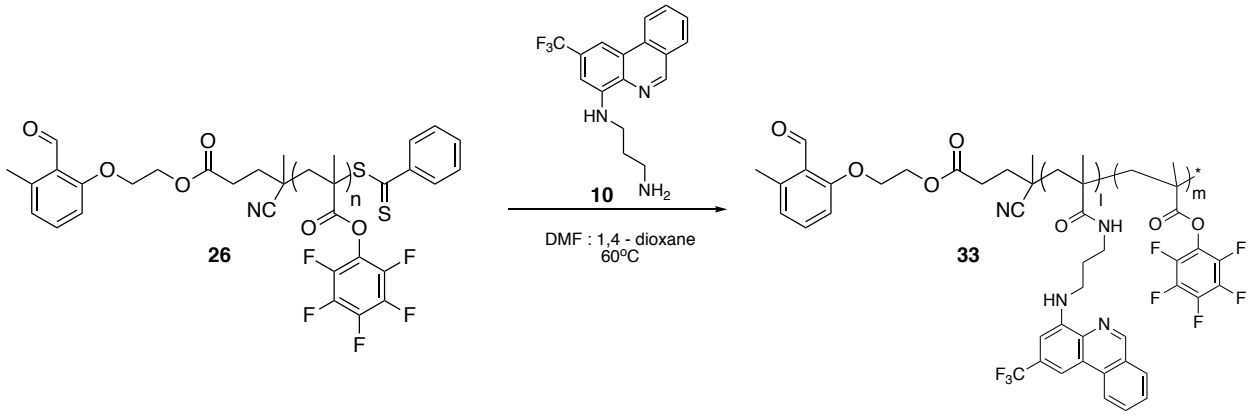


| Entry | Product | $MW_{n,cyclic}/MW_{n,linear}$ | % Conversion |
|---|---|---|---|
| 1 | **33** | 0.88 | 11 |
| 3 | **33b** | 1.00 | 36 |
| 4 | **33c** | 0.99 | >99 |
| 5 | **33d** | - | 50 |

PPM cyclic entries numbering followed from **Scheme 16**.
% conversion as determined by $^{19}F$ NMR

Polymers **32c** and **33c** with >99% of the side groups converted were made up into chloroform solutions with similar concentrations as confirmed with UV-Vis spectroscopy.

**Table 5**. UV-Vis spectrum comparing concentrations of modified linear and cyclic poly(pentafluorophenyl methacrylate).

| Wavelength (nm) | Linear (absorbance) | cyclic (absorbance) |
|---|---|---|
| 389 | 0.072369 | 0.074584 |

Then fluorescence measurements were made using identical cuvettes containing the polymers. The samples were excited at 389 nm and an emission spectrum was collected from 400 to 730 nm (**Fig. 18**). The fluorescence emission intensity was corrected by dividing by the absorbance value at 389 nm. The cyclic modified polymer displayed a larger intensity than the linear species for the same number of fluorophores in solution. The reduced conformational entropy of the cyclic scaffold augments the emitting capabilities of **1**. In an emission event the contribution of non-radiative relaxation is minimized by the cyclic polymer since the fluorophores are more isolated due to the rigidity of the ring leading to less aggregation-caused self-quenching[10] in comparison to the linear polymer.

The fluorescence measurements were repeated for **32** and **33** see **Figure 19** in **4.7 Experimental** for details.

**Figure 18.** Absorbance and fluorescence emission spectra of modified linear and cyclic polymers.

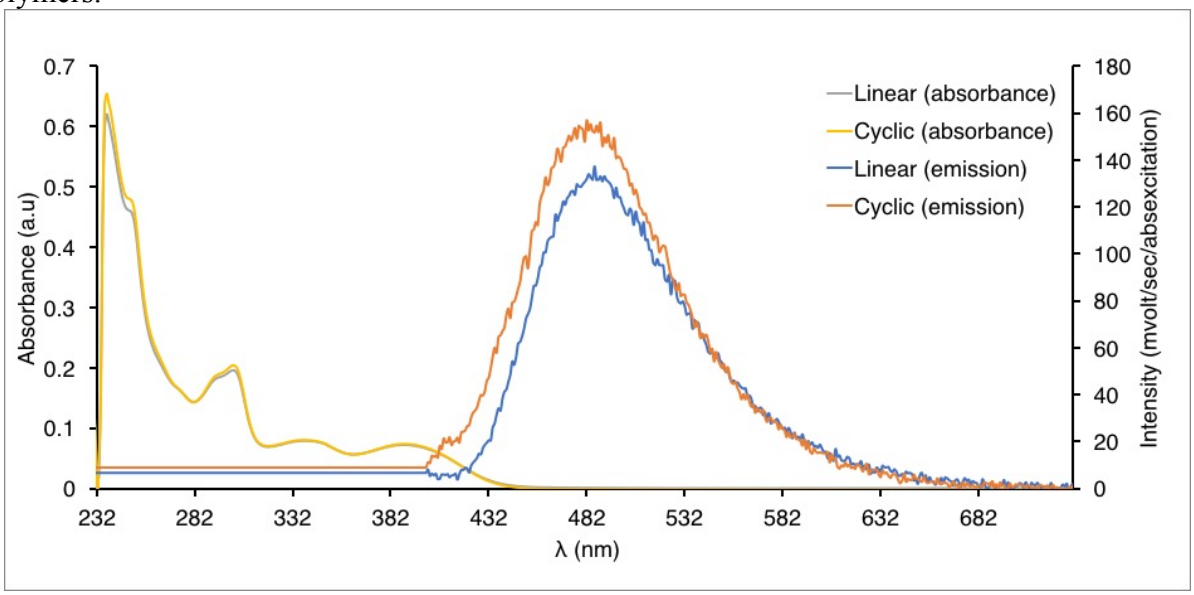


Stacked absorbance and fluorescence emission spectra of modified linear and cyclic polymers **Entry 4**, **Scheme 16** and **17**. $\lambda_{excitation}$ = 389 nm. Spectra collected in chloroform.

## 4.7 Experimental

### 4.7.1 Materials and Method

All reactions were handled using standard Schlenk line techniques (Ar) or in a $N_2$ filled glovebox (MBraun) unless otherwise specified. $^1$H NMR spectra were collected on a 300 MHz Bruker Avance spectrometer with spectra referenced to residual solvent peaks.[93] UV-Vis spectra were collected on a Helios Zeta UV-vis Thermo Scientific spectrophotometer. Gel permeation chromatography was performed on an Agilent 1100 Series with an Agilent PLgel 5μm MIXED-C column. Elution profiles were generated with THF or DCM (Sigma, HPLC grade) at 1 mL/min. A series of polystyrene standards were used to generate a 10-point calibration plot (Agilent). Solvents were removed using a rotoevaporator.

The following reagents were prepared for all reactions as follows: tetrahydrofuran (Sigma), acetonitrile (Sigma), and toluene (Sigma) were dried over sodium metal and

benzophenone and stored in the glovebox; dichloromethane (Sigma) and triethylamine (Alfa Aesar) were dried over $CaH_2$ and stored in the glovebox; acetone (Sigma) was pre-dried over silica, filtered and stored over 3Å sieves; dry dimethylformamide (Sigma), 1,4-dioxane (Sigma), pentane (Sigma), methanol (Sigma), hexanes (Sigma), ethanol, glacial acetic acid, concentrated sulfuric acid 18.4 M, and DMSO were used as received. 2-aminopropanol (Sigma), 4-aminoquinoline (Alfa Aesar), ethanolamine (Sigma), 5-aminopentanol (Sigma) was stored in the glovebox, potassium carbonate (Sigma), iron filings, sodium iodide, glycerol (Sigma), 2-chloropropionyl chloride (Aldrich), sec-butyl lithium (Fischer), sodium borohydride (Sigma), 1,3-propyldiamine, BINAP (Sigma), dppf, Tris(dibenzylideneacetone)dipalladium(0) (Sigma), sodium tert-butoxide, 12-bromo-1-dodecanol (Sigma), di-tert-butyl dicarbonate (Sigma), *para*-toluene sulfonyl chloride (Acros), 2-bromoethanol, 3-bromopropylamine hydrobromide (Aldrich), 4-quinolinol (Sigma), dodecanol (Sigma), *para*-toluene sulfonic acid (Sigma), and 4-dimethyl aminopyridine (Alfa) were all used as received.

## 4.7.2 Syntheses

**Preparation of phenanthridine-pincer fluorophores**

In a 50 mL Teflon stoppered flask charged with a stir bead a phenanthridine pincer, tether, base, and solvent were added in order. Amounts are summarized in **Table 6**. The contents were placed into a preheated oil bath for the specified times. The reaction flask was cooled to room temperature and the solvent was removed by rotoevaporation. **Entries 1 – 5** showed the reactants and no products along with unidentified impurities.

**Table 6**. Summary of phenanthridine-pincer fluorophores

| **Table 1** | Pincer, mg | Tether, mg | Base, mg | Solvent, mL | Temp. (°C) | Time (h) |
|---|---|---|---|---|---|---|
| **Entry 1** | **2**, 30.60 | **3**, 25.6 | NaOtBu, 7.8 | AN, 5 | 100 | overnight |
| **Entry 2** | **1**, 108.18 | **3**, 85 | TEA, 38μL | THF, 16 | 100 | 22 |
| **Entry 3** | **5**, 128.6 | **3**, 92.6 | - | THF, 11 | 100 | overnight |
| **Entry 4** | **1**, 20 | **4**, 18 | $K_2CO_3$, 21 | AN, 8 | 100 | overnight |
| **Entry 5** | **5**, 74 | **5**, 58 | - | THF, 14 | 100 | 20 |

**Preparation of phenanthridine fluorophores**

In a 50 mL Teflon stoppered flask charged with a stir bead **6**, tether, base, and solvent were added in order. Amounts are summarized in **Table 7**. The contents were placed onto a preheated oil bath for the specified times. The reaction flask was cooled to room temperature and the solvent was removed by rotoevaporation. **Entries 1 – 2** only showed the reactants and no products along with unidentified impurities.

**Table 7**. Summary of phenanthridine fluorophore reactions

| **Table 2** | **6**, mg | **4**, mg | $K_2CO_3$, mg | Solvent, mL | Temp. (°C) | Time (h) |
|---|---|---|---|---|---|---|
| **Entry 1** | 71.6 | 13.5 | - | THF, 6 | 105 | 20 |
| **Entry 2** | 49.1 | 84 | 13 | AN, 8 | 115 | 26 |

**Finkelstein reaction conditions for the alkylation of aromatic amine 6 (Scheme 3)**

In a 100 mL roundbottom flask equipped with a stir bead and condenser **6** (12.5 mg, 0.06 mmol), **7** (15.9 mg, 0.06 mmol), $Na_2CO_3$ (15.3 mg, 0.14 mmol), NaI (1 mg, 6,7 μmol), and anhydrous acetone (10 mL) were added together and refluxed overnight. The contents were cooled to room temperature and the solvent was removed.

**Buchwald Hartwig Cross Coupling Reactions**

In the glovebox, in a 50 mL Teflon stoppered flask charged with a stir bead the following were added: **8**, catalyst, ligand, and solvent. The flask was transferred onto a Schlenk line. 1,3-Propyldiamine and base were added. The flask was placed into a preheated oil bath and stirred for 36h. The contents were brought to room temperature and the solvent was removed. The contents were taken up in DCM and filtered through a plug of Celite and the solvent was removed. The amounts used are summarized in **Table 8**.

The compound described in **Entry 5 (repeat)** was purified by washing the solid on a plug of silica with DCM. The product was washed off with methanol and residual silica was removed. $^{1}$H NMR ($CDCl_3$, 300 MHz, 25°C) δ 9.16 (s, 1H), 8.56 (d, 1H, $J_{HH}$ = 9.1 Hz), 8.04 (t, 1H, $J_{HH}$ = 8Hz), 8.01 (s, 1H), 7.87 (t, 1H, $J_{HH}$ = 7.5 Hz), 7.72 (t, 1H, $J_{HH}$ = 7.3 Hz), 6.9 (s, 1H), 6.54 (br, NH), 3.45 (t, 2H, $J_{HH}$ = 6.3 Hz), 2.96 (t, 2H, $J_{HH}$ = 6.3 Hz), 1.98 (quin, 2H, $J_{HH}$ = 6.8 Hz), 1.84 (br, $NH_2$) ppm; $^{19}$F NMR ($CDCl_3$, 282 MHz, 25°C) δ: - 62.28 ppm; $^{13}$C{$^{1}$H} NMR ($CDCl_3$, 75 MHz, 25°C) δ 151.60, 146.35, 134.15, 132.90, 131.26, 128.85, 127.94, 127.00, 123.86, 122.56, 105.70, 101.22, 41.27, 40.1, 32.58 ppm.

**Table 8**. Buchwald Hartwig cross coupling reactions

| Amounts | **Table 2** | | |
|---|---|---|---|
| | Entry 4 | Entry 5 | Entry 5 (repeat) |
| **8**, mg | 43.3 | 35.8 | 1014.7 |
| 1, 3-propyldiamine, µL | 10.2 | 10.2 | 366 |
| $Pd_2dba_3$, mg | 2.3 | 2.3 | 70 |
| dppf, mg | 9.9 | - | - |
| BINAP, mg | - | 4.8 | 140.3 |
| NaOtBu, mg | 17.2 | 17 | 489.5 |
| Toluene, mL | 7 | 7 | 40 |
| Temperature (°C) | 150 | 150 | 150 |
| Reactions Time (h) | 48 | 48 | 50 |
| % Conversion | - | - | 74 |

**Preparation of 13**

In the glovebox **8** (0.98 g, 3 mmol), and anhydrous diethyl ether (6 mL) were added into a 50 mL Schlenk flask equipped with a stir bead. The flask was transferred onto a Schlenk line and brought to -78 °C. Over a period of 10 min a 1.3M solution in cyclohexane/hexane (92/8) of sec-butyl lithium (2.5 mL, 3 mmol) was added drop-wise while stirring. The contents were stirred for 6h at -78 °C. The reaction was quenched with anhydrous DMF (0.25 mL) and allowed to stir overnight at room temperature. Deionized water was degassed by bubbling Ar through it for 20 min. The water (10 mL) was added drop-wise to the reaction mixture and allowed to stir for 45 min.

The contents were washed DCM (35 mL x 4), dried ($Na_2SO_4$), and the solvent was removed. The contents were recrystallized from ethanol at -10°C to improve the purity minimally. The contents were then carried forward.

**Preparation of 15**

In the glovebox, to a 100 mL Schlenk flask equipped with a stir bead 5-aminopentanol **14** (174 mg, 1.7 mmol) was added. The flask was transferred onto a Schlenk line and compound **13** (66 mg, 0.24 mmol) and anhydrous ethanol (10 mL) was added. A condenser was attached and the contents were refluxed at 90 °C for 4 h. The flask was brought to room temperature and the was solvent removed.

**Preparation of 16**

In a 20 mL scintillation vial with a stir bead **15**, $NaBH_4$, and ACS grade solvent were added and the vial tightly sealed. The contents were stirred at room temperature overnight. The contents were quenched with a few drops of distilled water until bubbling stopped. The amounts

used are summarized in **Table 9**. The solvent was removed, taken up in DCM (35 mL), washed with water (10 mL x 3), and dried ($Na_2SO_4$).

**Table 9**. Sodium Borohydride reduction of **15**

| Location | **15**, mg | $NaBH_4$, mg | methanol, mL | ethanol, mL | Time (h) |
|---|---|---|---|---|---|
| **Entry 8** | 24.1 | 7.9 | - | 8 | overnight |
| **Entry 8** (repeat) | 228.1 | 47.9 | 10 | - | overnight |

**Preparation of 18**

An external oil bubble was attached to a 50 mL oven dried 3-necked round bottom flask on the Schlenk line. To the flask glycerol (2.0 mL, 27 mmol) was added and heated for 1h at 160°C and cooled to 100°C. Compound **17** (2.0 g, 9.7 mmol) and NaI (28.8 mg, 0.19 mmol) were added, stirred vigorously, and heated to 150°C. Concentrated sulfuric acid (1.2 mL) was added drop-wise and the contents were stirred for 1h at 150°C. Several sets of conditions for this reaction were tested, and these results are summarized in **Table 10** below. The contents were cooled to room temperature. The resulting black polymer was crushed and the contents were extracted with DCM (50 mL) and water (20 mL). The suspension was filtered over Celite and further washed with DCM (20 mL). The DCM fractions were washed with brine, dried ($Na_2SO_4$), and the solvent was removed.

**Table 10**. Skraup reaction of 2-nitro-4-(trifluoromethyl)aniline **17**

| **Scheme 6** | **17**, g | glycerol, mL | NaI, mg | $H_2SO_{4\ conc.}$ (mL) | Time (h) |
|---|---|---|---|---|---|
| **18** | 1 | 0.96 | 14.4 | 0.59 | 3 |
| **18** (duplicate) | 2 | 2 | 28.8 | 1.2 | 3 |
| **18** (triplicate) | 0.5 | 0.5 | 7.2 | 0.3 | 3 |

**Preparation of 19**

To a 100 mL Schlenk flask charged with a stir bead, glacial acetic acid (12.5 mL), **18** (100 mg, 0.410 mmol), and $Fe^0$ fillings (101 mg, 1.80 mmol) were added. The flask was placed

into a preheated oil bath at 65°C and heated for 2h. The contents were cooled to room temperature and filtered over Celite. The solvent was removed and taken up in DCM (25 mL), washed with water (15 mL x 2), brine (15 mL), and dried ($Na_2SO_4$). The product was recovered as a black solid, 86 mg (99%) yield.

**Preparation of 20**

To a 50 mL Schlenk flask with a stir bead **19** (32 mg, 0.15 mmol), pyridine (11.2 µL, 0.40 mmol), and anhydrous DCM (6 mL) were added and cooled to 0°C. 3-chloropropionyl chloride (58 µL, 0.61 mmol) was added drop-wise. The contents were stirred for 2h and brought to room temperature. Additional DCM (25 mL), washed with water (15 mL x 2), brine (15 mL), and dried ($Na_2SO_4$).

**General preparation procedure of miscellaneous phenanthridine fluorophores**

In a 50 mL Teflon stoppered flask charged with a stir bead a phenanthridine species, tether, base, and solvent were added in order. Amounts are summarized in **Table 11**. The flask was placed into a preheated oil bath for the specified times. The reaction flask was cooled to room temperature and the solvent was removed. **Entries 1 – 3, and 5** only showed the reactants and no products along with unidentified impurities.

**Table 11**. Summary of miscellaneous fluorophores

| **Table 3** | Phen. spp., mg | Tether, mag | Base, mg | Solvent, mL | Temp.(°C) | Time (h) |
|---|---|---|---|---|---|---|
| **Entry 1** | **21**, 45.5 | **7** / 80 | - | AN, 6 | 80 | overnight |
| **Entry 2** | **21**, 153 | **7** / 267 | TEA, 1 mL | AN, 4 | 110 | overnight |
| **Entry 3** | **22**, 33.23 | **7** / 34.43 | - | AN, 6 | 110 | 21 |
| **Entry 4** | **23**, 100 | 2-bromoethanol, 73 µL | $K_2CO_3$, 190 | DMF, 3 | 80 | overnight |
| **Entry 5** | **23**, 150 | 3-bromopropylamine hydrobromide, 340 | $K_2CO_3$, 357 | DMF, 5 | 65 | overnight |

**Attempts at post polymerization modification with 4-aminoquinoline 27**

In a 50 mL Teflon stoppered flask charged with a stir bead **26** (9.7 mg, 0.2 µmol), **27** (2.6 mg, 0.02 mmol), dimethyl aminopyridine/base (2.22 mg, 18 mmol), and solvent (2.2 mL) were

added. The flask was placed into a preheated oil bath and stirred for the specified time. The reaction flask was cooled to room temperature and the solvent was removed. The contents were dissolved in a minimal amount of THF and added drop-wise into a stirring solution of hexanes (15 mL) to precipitate the product. The mixture was centrifuged and the supernatant was decanted to isolate the product pellet. The purification steps were repeated for a total of three times and each time a minimal amount of THF was used to dissolve the pellet. The pellet was dried on a Schlenk line vacuum overnight at room temperature. Several sets of conditions for this reaction were tested, and these results are summarized in **Table 12** below.

**Table 12**. Post polymerization modification with 4-aminoquinoline **27**

| **Scheme 8** | **26**, mg | **27**, mg | solvent, mL | Base | Temp. (°C) | Time (h) |
|---|---|---|---|---|---|---|
| **Reaction 1** | 25.34 | 1.0 | DCM, 5 | - | 50 | 16 |
| **Reaction 2** | 24.70 | 2.0 | DCM, 5 | TEA, 1.94μL | 50 | 20 |
| **Reaction 3** | 12.79 | 3.5 | DCM, 5 | - | 60 | 24 |
| **Reaction 4** | 11.79 | 6.35 | DCM, 5 | - | 60 | 24 |
| **Reaction 5** | 12.35 | 3.8 | 1,4-dioxane, 4 | DMAP, 3.6 mg | 65 | overnight |
| **Reaction 6** | 9.70 | 2.6 | 1,4-dioxane/DMF (1:1), 2.2 | DMAP, 2.2 mg | 80 | 25.5 |
| **Reaction 7** | 12.35 | 3.3 | 1,4-dioxane/DMSO (1:1), 2.1 | - | 80 | 24 |

**Post polymerization modification with 2-amino-propanol 28**

In a 50 mL Teflon stoppered flask charged with a stir bead **26** (25 mg, 0.52 μmol), **28** (5.5 μL, 71 mmol), triethyl amine (9.9 μL, 71 mmol), and solvent (1.1 mL) were added. The flask was placed into a preheated oil bath and stirred for the specified time. The reaction flask was cooled to room temperature and the solvent was removed. The reaction mixture was dissolved in a minimal amount of DMF and added drop-wise to a stirring solution of diethyl ether (15 mL) to precipitate the product. The mixture was centrifuged and the supernatant was

decanted to isolate the product pellet. The purification steps were repeated for a total of three times and each time a minimal amount of DMF was used to dissolve the pellet. The pellet was then suspended in diethyl ether, centrifuged, and the supernatant was decanted. The polymer was then dried on a Schlenk line vacuum overnight at room temperature. Several sets of conditions for this reaction were tested, and these results are summarized in **Table 13** below.

**Table 13**. Post polymerization modification with 2-amino-propanol **28**

| **Scheme 9** | **26**, mg | **28**, µL | Solvent, mL | TEA, µL | Temp. (°C) | Time (h) | Conversion |
|---|---|---|---|---|---|---|---|
| **Reaction 1** | 14.56 | 3.1 | 1.1 | - | 70 | overnight | observed |
| **Reaction 2** | 25.11 | 5.5 | 1.1 | 9.9 | 60 | 23.5 | observed |
| **Reaction 3** | 14.90 | 4.8 | 1.1 | - | 60 | 48 | 100% conv. |
| **Reaction 4** | 10.00 | 1.5 | 1.1 | 2.6 | 60 | overnight | observed |
| **Reaction 5** | 29.50 | 4.3 | 2.0 | - | 90 | 23 | could not isolate |
| **Reaction 6** | 32.60 | 40 | 1.8 | - | 60 | 20 | 100% conv. |
| **Reaction 7** | 14.10 | 10 | 2.3 | - | 60 | 26.5 | 100% conv. |

**Post polymerization modification with 10**

In a 50 mL Teflon stoppered flask charged with a stir bead **26** (29 mg, 0.61 µmol), **10** (8.9 mg, 0.03 mmol), and solvent (1.8 mL) were added. The flask was placed into a preheated oil bath and stirred for the specified time. The reaction flask was cooled to room temperature and the solvent was removed. The reaction contents were dissolved in minimal THF and added drop-wise to a stirring solution of methanol (15 mL) to precipitate the product. The mixture was centrifuged and the supernatant was decanted to isolate the product pellet. The purification steps were repeated for a total of three times and each time a minimal amount of THF was used to dissolve the pellet. The pellet was then suspended in methanol, centrifuged, and the supernatant was decanted. The polymer was then dried on a Schlenk line vacuum overnight at room temperature. Several sets of conditions for this reaction were tested, and these results are summarized in **Table 14** below.

**Table 14**. Post Polymerization modification with **10**

| **Scheme 10** | **26**, mg | **10**, mg | solvent, mL | Temp. (°C) | Time (h) | % Conv. |
|---|---|---|---|---|---|---|
| **Reaction 1** | 29.3 | 8.90 | 1.8 | 60 | 18 | 2.3 |
| **Reaction 2** | 32.1 | 30.2 | 1.8 | 60 | 23 | 31 |
| **Reaction 3** | 25.7 | 10.4 | 1.8 | 60 | 19.5 | 12 |
| **Reaction 4** | 22.5 | 9.12 | 1.8 | 60 | 19.5 | 12 |

**Preparation of polymer 26e**

In a 50 mL Teflon stoppered flask charged with a stir bead **26d** (13.5 mg, 0.3 μmol), 2-aminopropanol (2 μL, 0.03 mmol), DMF (0.3 mL), and 1,4-dioxane (1.5 mL) were added. The flask was placed into a preheated oil bath and stirred for the specified time. The reaction flask was cooled to room temperature and methanol (15 mL) was added directly to the flask. The diluted reaction mixture was centrifuged and the supernatant was decanted. The pellet product was dissolved in a minimal amount of THF and added drop-wise into a stirring solution of methanol (15 mL) to re-precipitate the product. The mixture was centrifuged and the supernatant was decanted. The purification steps were repeated for a total of two times and each time a minimal amount of THF was used to dissolve the pellet. The pellet was dried on a Schlenk line vacuum overnight at room temperature. The polymer's solubility was qualitatively determined to be insoluble in $D_2O$ and partially soluble in $CDCl_3$.

**Preparation of poly(N-2-hydroxyethyl methacrylamide) 26f**

In a 50 mL Teflon stoppered flask charged with a stir bead **26** (18 mg, 0.37 μmol), **29** (200 μL, 3.3 mmol), triethyl amine (50 μL, 0.36 mmol), DMF (0.44 mL), and 1,4-dioxane (1.76 mL) were added. The flask was placed into a preheated oil bath and stirred for the specified time. The reaction flask was cooled to room temperature and the solvent was removed. The reaction contents were dissolved in minimal DMF and added drop-wise to a stirring solution of diethyl ether (15 mL) to precipitate the product. The mixture was centrifuged and the supernatant was

decanted to isolate the product pellet. The purification steps were repeated for a total of three times and each time a minimal amount of DMF was used to dissolve the pellet. The polymer was then dried on a Schlenk line vacuum overnight at room temperature. Several sets of conditions for this reaction were tested, and these results are summarized in **Table 15** below.

**Table 15**. Post polymerization modification with 2-amino-ethanol **29**

| **Scheme 12** | **26**, mg | **29**, μL | solvent, mL | TEA, μL | Temp. (°C) | Time (h) |
|---|---|---|---|---|---|---|
| **Entry 1** | 17.7 | 200 | 2.2 | 50 | 50 | overnight |
| **Entry 2** | 18.6 | 2 | 2.2 | 5 | 50 | overnight |

**Post polymerization modification with dodecanol 30 under neutral, basic, and acidic conditions**

In a 50 mL Teflon stoppered flask charged with a stir bead **26** (15 mg, 0.31 μmol), **30** (11 mg, 0.06 mmol), a catalyst, and solvent (1.7 mL) were added. The flask was placed into a preheated oil bath and stirred for the specified time. The reaction flask was cooled to room temperature and the solvent was removed. The reaction contents were dissolved in minimal THF and added drop-wise to a stirring solution of methanol (15 mL) to precipitate the product. The mixture was centrifuged and the supernatant was decanted to isolate the product pellet. The purification steps were repeated for a total of three times and each time a minimal amount of THF was used to dissolve the pellet. The polymer was then dried on a Schlenk line vacuum overnight at room temperature. Several sets of conditions for this reaction were tested, and these results are summarized in **Table 16** below.

**Table 16**. Post polymerization modification with dodecanol **30** under neutral, basic, and acidic conditions

| **Scheme 13** | **26**, mg | **30**, mg | Catalyst, mg | Solvent, mL | Temp. (°C) | Time (h) | Status |
|---|---|---|---|---|---|---|---|
| **Reaction 1** | 15 | 11 | - | 1.7 | 90 | 26 | x |
| **Reaction 2** | 19.22 | 6.6 | DMAP, 4.4 | 3 | 90 | 19 | x |
| **Reaction 3** | 12.8 | 4.6 | pTSA, 2.9 | 1.5 | 90 | 19 | observed |

**Post polymerization modification of cyclic poly(pentafluorophenyl methacrylate) 31 with 10**

In a 50 mL Teflon stoppered flask charged with a stir bead **32** (25.7 mg, 1.37 μmol), **10** (10.4 mg, 0.03 mmol), DMF (0.3 mL), and 1,4-dioxane (1.5 mL) were added. The flask was placed into a preheated oil bath and stirred for the specified time. The reaction flask was cooled to room temperature and the solvent was removed. The reaction contents were dissolved in minimal THF and added drop-wise to a stirring solution of methanol (15 mL) to precipitate the product. The mixture was centrifuged and the supernatant was decanted to isolate the product pellet. The purification steps were repeated for a total of three times and each time a minimal amount of THF was used to dissolve the pellet. The polymer was then dried on a Schlenk line vacuum overnight at room temperature. Several sets of conditions for this reaction were tested, and these results are summarized in **Table 17** below.

**Table 17**. Post polymerization modification of cyclic and linear poly(pentafluorophenyl methacrylate) with **10**.

| Species | Entry | pPFMA, mg | **10**, mg | solvent, mL | Temp. (°C) | Time (h) |
|---|---|---|---|---|---|---|
| Cyclic | **32** | 25.7 | 10.4 | 1.8 | 60 | 19.5 |
| Cyclic | **32a** | 20.0 | 9.20 | 1.8 | 60 | 19.5 |
| Cyclic | **32b** | 17.5 | 21.0 | 0.6 | 65 | 19 |
| Cyclic | **32c** | 14.8 | 22.6 | 0.8 | 65 | 17 |
| Cyclic | **32d** | 27.3 | 46.9 | 0.8 | 65 | overnight |
| Linear | **33** | 22.5 | 9.10 | 1.8 | 60 | 19.5 |
| Linear | **33b** | 20.1 | 24.2 | 0.8 | 65 | 19 |
| Linear | **33c** | 3.00 | 8.10 | 0.8 | 65 | 17 |
| Linear | **33d** | 35.4 | 46.7 | 0.8 | 65 | overnight |

**Figure 19**. Absorbance and fluorescence emission spectra of modified linear **33** and cyclic poly(pentafluorophenyl methacrylate).

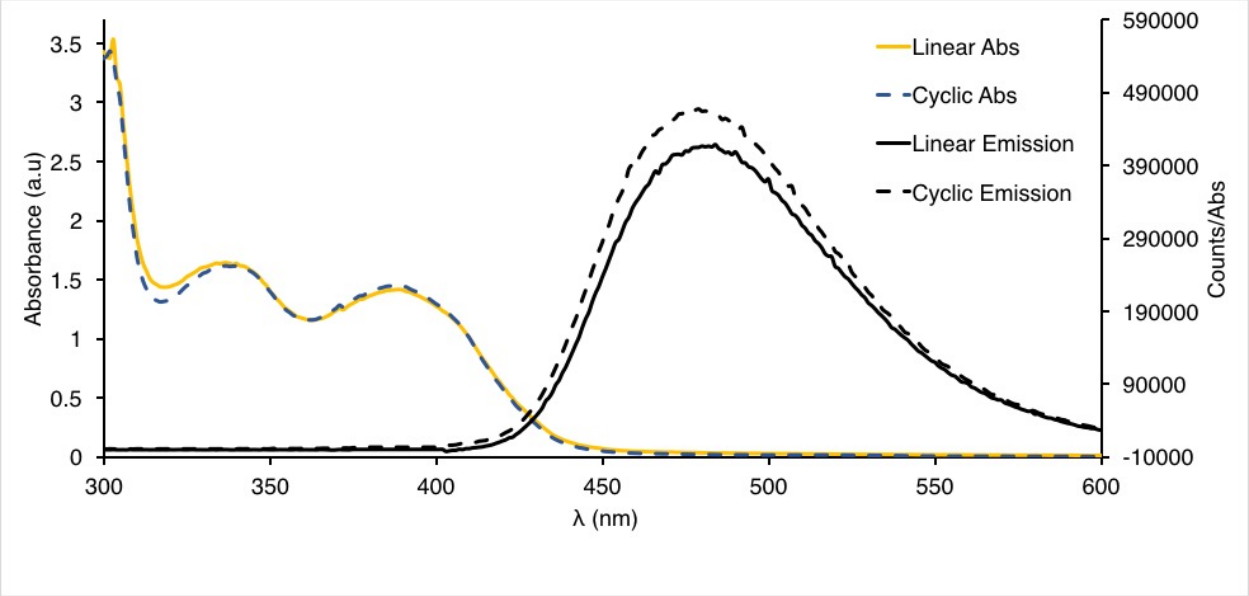

# 5 Conclusions and Outlook

It was demonstrated in this work that cyclic polymers bearing active esters were synthesized using the α-ω ring closure method as evidenced by $^{1}$H NMR, $^{19}$F NMR, Diffusion NMR, gel permeation chromatography, and UV-Vis spectroscopy. These materials were then subject to post polymerization modification (PPM) with a phenanthridyl fluorophore and by fluorescence spectrometry enhanced emission was demonstrated in comparison to their linear counterpart.

Since the synthesis of this material has been accomplished the next step would be to devise a method to try to increase the amount of material generated in a reaction and this can be achieved through Flow Chemistry. It required 45 min to irradiate a stirring solution with a concentration of ~ 40 mg/L at 500 mL to achieve ~ 20 mg of cyclic polymer. The HDA reaction has been previously performed to completion under flow[47] in 2 min with the additional advantage that larger volumes can be used by the lamp to generate larger amounts of material.

With larger amounts of material available other small molecules can be explored for post polymerization modification. This can include peptide tethered platinum anticancer drugs,[129] cross-linking precursors such as alkyl diamines, and a series of different fluorophores' emission could be compared to allow for the mechanism of aggregation induced emission enhancement (AIEE) to be further studied in detail.[130]

The pending questions that remain in this work include 1) determining the missing $^{1}$H NMR peaks in the isothiochroman group and its stability, 2) To improve the resolution in the gel permeation chromatography experiment, 3) As well, answering if this system's scope can be extended by utilizing other active esters.

1) Some aspects of the current project that have still to be explored are determining the presence of the tertiary proton and alcohol proton of the isothiochroman group by using either 2D NMR experiments or a $^{2}H$ NMR exchange experiment. As well, the robustness of the isothiochroman group has not been fully explored. It was demonstrated that after PPM with the phenanthridyl group that the cyclic integrity was maintained but what conditions, such as temperature and pH ranges, cause this cyclic polymer to break down back into a linear polymer.

2) Some cyclic polymers because of the nature of their side groups do not decrease substantially in hydrodynamic volume compared to their linear counterpart.[65,96] This leads to poor resolution (small change in retention volume) between peaks leading to ambiguity for a powerful piece of evidence for ring closure. In this work it remains to optimize the protocol for gel permeation chromatography to try to improve the resolution for linear and cyclic poly(pentafluorophenyl methacrylate) which might be subject by this effect.

3) The chain transfer agent employed in this work is applicable to vinyl benzoate monomers[81–85] with pentafluorophenyl groups. Further work can be done using the benzoate monomers to make cyclic polymers with polystyrene backbones whose kinetics are significantly faster[79] than pentafluorophenyl methacrylate.

The goal of this work was to provide a modular approach for the synthesis of new and interesting materials comprised of cyclic polymers and was achieved. Cyclic polymers are not widely used in many applications but have potential and have not been fully realized yet at this time.[6] This work is meant to streamline a route to applications by providing a tool and the possibilities for making different materials from cyclic poly(pentafluorophenyl methacrylate), like the topology, are ‘endless’.[19]

# References


(1) Kakuchi, R.; Theato, P. Post-Polymerization Modifications via Active Esters. In *Functional Polymers by Post-Polymerization Modification*; Theato, P., Klok, H.-A., Eds.; Wiley-VCH Verlag GmbH & Co. KGaA: Weinheim, Germany, 2013; pp 45–64.

(2) Zhang, K.; Lackey, M. A.; Wu, Y.; Tew, G. N. Universal Cyclic Polymer Templates. *J. Am. Chem. Soc.* **2011**, *133* (18), 6906–6909.

(3) Endo, K. Synthesis and Properties of Cyclic Polymers. In *New Frontiers in Polymer Synthesis*; Springer Berlin Heidelberg: Berlin, 2008; pp 121–183.

(4) Kricheldorf, H. R. Cyclic Polymers: Synthetic Strategies and Physical Properties. *J. Polym. Sci. Part A Polym. Chem.* **2010**, *48* (2), 251–284.

(5) Jia, Z.; Monteiro, M. J. Cyclic Polymers: Methods and Strategies. *J. Polym. Sci. Part A Polym. Chem.* **2012**, *50* (11), 2085–2097.

(6) Zhu, Y.; Hosmane, N. S. Advanced Developments in Cyclic Polymers: Synthesis, Applications, and Perspectives. *ChemistryOpen* **2015**, *4* (4), 408–417.

(7) Zhang, K.; Tew, G. N. Cyclic Polymers as a Building Block for Cyclic Brush Polymers and Gels. *React. Funct. Polym.* **2014**, *80*, 40–47.

(8) Honda, S.; Yamamoto, T.; Tezuka, Y. Topology-Directed Control on Thermal Stability: Micelles Formed from Linear and Cyclized Amphiphilic Block Copolymers. *J. Am. Chem. Soc.* **2010**, *132* (30), 10251–10253.

(9) Zhu, X.; Zhu, X.; Zhou, N.; Zhang, Z.; Sun, B.; Yang, Y.; Zhu, J. Cyclic Polymers with Pendent Carbazole Units: Enhanced Fluorescence and Redox Behavior. *Angew. Chemie - Int. Ed.* **2011**, *50* (29), 6615–6618.

(10) Zhang, H.; Zhou, N.; Zhu, X.; Chen, X.; Zhang, Z.; Zhang, W.; Zhu, J.; Hu, Z.; Zhu, X.

Cyclic Side-Chain Phenylazo Naphthalene Polymers: Enhanced Fluorescence Emission and Surface Relief Grating Formation. *Macromol. Rapid Commun.* **2012**, *33* (21), 1845–1851.

(11) Mu, B.; Li, Q.; Li, X.; Pan, S.; Zhou, Y.; Fang, J.; Chen, D. Cyclic Polymers with Pendant Triphenylene Discogens: Convenient Synthesis and Topological Effect on Thermotropic Liquid Crystal Behavior and Fluorescence Enhancement. *Polym. Chem.* **2016**, *7* (39), 6034–6038.

(12) Li, K.; Jiang, G.; Zhou, F.; Li, L.; Zhang, Z.; Hu, Z.; Zhou, N.; Zhu, X. Impact of Cyclic Topology: Odd-Even Glass Transition Temperatures and Fluorescence Quantum Yields in Molecularly-Defined Macrocycles. *Polym. Chem.* **2017**, 2686–2692.

(13) Nossarev, G. G.; Johnson, J.; Bradforth, S. E.; Hogen-Esch, T. E. Emission of Macrocyclic and Linear Poly(2-Vinylnaphthalene): Observation of Two Excimer Populations in Macrocycles. *J. Phys. Chem. C* **2013**, *117* (20), 10244–10256.

(14) Fox, M. E.; Szoka, F. C.; Fréchet, J. M. J. Soluble Polymer Carriers for the Treatment of Cancer: The Importance of Molecular Architecture. *Acc. Chem. Res.* **2009**, *42* (8), 1141–1151.

(15) Nasongkla, N.; Chen, B.; Macaraeg, N.; Fox, M. E.; Fréchet, J. M. J.; Szoka, F. C. Dependence of Pharmacokinetics and Biodistribution on Polymer Architecture: Effect of Cyclic versus Linear Polymers. *J. Am. Chem. Soc.* **2009**, *131* (11), 3842–3843.

(16) Torchilin, V. P. *Drug Delivery*; Schäfer-Korting, M., Ed.; Handbook of Experimental Pharmacology; Springer Berlin Heidelberg: Berlin, 2010; Vol. 197.

(17) Laurent, B. A.; Grayson, S. M. Synthetic Approaches for the Preparation of Cyclic Polymers. *Chem. Soc. Rev.* **2009**, *38* (8), 2202.

(18) Kricheldorf, H. R.; Lee, S.-R. Polylactones. 35. Macrocyclic and Stereoselective Polymerization of .beta.-D,L-Butyrolactone with Cyclic Dibutyltin Initiators. *Macromolecules* **1995**, *28* (20), 6718–6725.

(19) Bielawski, C. W. An "Endless" Route to Cyclic Polymers. *Science* **2002**, *297* (5589), 2041–2044.

(20) Boydston, A. J.; Xia, Y.; Kornfield, J. A.; Gorodetskaya, I. A.; Grubbs, R. H. Cyclic Ruthenium-Alkylidene Catalysts for Ring-Expansion Metathesis Polymerization. *J. Am. Chem. Soc.* **2008**, *130* (38), 12775–12782.

(21) *Encyclopedia of Polymeric Nanomaterials*; Kobayashi, S., Müllen, K., Eds.; Springer Berlin Heidelberg: Berlin, Heidelberg, 2015.

(22) Laurent, B. A.; Grayson, S. M. An Efficient Route to Well-Defined Macrocyclic Polymers Via "click" cyclization. *J. Am. Chem. Soc.* **2006**, *128* (13), 4238–4239.

(23) Zhu, X.; Zhou, N.; Zhu, J.; Zhang, Z.; Zhang, W.; Cheng, Z.; Tu, Y.; Zhu, X. A High-Efficiency Strategy for Synthesizing Cyclic Polymers of Methacryates in One Pot. *Macromol. Rapid Commun.* **2013**, *34* (12), 1014–1019.

(24) Matyjaszewski, K. Atom Transfer Radical Polymerization (ATRP): Current Status and Future Perspectives. *Macromolecules* **2012**, *45* (10), 4015–4039.

(25) Tsarevsky, S. *Fundamentals of Controlled/Living Radical Polymerization*; 2013.

(26) Fischer, H. The Persistent Radical Effect in Controlled Radical Polymerizations. *J. Polym. Sci. Part A Polym. Chem.* **1999**, *37* (13), 1885–1901.

(27) Fischer, H. The Persistent Radical Effect: A Principle for Selective Radical Reactions and Living Radical Polymerizations. *Chem. Rev.* **2001**, *101* (12), 3581–3610.

(28) Matyjaszewski, K.; Nanda, A. K.; Tang, W. Effect of [Cu II ] on the Rate of Activation in

ATRP. *Macromolecules* **2005**, *38* (5), 2015–2018.

(29) Liang, L.; Astruc, D. The copper(I)-Catalyzed Alkyne-Azide Cycloaddition (CuAAC) "click" Reaction and Its Applications. An Overview. *Coord. Chem. Rev.* **2011**, *255* (23–24), 2933–2945.

(30) Rostovtsev, V. V.; Green, L. G.; Fokin, V. V.; Sharpless, K. B. A Stepwise Huisgen Cycloaddition Process: Copper(I)-Catalyzed Regioselective "Ligation" of Azides and Terminal Alkynes. *Angew. Chemie Int. Ed.* **2002**, *41* (14), 2596–2599.

(31) Meldal, M. Polymer "clicking" by CuAAC Reactions. *Macromol. Rapid Commun.* **2008**, *29* (12–13), 1016–1051.

(32) Moad, Graeme; Rizzardo, Ezio; Thang, S. H. A RAFT Tutorial. *Strem Chem.* **2011**, *25* (1), 2–12.

(33) Moad, G.; Rizzardo, E.; Thang, S. H. RAFT Polymerization and Some of Its Applications. *Chem. - An Asian J.* **2013**, *8* (8), 1634–1644.

(34) Moad, G.; Rizzardo, E.; Thang, S. H. Living Radical Polymerization by the RAFT Process – A Second Update. *Aust. J. Chem.* **2009**, *62* (11), 1402.

(35) Moad, G.; Rizzardo, E.; Thang, S. H. CHAPTER 6 Fundamentals of RAFT Polymerization. In *Fundamentals of Controlled/Living Radical Polymerization*; The Royal Society of Chemistry, 2013; pp 205–249.

(36) Szwarc, M. "Living" Polymers. *Nature* **1956**, *178* (4543), 1168–1169.

(37) Glassner, M.; Delaittre, G.; Kaupp, M.; Blinco, J. P.; Barner-Kowollik, C. (Ultra)fast Catalyst-Free Macromolecular Conjugation in Aqueous Environment at Ambient Temperature. *J. Am. Chem. Soc.* **2012**, *134* (17), 7274–7277.

(38) Espinosa, E.; Glassner, M.; Boisson, C.; Barner-Kowollik, C.; D'Agosto, F. Synthesis of

Cyclopentadienyl Capped Polyethylene and Subsequent Block Copolymer Formation via Hetero Diels-Alder (HDA) Chemistry. *Macromol. Rapid Commun.* **2011**, *32* (18), 1447–1453.

(39) Wang, Z.; Ma, Z.; Zhang, Z.; Wu, F.; Jiang, H.; Jia, X. Mechanical Activation of a Dithioester Derivative-Based Retro RAFT-HDA Reaction. *Polym. Chem.* **2014**, *5* (24), 6893–6897.

(40) Langer, M.; Brandt, J.; Lederer, A.; Goldmann, A. S.; Schacher, F. H.; Barner-Kowollik, C. Amphiphilic Block Copolymers Featuring a Reversible Hetero Diels-Alder Linkage. *Polym. Chem.* **2014**, *5* (18), 5330–5338.

(41) Glassner, M.; Blinco, J. P.; Barner-Kowollik, C. Diels-Alder Reactions as an Efficient Route to High Purity Cyclic Polymers. *Macromol. Rapid Commun.* **2011**, *32* (9–10), 724–728.

(42) Winkler, M.; Mueller, J. O.; Oehlenschlaeger, K. K.; Montero de Espinosa, L.; Meier, M. A. R.; Barner-Kowollik, C. Highly Orthogonal Functionalization of ADMET Polymers via Photo-Induced Diels–Alder Reactions. *Macromolecules* **2012**, *45* (12), 5012–5019.

(43) Gruendling, T.; Oehlenschlaeger, K. K.; Frick, E.; Glassner, M.; Schmid, C.; Barner-Kowollik, C. Rapid UV Light-Triggered Macromolecular Click Conjugations via the Use of O-Quinodimethanes. *Macromol. Rapid Commun.* **2011**, *32* (11), 807–812.

(44) Inglis, A. J.; Sinnwell, S.; Stenzel, M. H.; Barner-Kowollik, C. Ultrafast Click Conjugation of Macromolecular Building Blocks at Ambient Temperature. *Angew. Chemie Int. Ed.* **2009**, *48* (13), 2411–2414.

(45) Oehlenschlaeger, K. K.; Mueller, J. O.; Heine, N. B.; Glassner, M.; Guimard, N. K.; Delaittre, G.; Schmidt, F. G.; Barner-Kowollik, C. Light-Induced Modular Ligation of

Conventional RAFT Polymers. *Angew. Chemie - Int. Ed.* **2013**, *52* (2), 762–766.

(46) Tang, Q.; Wu, Y.; Sun, P.; Chen, Y.; Zhang, K. Powerful Ring-Closure Method for Preparing Varied Cyclic Polymers. *Macromolecules* **2014**, *47*, 3775–3781.

(47) Sun, P.; Liu, J.; Zhang, Z.; Zhang, K. Scalable Preparation of Cyclic Polymers by the Ring-Closure Method Assisted by the Continuous-Flow Technique. *Polym. Chem.* **2016**, *7* (12), 2239–2244.

(48) Zhu, W.; Li, Z.; Zhao, Y.; Zhang, K. Cyclic Polymer with Alternating Monomer Sequence. *Macromol. Rapid Commun.* **2015**, *36* (22), 1987–1993.

(49) Segura, J. L.; Martín, N. O -Quinodimethanes: Efficient Intermediates in Organic Synthesis. *Chem. Rev.* **1999**, *99* (11), 3199–3246.

(50) Lavell, W. T. Photoenolization: An Organic Chemistry Laboratory Experiment. *J. Chem. Educ.* **1995**, *72* (6), 552.

(51) Sammes, P. Photoenolisation. *Tetrahedron* **1976**, *32* (Scheme 2), 405–422.

(52) Wagner, P. J. Solvent Effects on Type II Photoelimination of Phenyl Ketones. *J. Am. Chem. Soc.* **1967**, *89* (23), 5898–5901.

(53) Lonsdale, D. E.; Monteiro, M. J. Kinetic Simulations for Cyclization of A,ω-Telechelic Polymers. *J. Polym. Sci. Part A Polym. Chem.* **2010**, *48* (20), 4496–4503.

(54) Lonsdale, D. E.; Bell, C. A.; Monteiro, M. J. Strategy for Rapid and High-Purity Monocyclic Polymers by CuAAC “Click” Reactions. *Macromolecules* **2010**, *43* (7), 3331–3339.

(55) Jacobson, H.; Stockmayer, W. H. Intramolecular Reaction in Polycondensations. I. The Theory of Linear Systems. *J. Chem. Phys.* **1950**, *18* (12), 1600–1606.

(56) Semlyen, E. R. *Cyclic Polymers*; Semlyen, J. A., Ed.; Kluwer Academic Publishers:

Dordrecht, 2002.

(57) Tang, Q.; Wu, Y.; Sun, P.; Chen, Y.; Zhang, K. Powerful Ring-Closure Method for Preparing Varied Cyclic Polymers. *Macromolecules* **2014**, *47* (12), 3775–3781.

(58) Ma, X.; Sun, R.; Cheng, J.; Liu, J.; Gou, F.; Xiang, H.; Zhou, X. Fluorescence Aggregation-Caused Quenching versus Aggregation-Induced Emission: A Visual Teaching Technology for Undergraduate Chemistry Students. *J. Chem. Educ.* **2016**, *93* (2), 345–350.

(59) Chen, R.; Johnson, J. M.; Bradforth, S. E.; Hogen-Esch, T. E. Ultraviolet Absorption and Fluorescence Emission Spectroscopic Studies of Macrocyclic and Linear Poly(9,9-Dimethyl-2-Vinylfluorene). Evidence for Ground-State Chromophore Interactions. *Macromolecules* **2003**, *36* (26), 9966–9970.

(60) Rostovtsev, V. V.; Green, L. G.; Fokin, V. V.; Sharpless, K. B. A Stepwise Huisgen Cycloaddition Process: Copper(I)-Catalyzed Regioselective "Ligation" of Azides and Terminal Alkynes. *Angew. Chemie Int. Ed.* **2002**, *41* (14), 2596–2599.

(61) Barner-Kowollik, C.; Du Prez, F. E.; Espeel, P.; Hawker, C. J.; Junkers, T.; Schlaad, H.; Van Camp, W. "Clicking" polymers or Just Efficient Linking: What Is the Difference? *Angew. Chemie - Int. Ed.* **2011**, *50* (1), 60–62.

(62) Luedtke, A. E.; Timberlake, J. W. Effect of Oxidized States of Heteroatoms and of Orthogonal a Systems on Radical Stabilities. *J. Org. Chem.* **1985**, *50* (2), 268–270.

(63) Coessens, V.; Matyjaszewski, K. End Group Transformation of Polymers Prepared by ATRP, Substitution to Azides. *J. Macromol. Sci. Part A* **1999**, *36* (5–6), 667–679.

(64) Siegwart, D. J.; Oh, J. K.; Matyjaszewski, K. ATRP in the Design of Functional Materials for Biomedical Applications. *Prog. Polym. Sci.* **2012**, *37* (1), 18–37.

(65) Zhou, F.; Li, Y.; Jiang, G.; Zhang, Z.; Tu, Y.; Chen, X.; Zhou, N.; Zhu, X. Biomacrocyclic Side-Chain Liquid Crystalline Polymers Bearing Cholesterol Mesogens: Facile Synthesis and Topological Effect Study. *Polym. Chem.* **2015**, *6* (38), 6885–6893.

(66) Moad, G.; Rizzardo, E.; Thang, S. H. Living Radical Polymerization by the RAFT Process. *Aust. J. Chem.* **2005**, *58* (6), 379.

(67) Moad, G.; Rizzardo, E.; Thang, S. H. RAFT Polymerization and Some of Its Applications. *Chem. - An Asian J.* **2013**, *8* (8), 1634–1644.

(68) Walling, C.; El-Taliawi, G. M.; Zhao, C. Oxidation of Arylalkanols by Peroxydisulfate-copper(II). *J. Org. Chem.* **1983**, *48* (25), 4914–4917.

(69) Walling, C.; Zhao, C.; El-Taliawi, G. M. Oxidation of Alkylbenzenes by Peroxydisulfate-copper(II) in Acetic Acid and Acetonitrile. *J. Org. Chem.* **1983**, *48* (25), 4910–4914.

(70) Hauser, F. M.; Ellenberger, S. R. Regiospecific Oxidation of Methyl Groups in Dimethylanisoles. *Synthesis* **1987**, *1987* (8), 723–724.

(71) Bhatt, M. V.; Kulkarni, S. U. Cleavage of Ethers. *Synthesis* **1983**, *1983* (4), 249–282.

(72) McOmie, J. F. W.; Watts, M. L.; West, D. E. Demethylation of Aryl Methyl Ethers by Boron Tribromide. *Tetrahedron* **1968**, *24* (5), 2289–2292.

(73) Xia, Z.; Cao, X.; Rico-Bautista, E.; Yu, J.; Chen, L.; Chen, J.; Bobkov, A.; Wolf, D. A.; Zhang, X.-K.; Dawson, M. I. Relative Impact of 3- and 5-Hydroxyl Groups of Cytosporone B on Cancer Cell Viability. *Medchemcomm* **2013**, *4* (2), 332–339.

(74) Sc̈haefer W, F. Selective Ether Cleavage of 4-Hydroxymethoxyquinolinecarboxylic Acid Esters. *Chem. Ber.* **1966**, 160–164.

(75) Thang, S. H.; Chong, B. Y. K.; Mayadunne, R. T. a; Moad, G.; Rizzardo, E. A Novel Synthesis of Functional Dithioesters, Dithiocarbamates, Xynthates and Trithiocarbonates.

*Tetrahedron Lett.* **1999**, *40*, 2435–2438.

(76) Sun, P.; Liu, J.; Zhang, Z.; Zhang, K. Polymer Chemistry. *Polym. Chem.* **2016**, *7*, 2239–2244.

(77) Valeur, E.; Bradley, M. Amide Bond Formation: Beyond the Myth of Coupling Reagents. *Chem. Soc. Rev.* **2009**, *38* (2), 606–631.

(78) Nuhn, L.; Barz, M.; Zentel, R. New Perspectives of HPMA-Based Copolymers Derived by Post-Polymerization Modification. *Macromolecular Bioscience*. 2014, pp 607–618.

(79) Das, A.; Theato, P. Activated Ester Containing Polymers: Opportunities and Challenges for the Design of Functional Macromolecules. *Chemical Reviews*. 2016, pp 1434–1495.

(80) Yao, W.; Li, Y.; Huang, X. Fluorinated Poly(meth)acrylate: Synthesis and Properties. *Polym. (United Kingdom)* **2014**, *55* (24), 6197–6211.

(81) Nilles, K.; Theato, P. RAFT Polymerization of Activated 4-Vinylbenzoates. *J. Polym. Sci. Part A Polym. Chem.* **2009**, *47* (6), 1696–1705.

(82) Kakuchi, R.; Theato, P. Sequential Post-Polymerization Modification Reactions of Poly(pentafluorophenyl 4-Vinylbenzenesulfonate). *Polym. Chem.* **2014**, *5* (7), 2320.

(83) Nilles, K.; Theato, P. Sequential Conversion of Orthogonally Functionalized Diblock Copolymers Based on Pentafluorophenyl Esters. *J. Polym. Sci. Part A Polym. Chem.* **2010**, *48* (16), 3683–3692.

(84) Nilles, K.; Theato, P. Synthesis and Polymerization of Active Ester Monomers Based on 4-Vinylbenzoic Acid. *Eur. Polym. J.* **2007**, *43* (7), 2901–2912.

(85) Nilles, K.; Theato, P. Polymerization of an Activated Ester Monomer Based on 4-Vinylsulfonic Acid and Its Polymer Analogous Reaction. *Polym. Chem.* **2011**, *2* (2), 376–384.

(86) Gibson, M. I.; Fröhlich, E.; Klok, H.-A. Postpolymerization Modification of Poly(pentafluorophenyl Methacrylate): Synthesis of a Diverse Water-Soluble Polymer Library. *J. Polym. Sci. Part A Polym. Chem.* **2009**, *47* (17), 4332–4345.

(87) Vandenbergh, J.; Junkers, T. Alpha and Omega: Importance of the Nonliving Chain End in Raft Multiblock Copolymerization. *Macromolecules* **2014**, *47* (15), 5051–5059.

(88) Veloso, A.; Garcia, W.; Agirre, A.; Ballard, N.; Ruiperez, F.; de la Cal, J. C.; Asua, J. M. Determining the Effect of Side Reactions on Product Distributions in RAFT Polymerization by MALDI-TOF MS. *Polym. Chem.* **2015**, *6* (30), 5437–5450.

(89) Eberhardt, M.; Mruk, R.; Zentel, R.; Théato, P. Synthesis of Pentafluorophenyl(meth)acrylate Polymers: New Precursor Polymers for the Synthesis of Multifunctional Materials. *Eur. Polym. J.* **2005**, *41* (7), 1569–1575.

(90) Gody, G.; Maschmeyer, T.; Zetterlund, P. B. Polymerization for Synthesis of Polymer of High Livingness at Full. *Macromolecules* **2014**, *47*, 639–649.

(91) Gruendling, T.; Pickford, R.; Guilhaus, M.; Barner-Kowollik, C. Degradation of RAFT Polymers in a Cyclic Ether Studied via High Resolution ESI-MS: Implications for Synthesis, Storage, and End-Group Modification. *J. Polym. Sci. Part A Polym. Chem.* **2008**, *46* (22), 7447–7461.

(92) Claridge, T. *High-Resolution NMR Techniques in Organic Chemistry*; Tetrahedron Organic Chemistry; Elsevier Science, 1999.

(93) Fulmer, G. R.; Miller, A. J. M.; Sherden, N. H.; Gottlieb, H. E.; Nudelman, A.; Stoltz, B. M.; Bercaw, J. E.; Goldberg, K. I. NMR Chemical Shifts of Trace Impurities: Common Laboratory Solvents, Organics, and Gases in Deuterated Solvents Relevant to the Organometallic Chemist. *Organometallics* **2010**, *29* (9), 2176–2179.

(94) Harth, E.; Van Horn, B.; Lee, V. Y.; Germack, D. S.; Gonzales, C. P.; Miller, R. D.; Hawker, C. J. A Facile Approach to Architecturally Defined Nanoparticles via Intramolecular Chain Collapse. *J. Am. Chem. Soc.* **2002**, *124* (29), 8653–8660.

(95) Gruendling, T.; Oehlenschlaeger, K. K.; Frick, E.; Glassner, M.; Schmid, C.; Barner-Kowollik, C. Rapid UV Light-Triggered Macromolecular Click Conjugations via the Use of O-Quinodimethanes. *Macromol. Rapid Commun.* **2011**, *32* (11), 807–812.

(96) Zhou, F.; Zhang, Z.; Jiang, G.; Lu, J.; Chen, X.; Li, Y.; Zhou, N.; Zhu, X. Self-Assembly of Amphiphilic Macrocycles Containing Polymeric Liquid Crystal Grafts in Solution. *Polym. Chem.* **2016**, *7* (16), 2785–2789.

(97) Griffiths, P. C.; Stilbs, P.; Yu, G. E.; Booth, C. Role of Molecular Architecture in Polymer Diffusion: A PGSE-NMR Study of Linear and Cyclic Poly(ethylene Oxide). *J. Phys. Chem.* **1995**, *99* (45), 16752–16756.

(98) Ogawa, T.; Nakazono, K.; Aoki, D.; Uchida, S.; Takata, T. Effective Approach to Cyclic Polymer from Linear Polymer: Synthesis and Transformation of Macromolecular [1]Rotaxane. *ACS Macro Lett.* **2015**, *4* (4), 343–347.

(99) Kawaguchi, D.; Masuoka, K.; Takano, A.; Tanaka, K.; Nagamura, T.; Torikai, N.; Dalgliesh, R. M.; Langridge, S.; Matsushita, Y. Comparison of Interdiffusion Behavior between Cyclic and Linear Polystyrenes with High Molecular Weights. *Macromolecules* **2006**, *39* (16), 5180–5182.

(100) Hadziioannou, G.; Cotts, P. M.; ten Brinke, G.; Han, C. C.; Lutz, P.; Strazielle, C.; Rempp, P.; Kovacs, A. J. Thermodynamic and Hydrodynamic Properties of Dilute Solutions of Cyclic and Linear Polystyrenes. *Macromolecules* **1987**, *20* (3), 493–497.

(101) Zhu, X.; Zhou, N.; Zhang, Z.; Sun, B.; Yang, Y.; Zhu, J.; Zhu, X. Cyclic Polymers with

Pendent Carbazole Units: Enhanced Fluorescence and Redox Behavior. *Angew. Chemie Int. Ed.* **2011**, *50* (29), 6615–6618.

(102) Hoffman, R. Diffusion http://chem.ch.huji.ac.il/nmr/techniques/other/diff/diff.html (accessed Jun 2, 2017).

(103) Tumir, L.-M.; Radić Stojković, M.; Piantanida, I. Come-Back of Phenanthridine and Phenanthridinium Derivatives in the 21st Century. *Beilstein J. Org. Chem.* **2014**, *10*, 2930–2954.

(104) Krichevsky, O. Fluorescence Correlation Spectroscopy: The Technique and Its Applications. *Rep.Prog.Phys* **2002**, *65*, 251–297.

(105) Mandapati, P.; Giesbrecht, P. K.; Davis, R. L.; Herbert, D. E. Phenanthridine-Containing Pincer-like Amido Complexes of Nickel, Palladium, and Platinum. *Inorg. Chem.* **2017**, *56* (6), 3674–3685.

(106) Mondal, R.; Giesbrecht, P. K.; Herbert, D. E. Nickel(II), copper(I) and zinc(II) Complexes Supported by a (4-Diphenylphosphino)phenanthridine Ligand. *Polyhedron* **2016**, *108*, 156–162.

(107) Das, A.; Theato, P. Multifaceted Synthetic Route to Functional Polyacrylates by Transesterification of Poly(pentafluorophenyl Acrylates). *Macromolecules* **2015**, *48* (24), 8695–8707.

(108) He, L.; Szameit, K.; Zhao, H.; Hahn, U.; Theato, P. Postpolymerization Modification Using Less Cytotoxic Activated Ester Polymers for the Synthesis of Biological Active Polymers. *Biomacromolecules* **2014**, *15* (8), 3197–3205.

(109) Gan, Y.; Dong, D.; Carlotti, S.; Hogen-Esch, T. E. Enhanced Fluorescence of Macrocyclic Polystyrene. *J. Am. Chem. Soc.* **2000**, *122* (9), 2130–2131.

(110) Zhao, Y.; Duan, S.; Zeng, X.; Liu, C.; Davies, N. M.; Li, B.; Forrest, M. L. Prodrug Strategy for PSMA-Targeted Delivery of TGX-221 to Prostate Cancer Cells. *Mol. Pharm.* **2012**, *9* (6), 1705–1716.

(111) Choi, Y. W.; Lee, J. J.; Kim, C. A Highly Selective Fluorescent Chemosensor Based on a Quinoline Derivative for Zinc Ions in Pure Water. *RSC Adv.* **2015**, *5* (75), 60796–60803.

(112) Ottria, R.; Casati, S.; Ciuffreda, P. Optimized Synthesis and Characterization of N-Acylethanolamines and O-Acylethanolamines, Important Family of Lipid-Signalling Molecules. *Chem. Phys. Lipids* **2012**, *165* (7), 705–711.

(113) Smith, M. B.; March, J. *March's Advanced Organic Chemistry*; Hoboken Wiley, 2007.

(114) Deraeve, C.; Maraval, A.; Vendier, L.; Faugeroux, V.; Pitié, M.; Meunier, B. Preparation of New bis(8-Aminoquinoline) Ligands and Comparison with bis(8-Hydroxyquinoline) Ligands on Their Ability to Chelate CuII and ZnII. *Eur. J. Inorg. Chem.* **2008**, *1* (36), 5622–5631.

(115) Surry, D. S.; Buchwald, S. L. Dialkylbiaryl Phosphines in Pd-Catalyzed Amination: A User's Guide. *Chem. Sci.* **2011**, *2* (1), 27–50.

(116) Wolfe, J. P.; Buchwald, S. L. Scope and Limitations of the Pd/BINAP-Catalyzed Amination of Aryl Bromides. *J. Org. Chem.* **2000**, *65* (4), 1144–1157.

(117) Padilla, M.; Sanchez-quesada, J. Triple Substituted Phenanthroline Derivatives for the Treatment of Neurodegenerative or Haematological Diseases or Conditions, or Cancer. *United States Pat. Appl. Publ.* **2011**, *1* (19).

(118) Wu, Z.; He, Y.; Ma, C.; Zhou, X.; Liu, X.; Li, Y.; Hu, T.; Wen, P.; Huang, G. Oxidative Remote C−H Trifluoromethylation of Quinolineamides on the C5 Position with Iodobenzene Diacetate as the Oxidizing Agent. *Asian J. Org. Chem.* **2016**, *5* (6), 724–728.

(119) Yang, X.; Sun, Y.; Sun, T.; Rao, Y. Auxiliary-Assisted Palladium-Catalyzed Halogenation of Unactivated C(sp 3 )–H Bonds at Room Temperature. *Chem. Com* **2016**, *52* (38), 6423–6426.

(120) Willcock, H.; O'Reilly, R. K. End Group Removal and Modification of RAFT Polymers. *Polym. Chem.* **2010**, *1* (2), 149–157.

(121) Roth, P. J.; Boyer, C.; Lowe, A. B.; Davis, T. P. RAFT Polymerization and Thiol Chemistry: A Complementary Pairing for Implementing Modern Macromolecular Design. *Macromol. Rapid Commun.* **2011**, *32* (15), 1123–1143.

(122) Xu, J.; He, J.; Fan, D.; Wang, X.; Yang, Y. Aminolysis of Polymers with Thiocarbonylthio Termini Prepared by RAFT Polymerization: The Difference between Polystyrene and Polymethacrylates. *Macromolecules* **2006**, *39* (25), 8616–8624.

(123) Mohr, N.; Barz, M.; Forst, R.; Zentel, R. A Deeper Insight into the Postpolymerization Modification of Polypenta Fluorophenyl Methacrylates to Poly( N -(2-Hydroxypropyl) Methacrylamide). *Macromol. Rapid Commun.* **2014**, *35* (17), 1522–1527.

(124) Gibson, M. I.; Fröhlich, E.; Klok, H.-A. Postpolymerization Modification of Poly(pentafluorophenyl Methacrylate): Synthesis of a Diverse Water-Soluble Polymer Library. *J. Polym. Sci. Part A Polym. Chem.* **2009**, *47* (17), 4332–4345.

(125) Richards, S.; Jones, M. W.; Hunaban, M.; Haddleton, D. M.; Gibson, M. I. Probing Bacterial-Toxin Inhibition with Synthetic Glycopolymers Prepared by Tandem Post-Polymerization Modification: Role of Linker Length and Carbohydrate Density. *Angew. Chemie Int. Ed.* **2012**, *51* (31), 7812–7816.

(126) Singha, N. K.; Gibson, M. I.; Koiry, B. P.; Danial, M.; Klok, H. Side-Chain Peptide-Synthetic Polymer Conjugates via Tandem "Ester-Amide/Thiol–Ene" Post-Polymerization

Modification of Poly(pentafluorophenyl Methacrylate) Obtained Using ATRP. *Biomacromolecules* **2011**, *12* (8), 2908–2913.

(127) Kosvintsev, S. R.; Riande, E.; Velarde, M. G.; Guzmán, J. Rheological Behaviour of Solutions of poly(2-Hydroxyethyl Methacrylamide) in Glycerine. *Polymer (Guildf).* **2001**, *42* (17), 7395–7401.

(128) Günay, K. A.; Schüwer, N.; Klok, H.-A. Synthesis and Post-Polymerization Modification of Poly(pentafluorophenyl Methacrylate) Brushes. *Polym. Chem.* **2012**, *3* (8), 2186.

(129) Yoshida, T.; Lai, T. C.; Kwon, G. S.; Sako, K. pH- and Ion-Sensitive Polymers for Drug Delivery. *Expert Opin. Drug Deliv.* **2013**, *10* (11), 1497–1513.

(130) Hong, Y.; Lam, J. W. Y.; Tang, B. Z. Aggregation-Induced Emission: Phenomenon, Mechanism and Applications. *Chem. Commun.* **2009**, No. 29, 4332.